# Modeling and Analysis of a Traveling Wave Tube Under Multitone Excitation

by

**John Greaton Wöhlbier**

A thesis submitted in partial fulfillment of

the requirements for the degree of

Masters of Science

(Electrical and Computer Engineering)

at the

University of Wisconsin - Madison

2000

This thesis entitled:
Modeling and Analysis of a Traveling Wave Tube Under Multitone Excitation
written by John Greaton Wöhlbier
has been approved for the Department of Electrical and Computer Engineering

Ian Dobson

John H. Booske

Date

The final copy of this thesis has been examined by the signatories, and we find that both the content and the form meet acceptable presentation standards of scholarly work in the above mentioned discipline.

Wöhlbier, John Greaton (M.S., Electrical and Computer Engineering)

Modeling and Analysis of a Traveling Wave Tube Under Multitone Excitation

Thesis directed by Professor Ian Dobson and Professor John H. Booske

When a Traveling Wave Tube (TWT) is driven at a sufficient level by an input containing multiple frequencies, the output spectrum of the amplifier is distorted due to the nonlinear response of the electron beam to the drive signals. With the improvement of TWT technology device bandwidths continue to increase, and it is ever more important to have a qualitative and quantitative understanding of the nonlinear interactions. Therefore, in this thesis we reformulate and analyze a model of a TWT under multitone drive that was originally developed in 1968 by A.J. Giarola. First we present a single tone model where analysis techniques are developed, and then we derive the multitone model and perform a similar analysis. Included in the analyses are linearizations of finite dimensional approximations of the models and linearization by the method of collective variables. Numerical solutions and physical interpretations of the model equations are included.

## Dedication

To Kathryn and Carl.

**Acknowledgements**

I thank Professors Dobson and Booske for their patience, guidance, friendship, and for their willingness to let me guide the research.

This work was supported in part by AFOSR Grant 49620-00-1-0088 and by DUSD(S&T) under the Innovative Microwave Vacuum Electronics Multidisciplinary University Research Initiative (MURI) program, managed by the Air Force Office of Scientific Research under Grant F49620-99-1-0297.

## Contents

**Chapter**

## Figures

**Figure**

## Tables

### Table

# Chapter 1

# Introduction

## 1.1 Motivation

Traveling Wave Tubes (TWTs) are amplifiers used in satellite communications (e.g. cellular phones, television broadcast, or scientific satellites) or electronic countermeasures (e.g. radar jamming). The possibility of several simultaneous communications channels in one TWT is attractive since it increases "communication density" for a given satellite, or, alternatively, reduces satellite payload. When a standard TWT is used with multiple simultaneous communications channels (multitone drive) there are unwanted consequences, most notably distortion of the output.

This thesis investigates the modeling of a Traveling Wave Tube (TWT) under multitone drive. Multitone drive means that the spectrum of the input signal, or drive signal, fed to the amplifier has several distinct tones, or carriers, each of which is intended to transmit information not related to the information on the other carriers. For even moderate levels of drive signals the spectrum on the output of the amplifier contains frequency content not found in the input, i.e. the output is not just a scaled version of the input. This distortion of the input signal makes the subsequent decoding of the information on the carriers difficult. We study the physics, modeling, and analysis of the TWT with the aim of improving the device performance.

### 1.1.1 The Traveling Wave Tube

The Traveling Wave Tube is a device which is used for the amplification of coherent electromagnetic waves, typically in the microwave ($1 - 100$ GHz) range. The free energy required for the amplification of the wave comes from DC energy stored in an electron beam that is passed in near proximity to the electromagnetic (EM) wave. If the electron beam and the EM wave have nearly the same velocities, energy in the beam is given to the wave which manifests in wave amplitude growth; the growth is due to an inherent instability in the beam-wave system.

Before qualitatively describing the interaction we need to briefly explain the slow-wave guiding structure required for the interaction. There are several guiding structures that are used in practice but we shall restrict our attention to the helical wire, or helix, waveguide. The helix waveguide is composed of a helical wire surrounded by a metal cylindrical sheath; the sheath acts as the ground plane for the waveguide. The shape of the wire has the effect of reducing the phase velocity of a wave propagating on the structure. One may think of the wave propagating along the line of the helix so that the reduction of phase velocity from the vacuum speed corresponds to the time for the wave to propagate over one twist of the helix. A helix with a smaller pitch will therefore have a slower phase velocity. The mode structure of the helix has most of the field intensity concentrated between the helix and the ground plane, but there are also fringing electric fields that extend from turn to turn of the helix; a portion of these fields extend into the center of the helix and have an axial component of electric field. Since the electron beam is sent down the center of the helix it is easy to imagine that these longitudinal fringing fields are those that the beam interacts with; this is in fact the case. Note that any guiding structure used in TWT design must have a longitudinal component of electric field.

Lastly, the presence of the electron beam in the waveguide modifies the vacuum

field structure, and hence changes the dispersion relation for the beam-circuit system. This phenomena is referred to as beam loading. Often in analysis we will speak of cold circuit phase velocity, which is the phase velocity when no electron beam is present in the waveguide. One should keep in mind that if an electron beam is present the circuit wave will never propagate with this cold circuit phase velocity, and in fact the actual wave will always propagate slower than the electron beam.

This is all the detail required for appreciating the role of the waveguide in the TWT interaction. There is a substantial body of literature dealing exclusively with these waveguiding structures (for a taste of what has been known for some time see [52]). We are more interested in analyzing the beam-wave interaction so will take a naive view of the helix and treat it as a simple transmission line. We will try to mention the shortcomings of this approach where applicable.

To aid in understanding the interaction imagine the following "Gedanken TWT". Consider a propagating sinusoidal electromagnetic wave in the presence of a uniformly distributed monoenergetic electron beam in which the velocities of the electrons in the beam are very close to the wave velocity. Imagine that there is initially no interaction so we simply have the copropagation of the wave and the electron beam. At time $t = 0$ the interaction is turned on at $z = 0$ and this boundary, or wave front, between the regions of no interaction and interaction propagates down the tube; furthermore require that at time $t = 0$ a voltage peak of the electromagnetic sinusoid is at $z = 0$. We are obviously interested in what happens behind the wave front. If we picture the negative of the voltage wave we can imagine that electrons will roll down into this sinusoid and we can hence easily picture whether they are accelerated or decelerated.[1] The interaction can then be summarized in three steps:

(1) Charges that are in the decelerating regions of the electromagnetic wave are

[1] We could also imagine positive charge in the beam for the same effect.

slowed down (fall back into the well) and charges that are in the accelerating regions of the wave are sped up (fall forward into the well). Notice that not all electrons feel the same force, e.g. those in the bottom of the well feel no force, while those half way up the sinusoid feel maximum force.

(2) The redistribution of charge in the beam forces charges in the circuit to deviate from their unforced trajectories (i.e. the charge trajectories when no beam is present). This amounts to a perturbation in the unforced current, and hence a modification of the circuit voltage.

(3) The induced voltage on the circuit, combined with the original impressed voltage, further modify the beam electron trajectories. Due to the beam loading of the circuit, the electrons tend to bunch in the decelerating phase of the circuit wave; therefore, there is a higher concentration of charge in the decelerating phase. Reapplication of step (1) will imply energy is given to the wave and the amplitude of the wave grows.

The above steps do not indeed happen in such a discrete cause and effect manner; rather, they evolve self consistently.

### 1.1.2 The Multitone Problem

With the above picture, the problem of multitone drive may be simply motivated. In place of the single tone above we introduce multiple forcing tones. Each tone has its own wavelength which is calculated from the dispersion relation of the circuit. Then in step (1) above the net force an electron in the beam feels is not only due to the single sinusoid, rather it gets a kick from each tone. The amount of kick depends both on its phase with respect to the various tones as well as the tone amplitudes. Each particle then gets it own trajectory modification and the sum

of these modifications forces the redistribution of charge on the circuit, which further influences the trajectories of the electrons. The self-consistent solution of the interaction results in the growth of the imposed tones.

One can imagine that the bunching that results from multitone drive has spatial (and hence temporal) characteristics of the driving tones. Moreover these characteristics will reflect not only frequencies (in the spatial distribution of bunches) but also amplitudes of the tones (in the intensity of bunching at the particular frequency, maybe measured by a Fourier transform). In fact this bunching structure combined with the ballistic response of the electron beam can induce tones on the circuit that were not imposed. In a communications application, spectral content on the output that was not present on the input is clearly undesired as it complicates decoding of the information. Indeed the motivation of this thesis is to physically understand the dynamics of multitone drive and the resulting spectrum.

## 1.2 Literature Review

The TWT was invented in 1944 [26] and a substantial amount of work has gone into understanding the principles of its operation. In this section we try to highlight the portions of that work that have the most relevance to us. In particular we will make no attempt to cover aspects of the device unrelated to our work, such as the effect of helix support structures on helix dispersion; rather, we will focus on the literature dealing with the physics of the beam-wave interaction. The material discussed will mostly be theoretical in nature, but experimental results will be alluded to when relevant.

### 1.2.1 Overview of TWT Modeling Techniques and Review of the Literature

The classic model of a TWT was established by J. R. Pierce and published in 1947 [44]. The analysis uses a one-dimensional transmission line equivalent to represent the waveguide, and models the electron beam as a one dimensional fluid. The two fluid equations for the electron beam are a Newton's Law relation and an equation of continuity, written in Eulerian coordinates. As these equations are quasi-linear (linear in the highest order derivative) the first step of the analysis is to linearize. The solution to the linearized equations does a good job of predicting TWT performance in the small-signal regime. There is a substantial amount of physics that can be added to the model, the details of which have been presented in several text books such as [24, 26, 33, 45].

Even the most basic one-dimensional TWT equations are not linear. The effect of the nonlinearities on the beam-wave interaction and its manifestation in the circuit voltage is very important. One consequence was mentioned earlier in motivating the multitone problem. Indeed the unwanted spectral content on the output is due to the nonlinear response of the electron beam to the voltage on the transmission line. This is an issue not only in communications applications, but even under single tone drive when one wants to predict the amount of power in the wave at the fundamental driving frequency. Another nonlinear effect is that of saturation in which the electron bunch that had formed in the decelerating phase is decelerated so much so that it falls back into the accelerating phase of the wave. At this point the wave starts giving energy back to the beam and the circuit voltage saturates and starts decreasing.

In the classic Pierce model the beam fluid equations were written in Eulerian coordinates. An alternative set of coordinates, which will be used in this thesis, are Lagrangian coordinates. Since the choice of coordinates plays a major role in this

thesis, we briefly describe Eulerian and Lagrangian fluid coordinates here. Eulerian coordinates are the conventional space-time coordinates, e.g. $(\mathbf{r}, t)$. Then, for instance, the fluid velocity function is written $\mathbf{v}(\mathbf{r}, t)$; this function gives, at time $t$ and location $\mathbf{r}$ the velocity of the fluid element occupying that location. Notice for $\mathbf{v}(\mathbf{r}, t)$ to be a well defined function there may be only one value of velocity at each point in space at a fixed time; there may only be one fluid element at the position $\mathbf{r}$ at a fixed time. Alternatively in Lagrangian coordinates, as independent variables one may use the initial position of the fluid elements, $\mathbf{r}_0$, and time, $t$; thus a fluid element position function would be written as $\mathbf{r}(\mathbf{r}_0, t)$. This way of describing the fluid has the advantage that two different fluid elements, labeled by different values of $\mathbf{r}_0$, may occupy the same $\mathbf{r}$ position without violating the well-behavedness of the function $\mathbf{r}(\mathbf{r}_0, t)$. The model equations for a fluid in the two different sets of coordinates will be slightly different, but they will model the same physical situation.

When the early TWT researchers did nonlinear analyses most of their attention turned to the Lagrangian description. One researcher not in this group, F. Paschke, retained the Eulerian description for Klystron analysis (a device closely related to the TWT). In particular he studied space-charge waves and harmonic generation in a velocity modulated beam using a successive approximation type of analysis [39, 40, 41]. Recently there has been some work done by a group of authors who extend Paschke's methods and apply them to a TWT. Using an Eulerian description, they study power in the fundamental and harmonic frequencies at saturation, and propose methods for suppression of harmonics based on their results. In their work they compare their results to what is considered a more accurate Lagrangian theory [14, 15, 16, 17].

It was realized early on that electron overtaking occurs at lengths even before saturation. As discussed, the Eulerian description cannot describe the situation where

two fluid elements occupy the same position at an instant of time. Thus in 1953, only 6 years after Pierce's seminal paper, A. Nordsieck formulated the TWT equations using a Lagrangian fluid description [38]. The assumptions made in this work were severe, but nonetheless it developed a framework on which several authors built. The number of theoretical papers written using this foundational method, or something very similar, are numerous. Each paper makes its own modification or improvement to the model. Rather than list all of the papers here we refer to the book by Rowe [49] in which he exhaustively covers the details of the modeling choices, applies the modeling technique to several microwave devices, and includes references to much of the literature mentioned. A very good paper that compares experimental data on the nonlinear saturation phenomena to much of the above mentioned modeling is [12].

In this thesis we are interested in modeling the TWT when it is driven by several tones. The first attempt to formulate the Lagrangian model discussed for the multitone drive case was Giarola [25]. Like Nordsieck's paper this treatment made several severe assumptions, but was a framework for other authors to study and improve upon [20, 50]. In fact in this thesis we will formulate a version of Giarola's model and study it in ways it has not been studied in the literature.

### 1.2.2 More TWT Modeling Literature

The literature review required for the thesis has been presented. Since we do not want to give the impression that Giarola's model is the current state of the art, we now discuss the work that has been done in the 30 years following Giarola's paper. It is not unreasonable to say that the foundational work for modern day modeling was done in the papers previously mentioned.[2] Activities today are increasing the level of detail included in modeling both the circuit and the electron beam. In general the

[2] For a nice summary of microwave device modeling in 1999 one should see the article by Antonsen, *et al.* [4].

electron beam is treated as a one, two, or three dimensional "macro-particle" beam and the circuit is represented by either a sheath or tape helix model. The circuit analysis may be done in the frequency or time domain. In some instances the circuit is just represented by frequency dependent parameters that are calculated from a different electromagnetics solver. Examples of some of these models may be found in [2, 3] and [21, 22]. Finally, with regard to the macro-particle approach, there have been other papers that are similar in spirit but take a slightly different approach to modeling the beam-wave interaction [18, 53].

At this time a fully 3-dimensional "First Principles", or particle-in-cell (PIC) model of the TWT is impractical for computing resources. While the required tools exist, not much TWT modeling has been done with them. Some researchers have developed one-dimensional PIC codes that display the fundamental beam-wave interaction physics [11, 37].

## 1.3 The Contribution of this Thesis

Since we have stated that we will study a model similar to Giarola's in this thesis, the purpose of this thesis is not to advance the state of the art TWT modeling. Instead the purpose of this work is to carefully analyze the fundamental beam-wave interaction for a TWT with multitone drive. This careful analysis, it is hoped, will set the stage for suggested methods of improving the performance of a TWT under multitone drive. To this end we employ a few mathematical techniques that have not previously been applied to the multitone TWT model. The contributions of this thesis can be summarized as:

(1) Redeveloping Giarola's equations in coordinates more amenable to analysis and physical interpretation.

(2) Linearizing the Lagrangian model, including a study of the Jacobian matrix

(single tone and multitone).

(3) Linearization by the method of collective variables (single tone and multitone).

# Chapter 2

## Single Tone Analysis

As a starting point for our analysis of the TWT under multitone excitation we elect to first consider a single tone model. Since the single tone model is very similar to the multitone model, analysis on this simpler case will be easily extendable to the multitone case. Furthermore, intuitions developed here will greatly aid in understanding the multitone model.

We outline the model originally presented by Nordsieck [38] taking time to clearly spell out differences between this model and the classic modeling by Pierce ([44], [45], [26]), as well as offering an interpretation of the physical meaning of the variables and equations. Next we cast the model into a Hamiltonian form similar to that of a high gain Free Electron Laser (FEL) model [8] along with changing the reference frame from the cold circuit wave frame to the unperturbed electron beam frame. Since the numerical solutions to the model will be important, we spend some time discussing the numerical issue of stiffness found in our system and present some solutions for a few cases. We then identify a system equilibrium and investigate the eigenvalue structure for a TWT under single tone excitation. Lastly, a linearization of the model about the equilibrium using the method of collective variables is performed and results are presented.

## 2.1 Single Tone Model

The "large signal" model of Nordsieck was widely used and improved upon for many years following its publication. For an extensive treatment of the model as applied to TWTs and other microwave devices see Rowe [49]. Here we discuss the foundations for the model, including physical and mathematical assumptions made in the derivation, and present the model in one of its original forms.

### 2.1.1 Presentation of the Nordsieck Model

#### Model Foundations

As discussed in Chapter 1, to describe the behavior of a TWT one must model the interaction of the radiation field of the slow wave circuit and the dynamics of the electron beam. In general this is a very ambitious task. Efforts prior to Nordsieck's paper were linearizations of the fundamental equations and thus lacked substantially in their predictive power. To model nonlinear effects Nordsieck discovered that one may formulate the equations in Lagrangian coordinates. This formulation allows modeling of electrons in a beam overtaking each other, whereas modeling electron overtaking is not possible in an Eulerian formulation.

Before proceeding we should introduce the differences between an Eulerian description and a Lagrangian description as this is the essence of what separates Nordsieck's model from earlier analyses (e.g. Pierce).[1] The terms Eulerian and Lagrangian have their origins in fluid dynamics and continuum mechanics and are applicable since we are modeling the electron beam as a fluid. It is vital to understand that the fundamental modeling equations are the same in both cases, the difference being what one chooses as the independent variables. An Eulerian description treats

[1] For textbook presentations of the two fluid descriptions one should see for example fluid dynamics texts such as [36] or a text on continuum mechanics such as [47, 55]. An instructive video also exists [29].

configuration space variables as independent variables where fluid quantities such as density are evaluated at points in space-time, e.g. $\rho(\mathbf{r}, t)$. A Lagrangian description uses fluid element initial position and time as independent variables; thus, a fluid quantity such as density is parameterized by time and fluid element label, e.g. $\tilde{\rho}(\mathbf{r}_0, t)$. If one wants to calculate density in configuration space from $\tilde{\rho}(\mathbf{r}_0, t)$ one would need a trajectory function for each fluid element, i.e. $\mathbf{r}(\mathbf{r}_0, t)$ where $\mathbf{r}$ is the configuration space coordinate, $\mathbf{r}_0$ is initial fluid element position, and $t$ is time. To get $\rho(\mathbf{r}, t)$ one would invert $\mathbf{r}(\mathbf{r}_0, t)$ giving $\mathbf{r}_0(\mathbf{r}, t)$, and substitute this function into $\tilde{\rho}(\mathbf{r}_0, t)$.

To start modeling, several simplifying assumptions need to be made. The assumptions regarding the helix circuit are discussed first. The circuit is replaced by a dispersionless transmission line and instead of solving for fields one solves for voltages on the transmission line. This is a common simplification and was used in several of the earlier analyses. Next, we ignore reflections on the transmission line and assume only a forward wave exists. Lastly, the impedance of the circuit is assumed to be only at the fundamental frequency so that the only frequency component of the charge density that induces voltage on the circuit is the fundamental tone.[2]

The electron beam is made tractable by assuming it is a one-dimensional fluid in which repulsive forces between electron fluid elements are ignored. The interaction is considered to be periodic in time; choosing any point in space we see a periodic voltage wave of a constant amplitude and a periodic beam density profile pass by in time. Although there is time periodicity at points in space, there is no spatial periodicity at points in time; indeed, if there were spatial periodicity there would be no growth of the wave nor bunching of the beam. Because of the periodicity assumption we may consider only one period of the wave and the corresponding

[2] To understand this last assumption consider that a pure tone excitation will bunch the beam sufficiently to give density modulation with high frequency content; we assume only the excitation frequency induced into the beam feeds back and induces voltage on the circuit. If one lets the other frequencies induce voltages one has a multitone model, which is the subject of Chapter 3.

piece of the beam. These are the assumptions required for deriving the model. For further analysis, including calculating numerical solutions, one effectively chops the beam into disks[3] and treats the disks as "particles".

The model is derived from three fundamental equations. For the evolution of the voltage on the transmission line an inhomogeneous telegrapher's transmission line equation is used. The source term in this equation is a function of the electron beam charge density as charges in the beam influence the motion of charges (currents) in the circuit (and hence voltages). For the evolution of the electron beam Newton's law is used in conjunction with an equation of continuity. The continuity equation used is not the standard Eulerian form, rather a Lagrangian form that comes from requiring conservation of charge. Intuitively charge conservation can be understood by considering the fact that a charge element of width $\Delta z_0$ that enters the interaction region at time $t_0$ must be accounted for at some later time $t_1$ within a different elemental width $\Delta z_1$. Newton's law is used to determine the trajectories of these charge elements by relating the force on the charge in the beam to the gradient of the voltage on the transmission line.[4] All of the equations are one dimensional in space with an additional dimension for time. For a detailed exposition on the validity of these equations see Rowe [49]. The equations are presented below:

$$\frac{\partial^2 V(z,t)}{\partial t^2} - {v_0}^2 \frac{\partial^2 V(z,t)}{\partial z^2} = v_0 Z_0 \frac{\partial^2 \rho(z,t)}{\partial t^2} \tag{2.1}$$

$$\frac{\partial^2 z(z_0,t)}{\partial t^2} = -\frac{e}{m_e} \frac{\partial V(z,t)}{\partial z} \tag{2.2}$$

$$\rho(z,t) = \frac{I_0}{u_0} \left| \frac{\partial z_0(z,t)}{\partial z} \right|_t \tag{2.3}$$

[3] In the literature the discretization is an implied feature of a Lagrangian model, which is described by a system of ordinary differential equations. These models are also sometimes called "large-particle", or "macro-particle" models. In this thesis we maintain a fluid description, which is described by partial differential equations, until we explicitly discretize.

[4] As mentioned the description of the electron beam is a fluid one and when we talk of charge elements of width $\Delta z$ we really mean differentially small elements. In this way we will use the word fluid element as a differentially small "chunk" of fluid.

In equations (2.1)-(2.3) $V(z,t)$ is the transmission line voltage, $\rho(z,t)$ is the electron beam fluid charge density, $v_0$ is the cold helix phase velocity (i.e. the phase velocity of the circuit when no electron beam is present), $Z_0$ is the transmission line impedance, $z(z_0,t)$ is the position function of a fluid element at time $t$ whose value at time $t=0$ was $z(z_0,0)=z_0$; $z_0$ takes a continuum of values corresponding to the space the beam occupies at $t=0$, $\frac{e}{m_e}$ is an electron charge to mass ratio ($e<0$ for an electron), $I_0$ is the value of beam current at $(z,t)=(0,0)$ ($I_0<0$ for electron current), $u_0$ is the electron beam velocity at $(z,t)=(0,0)$, $\frac{I_0}{u_0}$ is therefore the charge density at $(z,t)=(0,0)$, and $z_0(z,t)$ is a function whose value is, for the fluid element at position $z$ at time $t$, its $z$ value at time $t=0$, $z=z_0$. The functions $z(z_0,t)$ and $z_0(z,t)$ are related in that for a fixed $t$ the function $z_0(z,t)$ is the inverse (pending its existence) of $z(z_0,t)$. One of the benefits of the Lagrangian formulation is that it allows for overtaking of electrons in a beam, which means at some time $t$, $z(z_0,t)$ will have the same value for at least two different values of $z_0$. Therefore its inverse function, $z_0(z,t)$, will not be well defined; the $|\cdot|_t$ notation is introduced to take "...the sum of [$\frac{\partial z_0}{\partial z}$'s] values for all branches of the multivalued function $z_0$."[38].

In our final Lagrangian model, the independent variables will be scaled versions of $z$ and $z_0$. When $(z,z_0)$ are the independent variables we have a fluid element time function $t(z,z_0)$; the time it takes fluid element $z_0$ to get to position $z$. Notice then in equation (2.1) the dependent variable $t$ appears as an argument of the dependent variables $V$ and $\rho$, and some differentiations are with respect to $t$. Furthermore, in equations (2.2) and (2.3) functions $z_0(z,t)$ and $z(z_0,t)$ appear, so clearly $(z,z_0)$ are not explicitly the independent variables of the system. This is one of the complications with equations (2.1)-(2.3) which is why we must do some work to get them in usable form.

**Variable Definitions**

The first step in the formulation involves changing from the laboratory frame to a reference frame moving with the unperturbed circuit phase velocity $v_0$. To change reference frame is simply to define new independent variables such that sitting at the origin of the new coordinate system (i.e. traveling at the reference frame velocity with respect to the lab frame) implies that your new coordinate remains zero. The equations are then written in the new coordinates.

The lab frame space variable $z$ is transformed into a frequency normalized variable $y$ as defined by the following relation:

$$y \equiv C\frac{\omega z}{v_0} \tag{2.4}$$

In (2.4) $C$ is the Pierce growth parameter, and $\omega$ is the radian frequency of the single tone assumed to be on the TWT. The growth parameter is defined by $C^3 \equiv \frac{Z_0 I_0}{4V_0}$, where $Z_0$ is the circuit impedance, $I_0$ is the DC beam current, and $V_0$ is the beam voltage. The second variable is a phase variable which combines $z$ and $t$:

$$\Phi \equiv \omega\left(\frac{z}{v_0} - t\right) \tag{2.5}$$

The phase it describes is that with respect to a traveling wave of frequency $\omega$ and speed $v_0$, namely the cold circuit wave. In other words a point of constant phase on the cold circuit wave has a trajectory given by $z(t) = v_0 t$, evaluating (2.5) along this trajectory (i.e. plugging $v_0 t$ into the $z$ component of (2.5)) one sees that $\Phi(v_0 t, t) = 0$, so for any other pairs of $(z, t)$ equation (2.5) computes phase with respect to this constant phase point. In this way we are defining a moving coordinate system in that our coordinate only takes a nonzero value if a $z$ value deviates from $z = v_0 t$.

At $t = 0$ the portion of the beam corresponding to one period of the interaction occupies a region of space; each point $z_0$ in that region has a value of phase with respect to a traveling wave and this phase could be calculated by setting $t = 0$

in (2.5). In fact we choose the phase at time $t = 0$ relative to a wave of frequency $\omega$ traveling at the initial beam velocity, $u_0$ (referred to as the stream wave). This is given by:

$$\Phi_0 \equiv \omega \frac{z_0}{u_0} \tag{2.6}$$

Eventually $\Phi_0$ will become our independent variable while $\Phi$ will be a dependent variable. To represent the amount of electron beam in one wavelength of the stream wave we will let $\Phi_0$ take values in the interval $[0, 2\pi]$.

Now we consider dependent variables that will describe the evolution of the electron beam fluid and describe the evolution of the circuit voltage wave. First we consider the electron beam description. The Lagrangian "position" coordinate function of a fluid element we will define as $\Phi(y, \Phi_0)$; this is the same $\Phi$ as in equation (2.5). That is, $\Phi$ in (2.5) can be viewed as a general coordinate transformation and inserting the fluid element time function, $t(z, z_0)$ into the $t$ coordinate of $\Phi$ gives $\Phi(y, \Phi_0)$ if $(z, z_0)$ is further transformed to $(y, \Phi_0)$. Note how $\Phi_0$ appears as an independent variable in $\Phi(y, \Phi_0)$ as one would expect for a Lagrangian dependent variable; this implies that different fluid elements will take different trajectories, or the fluid might stretch, squish, and/or cross over itself.

For a total specification of the fluid state we define a variable for the velocity of a fluid element. We define the velocity with respect to the moving coordinate system. That is, if a fluid element has a value of velocity equal to zero in the moving frame variable it would have a velocity of $v_0$ in the lab frame. This is accomplished by the following definition:[5]

$$\frac{\partial z(z_0, t)}{\partial t} \equiv v_0 \left[1 + C w(y, \Phi_0)\right] \tag{2.7}$$

We see again that $\Phi_0$ appears as an argument of $w(y, \Phi_0)$ as it should. Note that $\Phi(y, \Phi_0)$ and $w(y, \Phi_0)$ are total fluid functions in that they track every initial fluid

[5] In this thesis we allow the $\equiv$ symbol to implicitly define quantities on the right hand side of the expression in terms of known quantities on the left hand side of the expression.

element as parameterized by $\Phi_0$.

As a last note regarding $\Phi(y, \Phi_0)$ and $w(y, \Phi_0)$ as fluid functions notice that a fluid element's state is parameterized by space rather than time as we are used to. The effect of this is that if we fix $y$ in $\Phi$ or $w$ and vary $\Phi_0$, we get the phases and velocities of all of the elements at the specific point in space, $y$. Obviously the elements do not all occupy this point in space at the same time.

Lastly, we assume a particular form for the voltage solution. The phase of the voltage with respect to the cold circuit wave will change as the beam-wave interaction progresses and therefore we need our circuit voltage solution to model this phenomena. More specifically, we assume a voltage wave solution as a single tone traveling wave that may have $y$ dependent phase shift and substitute this form into our model equations. The components of the voltage wave are defined by:

$$V(y, \Phi) \equiv \frac{Z_0 I_0}{4C} \left[ a_1(y) \cos \Phi - a_2(y) \sin \Phi \right] \tag{2.8}$$

The relative weighting of the sine and cosine terms determines the phase of the total voltage wave. We will need evolution equations for both $a_1(y)$ and $a_2(y)$ as they both appear in (2.8). Notice the phase $\Phi$ as it appears in (2.8); along with being a traveling wave phase, if one considers $\Phi(y, \Phi_0)$ as the function ascribing a phase value, relative to the voltage wave, of a fluid element based on the fluid element's space-time coordinates, then for a given fluid element $V(y, \Phi(y, \Phi_0))$ is the voltage the fluid element sees as it passes through the interaction region.

**Transformed Equations**

We are now ready to present equations (2.1)-(2.3) written in transformed Lagrangian coordinates. There are details such as transforming the differential operators from lab coordinates to the new coordinates and assuming a Fourier series form for the charge density $\rho(y, \Phi)$ that will be skipped here but covered in detail in Chapter 3.

The transformation yields:

$$\frac{da_1(y)}{dy} = -\frac{2}{\pi}\int_0^{2\pi} \frac{\sin\Phi(y,\Phi_0)}{1+Cw(y,\Phi_0)}\, d\Phi_0 \tag{2.9}$$

$$\frac{da_2(y)}{dy} = -\frac{2}{\pi}\int_0^{2\pi} \frac{\cos\Phi(y,\Phi_0)}{1+Cw(y,\Phi_0)}\, d\Phi_0 \tag{2.10}$$

$$\begin{aligned}\frac{\partial}{\partial y}\left[1+Cw(y,\Phi_0)\right]^2 &= C\left[\left(a_1(y)+C\frac{da_2(y)}{dy}\right)\sin\Phi(y,\Phi_0)\right.\\ &\quad\left.+\left(a_2(y)-C\frac{da_1(y)}{dy}\right)\cos\Phi(y,\Phi_0)\right]\end{aligned} \tag{2.11}$$

$$\frac{\partial\Phi(y,\Phi_0)}{\partial y} = \frac{w(y,\Phi_0)}{1+Cw(y,\Phi_0)} \tag{2.12}$$

These are identical to the third set of equations in [38], namely (13′), (14′), (17′), and (20′).

If one prefers a magnitude and phase type description of the wave it can be calculated from:

$$A(y) = \frac{1}{4}\left[a_1^2(y)+a_2^2(y)\right]^{\frac{1}{2}} \tag{2.13}$$

$$\tan(-\theta(y)-by) = \frac{a_2(y)}{a_1(y)} \tag{2.14}$$

In (2.14) $\theta(y)$ is the phase of the actual wave with respect to the stream wave (which does not exist, but again is a convenient reference) and the detuning parameter $b$ is given by:

$$b \equiv \frac{u_0 - v_0}{Cu_0} \tag{2.15}$$

Equations (2.9)-(2.12) are partial integro-differential equations and indeed quite formidable. What we have gained by writing the equations in the Lagrangian form is the ability of our model to represent the beam crossover in that $\Phi(y,\Phi_0)$ is allowed to have the same value for more than one value of $\Phi_0$ (and will be seen to indeed behave in this way when results of numerical simulations are presented). This was not possible in an Eulerian analysis such as Pierce's where the dependent variables could only take on one value for a particular space-time point.

**The Small $C$ Equations**

Admittedly equations (2.9)-(2.12) are still somewhat complicated. Further, physical insight into TWT behavior on initial inspection of these equations is difficult to gain to say the least. To simplify matters we consider the "small $C$" limit of equations (2.9)-(2.12). This limit of $C$ values turns out to apply to a wide range of real devices. The result of assuming $C \ll 1$ is:

$$\frac{da_1(y)}{dy} = -\frac{2}{\pi}\int_0^{2\pi} \sin\Phi(y,\Phi_0)\; d\Phi_0 \tag{2.16}$$

$$\frac{da_2(y)}{dy} = -\frac{2}{\pi}\int_0^{2\pi} \cos\Phi(y,\Phi_0)\; d\Phi_0 \tag{2.17}$$

$$\frac{\partial w(y,\Phi_0)}{\partial y} = \frac{1}{2}\left[a_1(y)\sin\Phi(y,\Phi_0) + a_2(y)\cos\Phi(y,\Phi_0)\right] \tag{2.18}$$

$$\frac{\partial \Phi(y,\Phi_0)}{\partial y} = w(y,\Phi_0) \tag{2.19}$$

For predicting TWT performance with this model one should restrict themselves to roughly $C < 0.1$ [12].

Equations (2.16)-(2.19)[6] are the model equations we will work with throughout the remainder of the chapter. It is the simplest form of the Lagrangian equations and therefore easiest to consider for interpretations. Also, this is the most desirable starting point for analysis, again due to the system "simplicity".

### 2.1.2 Physical Interpretation of the Nordsieck Equations

It is worthwhile to consider a physical interpretation of our equations as the multitone equations which we will work with in the end have a very similar form. First we consider the motion of the electron beam in response to the wave on the

[6] These equations and variations on this theme are often referred to as the nonlinear pendulum equations. Notice that the right hand sides of equations (2.18) and (2.19) are essentially the classical pendulum equations modified by the amplitude variables on the sinusoidal terms. When one discretizes and reduces the system to a finite number of equations, $2 + 2N$, one has $N$ coupled pendula with coupling parameters $a_1(y)$ and $a_2(y)$.

circuit, then the growth of the wave due to its interactions with the electron beam. These two effects are accounted for self-consistently in (2.16)-(2.19).

**Electron Beam Response to Circuit Voltage**

The operation of the TWT requires an electron beam as a source of energy which is converted into the circuit voltage wave amplitude. The signal wave initially introduced to the circuit tends to cause a bunching of electrons in the beam which in turn induce electron bunches on the circuit with the net result being an amplified wave. We discuss how equations (2.16)-(2.19) describe the accelerations of fluid elements that leads to this bunching. First of all recall that the effect of neighboring fluid elements debunching due to space charge interaction has been neglected in this model. Techniques have been developed to account for this effect (see Rowe [49] for a complete account), but it turns out its inclusion substantially complicates matters while only improving model accuracy rather than capturing essential beam-wave interaction physics. All of the elements do however interact with each other in that they each influence the amplitude of the wave which in turn influences the individual element trajectories.

The force on an electron is due to the longitudinal fringing electric field at the center of a helical waveguide. As can be seen in equation (2.2) the force is proportional to the gradient of the circuit voltage. Equation (2.18) is this statement in the transformed coordinates. If one takes $\frac{\partial}{\partial z}$, in the new coordinates, of (2.8), one gets the right hand side of (2.11); dropping terms multiplied by $C$ we get the right hand side of (2.18). While this seems straight forward there is a subtlety involved in the interpretation. The subtlety is that fluid element trajectories are parameterized by space instead of time. Thus acceleration for all fluid elements are evaluated at the same point in space for each value of $y$, and not at instants of time. The right hand

sides of (2.18) and (2.19) being evaluated at fixed $y$ implies that differing values of $\Phi$ correspond to fluid element displacement in time.

As seen by (2.8) we can picture our voltage solution as a spatial voltage amplitude profile given by (2.13) under which a traveling wave travels. Equation (2.18) is calculating fluid acceleration at a point in space. Since the voltage is time periodic the voltage at that point in space will vary sinusoidally in time; the force a fluid element feels as it passes that point in space depends on its phase with respect to the traveling wave. Therefore, we calculate fluid acceleration by considering what the instantaneous value of the force on a fluid element will be when it arrives at point $y$ along its self-consistent trajectory.[7]

Finally, equation (2.19) is a statement of $\frac{dx}{dt} = v$ for the fluid function $\Phi$.

**Wave Growth**

Just as wave amplitude affects fluid element trajectories and thus fluid element positions at instants of time, the fluid element positions affect the growth of the voltage wave. Equations (2.16) and (2.17) determine how the voltage wave will grow based on the fluid element positions. The principle of operation for a TWT is that the formation of an electron bunch in the decelerating region of the helix electric fringing field decelerates the electrons, which thus give their energy to the radiation field. This energy exchange is manifested in a growth of the amplitude of the wave; therefore, we must investigate just how equations (2.16) and (2.17) predict this action.

Before considering equations (2.16) and (2.17), recall that in the wave equation (2.1) the second time derivative of the charge density appears on the right hand side as a source term. This term will cause $V(z,t)$ to grow in this equation, but on

[7] The word self-consistent in this context refers to the solution of the differential equations. In other words, the motion of the fluid elements influence the wave growth which in turn influences the motion of the fluid elements; the fluid element trajectories which satisfy these constraints are the self-consistent trajectories.

first inspection it might not be physically or mathematically obvious how it causes it to grow. We try to shed some light on the meaning of the wave equation and the source term. For a homogeneous wave equation (the right hand side of (2.1) equal to zero) we have that the spatial acceleration of the solution is proportional to the time acceleration of the solution. To understand what is meant by time acceleration, consider starting at a fixed point in space-time and taking a very small step in time while holding spatial position fixed. The rate at which the rate of change is changing is the time acceleration of the function. Similarly taking a small step in space and calculating the rate at which the spatial rate of change is changing measures the spatial acceleration. A solution to a homogeneous wave equation must have these accelerations proportional. We can make sense out of this by considering, for instance, a traveling pulse shape on a spring. Imagine freezing time and looking at the spatial profile of the pulse, then considering that since the pulse is traveling we may choose a point to stand in its path and let the pulse pass by us in time. We can trace out the spring height we see as a function of time and recognize that we have a scaled, reflected image of the spatial profile of the pulse (assuming no dispersion). In this way it is not hard to see that the spatial and time accelerations of the pulse must be related. Freezing time a moment while the pulse moves by you, the time acceleration you will measure in the next instant is proportional to what is spatially coming at you. Returning to the TWT and considering that the charge density in the beam will influence the growth of the voltage wave on the circuit, one can imagine that the time acceleration of the charge density at a particular point in space will contribute to the spatial acceleration of the voltage wave; the spatial acceleration of the voltage wave is the sum of the time acceleration of the voltage wave and the time acceleration of the charge density nearby.

Based on the previous paragraph we want to consider how a time acceleration of

the charge density manifests as the integrals on the right hand sides of (2.16) and (2.17). Consider sitting at a point in space and watching a charge density profile pass by. If the charge density is uniform there will be no time acceleration and therefore no source term on the right hand side of (2.1). This agrees with the notion that a properly placed bunch is required to get voltage amplitude growth. One can verify that for a uniform distribution of $\Phi$ the integrations in (2.16) and (2.17) are zero.[8] We are assuming time periodicity in our solutions for a fixed point in space so we need only consider one bunch pass by and assume that identical bunches will follow. In one period the charge bunch that passes by may have several different values of time acceleration. For example one could imagine a sharp front edge and a tapering trailing edge. A legitimate way to measure the net time acceleration of the charge density and its location with respect to the circuit wave is to integrate over one time period. This will result in a number reflecting how much net contribution to a spatially growing wave the charge density has. The assumption of periodicity (in $\Phi$ for fixed $y$) also implies that we may write a Fourier series for $\rho(y, \Phi)$ at a particular $y$. The Fourier coefficients measure this time acceleration and its placement with respect to the voltage wave by multiplying the second time derivative (acceleration) of the charge density profile by sines and cosines and integrating; this calculation manifests in the integrals in the model equations.

We now explore the integrations in equations (2.16) and (2.17) further and see that they are in line with the physical notions we expect will lead to wave growth. Based on our physical knowledge of how the device works we expect to see that beam bunching in a decelerating phase of the voltage should imply wave growth. Recall $\Phi(y, \Phi_0)$ as it appears in (2.16) and (2.17) is a function that keeps track of the beam squishing and stretching. That is, for an initially unbunched beam, $\Phi(0, \Phi_0)$ is

[8] For a uniform distribution the graph of $\Phi(0, \Phi_0)$ vs. $\Phi_0$ is a line of slope 1, and $\int_0^{2\pi} \sin \Phi(0, \Phi_0) d\Phi_0 = \int_0^{2\pi} \cos \Phi(0, \Phi_0) d\Phi_0 = 0$.

straight line of slope 1 and as $y$ evolves the straight line distorts to reflect bunching or stretching in time for a fixed point in space. For bunching, two initial values of $\Phi_0$ that were a certain distance apart will become closer together (the graph of $\Phi(y^*, \Phi_0)$, where $y^* = \text{const.}$, will become flatter in this region) where for beam stretching the same two initial values will spread out (the graph of $\Phi(y^*, \Phi_0)$ will become steeper in this region). See Section 2.1.4, Figure 2.5 for simulated results of this phenomena. Also recall that our wave is postulated as the combination of a sine term and a cosine term; equation (2.16) computes the evolution of the cosine term and (2.17) calculates the evolution of the sine term. If, for example, the amplitude of the cosine term is to grow at some point $y = y^*$ we would expect the beam to be bunched in the decelerating phase of the cosine wave (i.e. a flatness in the graph of $\Phi(y^*, \Phi_0)$ in the interval $\pi \leq \Phi(y^*, \Phi_0) \leq 2\pi$, $0 \leq \Phi_0 \leq 2\pi$). For this to happen $\Phi(y^*, \Phi_0)$ must have form such that the integral of the sine of $\Phi(y^*, \Phi_0)$ is less than zero and after multiplication by $-\frac{2}{\pi}$ we have $\frac{da_1(y^*)}{dy} > 0$ or net growth for the particular value of $y^*$. We should expect the sine function in the integrand for $a_1$ since if, for example, $\Phi(\cdot, \cdot) = \frac{3\pi}{2}$ then we expect a growth type contribution to the cosine wave amplitude $a_1(\cdot)$, and need to take the sine of the position to get a nonzero contribution. Similarly the growth of the sine wave amplitude is determined by integration of $\Phi(y, \Phi_0)$ as an argument of the cosine function.

Only one integral appears on the right hand side of both (2.16) and (2.17) because we have restricted contributions to the growth of the voltage to be only due to the fundamental frequency component of the charge density. If we wanted to account for contributions by other harmonic frequencies we would need to know the frequency dependence of the circuit impedance $Z_0(\omega)$ and would require an additional integral term on the right hand side of (2.16) and (2.17) per harmonic frequency included.

### 2.1.3 Development of Discretized Nordsieck Small $C$ Model

We have now completed the presentation of the Nordsieck model along with enough information to develop a reasonable understanding of the physics of the interaction. At this point we consider a further mathematical analysis of the model focusing primarily on the Hamiltonian structure in the equations. As it turns out the discretized model for the TWT is identical to a model describing a high gain FEL [8]. In this section we present the discretization and associated notation, present a Hamiltonian formulation of the discretized model, and formulate the Hamiltonian model in the electron beam reference frame.

#### Discretized Model

Equations (2.16)-(2.19) are partial integro-differential equations that model the TWT interaction. In general finite dimensional[9] ordinary differential equations are easier to work with. We have stated previously that breaking the electron beam into a finite number of chunks will allow us to write our model as a system of ordinary differential equations. We perform the discretization here.

In the fluid picture of the electron beam the function $\Phi(y, \Phi_0)$ is parameterized by a continuum of values of $\Phi_0$ in the interval $[0, 2\pi]$. We shall now consider that there are only a finite number, $N$, of initial values of phase, or $N$ "disks". Each of these initial conditions then will be tracked through the interaction. Therefore, instead of writing $\Phi(y, \Phi_0)$ we will write $\Phi_j(y)$ where the subscript $j$ indicates we are considering the phase of the particle corresponding to the $j^{\text{th}}$ initial condition at spatial position $y$. The value of the $j^{\text{th}}$ initial phase is $\Phi_j(0)$. We treat the velocity

[9] Partial differential equations can be considered infinite in dimension in that one of the independent variables of the solution parameterizes a function in the other variable. The function belongs to a vector space that requires an infinite number of basis vectors to represent the function. Similarly, ordinary differential equations are finite in dimension since the variable of integration parameterizes a solution curve in a finite dimensional vector space.

variable similarly and $w(y, \Phi_0) \to w_j(y)$ with initial value of the $j^{\text{th}}$ velocity written as $w_j(0)$. The variables $a_1(y)$ and $a_2(y)$ do not change as they were functions of only one variable to begin with.

We now present equations (2.16) and (2.17) in discretized form making the following notes: the integrals in equations (2.16) and (2.17) become sums; the equations for the phase and velocity variables are each $N$ in number. The overdot represents differentiation with respect to $y$ and the functional dependence on $y$ is not explicitly shown.

$$\dot{a}_1 = -\frac{4}{N}\sum_{j=1}^{N}\sin\Phi_j \tag{2.20}$$

$$\dot{a}_2 = -\frac{4}{N}\sum_{j=1}^{N}\cos\Phi_j \tag{2.21}$$

$$\dot{w}_j = \frac{1}{2}\left[a_1\sin\Phi_j + a_2\cos\Phi_j\right] \qquad j = 1,\ldots,N \tag{2.22}$$

$$\dot{\Phi}_j = w_j \qquad j = 1,\ldots,N \tag{2.23}$$

This form of the TWT model is nearly identical to the model for a high gain FEL[10] as given in [8]. In [8] the equations are written slightly differently in that the wave amplitudes are combined into one complex variable; see Section B.1.1 in Appendix B for our model in a form similar to [8]. If one desires our model to be exactly that of [8] one must assume a voltage solution of the form (A.2) whereas we have presented the results of Nordsieck's choice (A.1).

### Hamiltonian Formulation of Discretized Model

Equations (2.20)-(2.23) can be derived from a Hamiltonian function, but $a_1$ and $a_2$ are not symplectic variables.[11] See B.1.1 for a Hamiltonian and modifications that

[10] It is also interesting that an earlier incarnation of the FEL equations were determined by the authors of [8] to be the same equations that model an array of Josephson Junctions [7].

[11] For an undergraduate introduction to Hamiltonian systems see [6]. One of the classic graduate level references covering the topic is [27]. A fairly accessible overview to the mathematics of Hamil-

need to be made to the equations of motion to generate (2.20)-(2.23). For symplectic variables we make the following transformation:

$$\Phi_0 \equiv \sqrt{\frac{N}{8}}\, a_1 \tag{2.24}$$

$$w_0 \equiv \sqrt{\frac{N}{8}}\, a_2 \tag{2.25}$$

We emphasize that $\Phi_0$ in (2.24) is not the same $\Phi_0$ that was used in the Nordsieck partial differential equation model. Substituting (2.24) and (2.25) into equations (2.20)-(2.23) results in the following equations:

$$\dot{w}_0 = -\sqrt{\frac{2}{N}} \sum_{j=1}^{N} \cos \Phi_j \tag{2.26}$$

$$\dot{\Phi}_0 = -\sqrt{\frac{2}{N}} \sum_{j=1}^{N} \sin \Phi_j \tag{2.27}$$

$$\dot{w}_j = \sqrt{\frac{2}{N}} \left[\Phi_0 \sin \Phi_j + w_0 \cos \Phi_j\right] \qquad j = 1, \ldots, N \tag{2.28}$$

$$\dot{\Phi}_j = w_j \qquad j = 1, \ldots, N \tag{2.29}$$

These equations can be generated from the Hamiltonian system:

$$H = \sum_{j=1}^{N} \frac{{w_j}^2}{2} + \sqrt{\frac{2}{N}} \left[\Phi_0 \sum_{j=1}^{N} \cos \Phi_j - w_0 \sum_{j=1}^{N} \sin \Phi_j\right] \tag{2.30}$$

$$\dot{\Phi}_i = \frac{\partial H}{\partial w_i} \qquad i = 0, \ldots, N \tag{2.31}$$

$$\dot{w}_i = -\frac{\partial H}{\partial \Phi_i} \qquad i = 0, \ldots, N \tag{2.32}$$

The index $i$ runs from 0 to $N$ with the equations for $i = 0$ that of the voltage components as defined in (2.24) and (2.25).

tonian systems for the non-mathematician is given in [34]. Sophisticated mathematical treatments are given in [1, 5].

**Transformation to Beam Reference Frame**

There are no known analytical solutions to equations (2.26)-(2.29). To make progress in an analysis we will use techniques from dynamical systems theory. Typically the first step in the analysis of a nonlinear system is a local investigation about the fixed point(s) of the system. For an undergraduate level introduction to dynamical systems theory see [54]. More advanced treatments can be found in [28, 30, 43, 48].

We physically motivate a fixed point of our system and then express it mathematically. Consider the initial condition in which there are $N$ disks uniformly distributed in space each having initial velocity $u_0$. Also consider the initial value of the voltage to be vanishingly small or zero, which will therefore have no forcing effect on the $N$ disks. The $N$ disks will then continue to propagate and because of their even distribution induce no voltage on the circuit. This condition is obviously a steady state and in fact a fixed point of the system.

To see that it is a fixed point we must consider the reference frame in which the formulation is written. Consider sitting in either the lab frame or the initial circuit velocity frame when the initial circuit velocity and initial beam velocity are not equal; the velocities of the electrons are not changing as a fixed point would require, but their positions are. The voltage is not changing as it requires some uneven distribution of particle phases to start the interaction process. The proper reference frame to manifest a fixed point is therefore the frame moving with the initial velocity of the electrons. In this frame the positions of the electrons are not changing, nor are their velocities, nor is the amplitude of the radiation field.[12] It is therefore desired to transform our model into this reference frame. Recall that our current

[12] No mention of the stability of this fixed point is being made. Loosely speaking, stability of the fixed point refers to whether solutions starting nearby will tend towards the point or away from the point. The determination of stability is in fact one of the questions the tools will address. Physically one would expect the point to be unstable as perturbation of the radiation field away from zero would initialize the growth phenomenon that the TWT relies upon for its operation.

formulation is in the reference frame which is traveling with respect to the lab frame at $v_0$, the cold circuit velocity, which may be different than the initial velocity of the beam electrons, $u_0$.

In transforming to the beam reference frame we define new variables. The velocity and phase of electrons will be given by $\Gamma_j$ and $\psi_j$ respectively, and the voltage terms will be given by $\psi_0$ and $\Gamma_0$. The transformation is Galilean where the variables are related by:

$$\psi_0 \equiv \Phi_0 \cos by - w_0 \sin by \tag{2.33}$$

$$\Gamma_0 \equiv \Phi_0 \sin by + w_0 \cos by \tag{2.34}$$

$$\psi_j \equiv \Phi_j - by \qquad j = 1, \ldots, N \tag{2.35}$$

$$\Gamma_j \equiv w_j - b \qquad j = 1, \ldots, N \tag{2.36}$$

Making substitutions the system becomes:[13]

$$\dot{\Gamma}_0 = -\sqrt{\frac{2}{N}} \sum_{j=1}^{N} \cos \psi_j + b\psi_0 \tag{2.37}$$

$$\dot{\psi}_0 = -\sqrt{\frac{2}{N}} \sum_{j=1}^{N} \sin \psi_j - b\Gamma_0 \tag{2.38}$$

$$\dot{\Gamma}_j = \sqrt{\frac{2}{N}} \left[\psi_0 \sin \psi_j + \Gamma_0 \cos \psi_j\right] \qquad j = 1, \ldots, N \tag{2.39}$$

$$\dot{\psi}_j = \Gamma_j \qquad j = 1, \ldots, N \tag{2.40}$$

The Hamiltonian is:

$$H = \sum_{j=1}^{N} \frac{\Gamma_j^2}{2} + \sqrt{\frac{2}{N}} \left[\psi_0 \sum_{j=1}^{N} \cos \psi_j - \Gamma_0 \sum_{j=1}^{N} \sin \psi_j\right] - \frac{b}{2}\left(\psi_0^2 + \Gamma_0^2\right) \tag{2.41}$$

The equations are generated by:

$$\dot{\psi}_i = \frac{\partial H}{\partial \Gamma_i} \qquad i = 0, \ldots, N \tag{2.42}$$

[13] Although the voltage term transforms are written as sums of sines and cosines in (2.33) and (2.34) the transformations are more conveniently done using complex exponentials and identities in Appendix A. Equations (2.33) and (2.34) are derived from the complex variable transformation $\psi_0 + i\Gamma_0 \equiv (\Phi_0 + iw_0)\, e^{iby}$.

$$\dot{\Gamma}_i = -\frac{\partial H}{\partial \psi_i} \qquad i = 0, \ldots, N \tag{2.43}$$

Note that due to the reference frame transformation, the Hamiltonian is not simply attained by substitution of the transformations (2.33)-(2.36) into (2.30). For details on changing reference frames of Hamiltonians see for example [42].

We will use equations (2.37)-(2.40) for analysis and equations (2.26)-(2.29) for numerical solutions.

#### Conserved Quantities

With the Hamiltonian formulation just presented this is an appropriate place to mention conserved quantities of the system. In addition to the obvious conserved quantity of the Hamiltonian, one other conserved quantity has been identified in the FEL work [8]. Following [8] we define the conserved quantity as:

$$\Delta_{\text{st}} \equiv \sum_{j=1}^{N} \Gamma_j + \frac{1}{2}\left(\psi_0^2 + \Gamma_0^2\right) \tag{2.44}$$

See B.1.3 in Appendix B for equations (2.37)-(2.44) in complex form.

### 2.1.4 Numerical Solution to Equations

#### Defining the Numerical Problem

As a final step in the model presentation and interpretation we consider a numerical example. Before presenting the example there are several items worthy of mention regarding the simulation of the equations. First, we emphasize that the equations that will be numerically integrated are the discretized Hamiltonian equations in (2.26)-(2.29). The equations in (2.26)-(2.29) are ordinary differential equations and we will use standard ordinary differential equation integration techniques. The problem we will be solving is an initial value problem, where the initial values we

specify are the voltage amplitude components, the initial phases of the disks, and the initial velocities of the disks.

### Integration Methods and Stiffness

Among the issues involved with numerical integration is the determination of whether or not the system in question is "stiff" [23, 32, 46]. Loosely speaking, a system is stiff if state variables are changing on largely disparate time[14] scales. The most common implication of having a stiff system is that explicit methods like fourth-order Runge-Kutta are not reliable. Equations (2.26)-(2.29) are indeed stiff.

To determine stiffness of a nonlinear system of equations one looks at the linearization of the system. In particular, the eigenvalues of the Jacobian matrix are a measure of the time scales of the system, and therefore comparing magnitudes of the most disparate eigenvalues one can determine whether the system is stiff. Furthermore, one can perform this calculation along the solution to see if the stiffness property changes as the trajectory moves through state space. We have performed computations along the trajectory and found the system is stiff for roughly one third of the distance to saturation (for the parameters in Table 2.1). We will not present the results of our computations here, but one may see Section 2.2.2 for the Jacobian matrix with which we tested for stiffness.

Commonly, alternative integration algorithms are required for stiff systems. Interestingly, stiffness is more of a concern for stable systems ([32], pg. 268). Our system is inherently unstable, as will be shown and discussed in more detail in Section 2.2.2, so we might guess that the stiffness may not be a great concern for us. Indeed integrating the system using algorithms for stiff equations one sees that the Bulirsch-Stoer, Rosenbrock, and fourth-order Runge-Kutta algorithms, all with adap-

[14] Actually, the word "time" refers to the variable of integration, which is in our case length.

| Parameter | Value |
|---|---|
| $b$ | 1.0 |
| $N$ | 28 |
| $a_1(0)$ | 0.001 |
| $a_2(0)$ | 0.0 |
| $w_j(0)$ | 1.0 |
| $\Phi_j(0)$ | $2\pi(j-1)/N$ |

Table 2.1: Simulation parameters and initial data for presented results. The values for $w_0$ and $\Phi_0$ are obtained from (2.24) and (2.25). For $w_j(0)$ and $\Phi_j(0)$ $j$ takes on values $1, \ldots, N$.

tive stepsize,[15] produce similar results with the major difference being computation time. Unfortunately one method is not always faster than the others so each initial condition must be tested with all of the methods to determine the fastest one.

**Simulations**

We now present the results of integrating equations (2.26)-(2.29) for one set of parameters and initial conditions. The parameter values and initial conditions are listed in Table 2.1. In Figure 2.1 we plot normalized amplitude $A(y)$ from equation (2.13) in which we used (2.24) and (2.25). In Figure 2.2 we plot phase $\theta(y)$ from equation (2.14). In Figure 2.3 we plot the functions $w_0(y)$ and $\Phi_0(y)$. In Figure 2.4 we plot what could be considered representative electron phase trajectories as a function of distance.[16] In Figure 2.5 we plot the approximate fluid function $\Phi(y, \Phi_0)$ as constructed from $\Phi_j(y)$. Note that in $\Phi(y, \Phi_0)$ the argument $\Phi_0$ is not the wave amplitude $\Phi_0(y)$. Also note that the simulation parameters are different for this graph so the features are better seen: the differences from Table 2.1 are $b = 0$ and $N = 100$.

[15] All of the algorithms are taken from [46].

[16] Note that these are not position vs. time trajectories as one is accustomed to considering. Rather, following an electron down the interaction region, the functions give the particle's phase with respect to the cold circuit wave at each value of space, $y$.

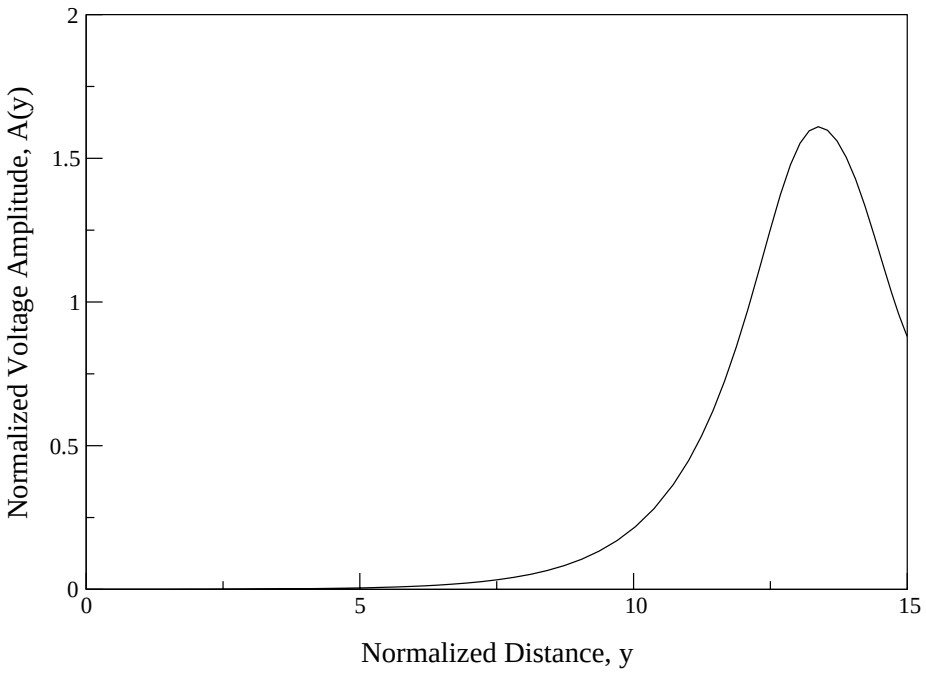


Figure 2.1: Normalized amplitude, $A(y)$, as in (2.13) versus normalized distance $y$.

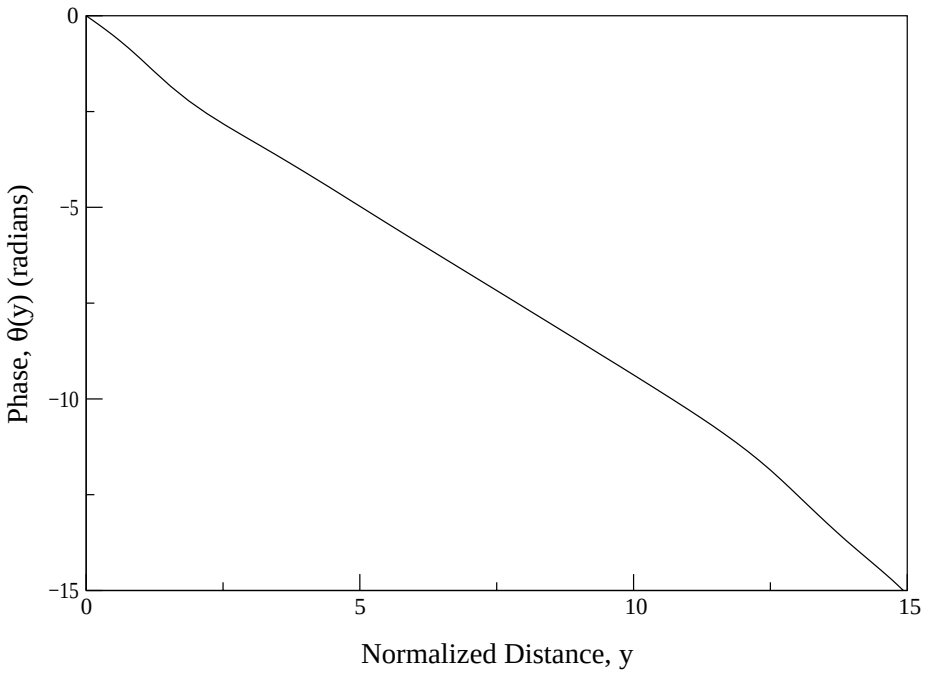


Figure 2.2: Phase, $\theta(y)$, as in (2.14) versus normalized distance $y$.

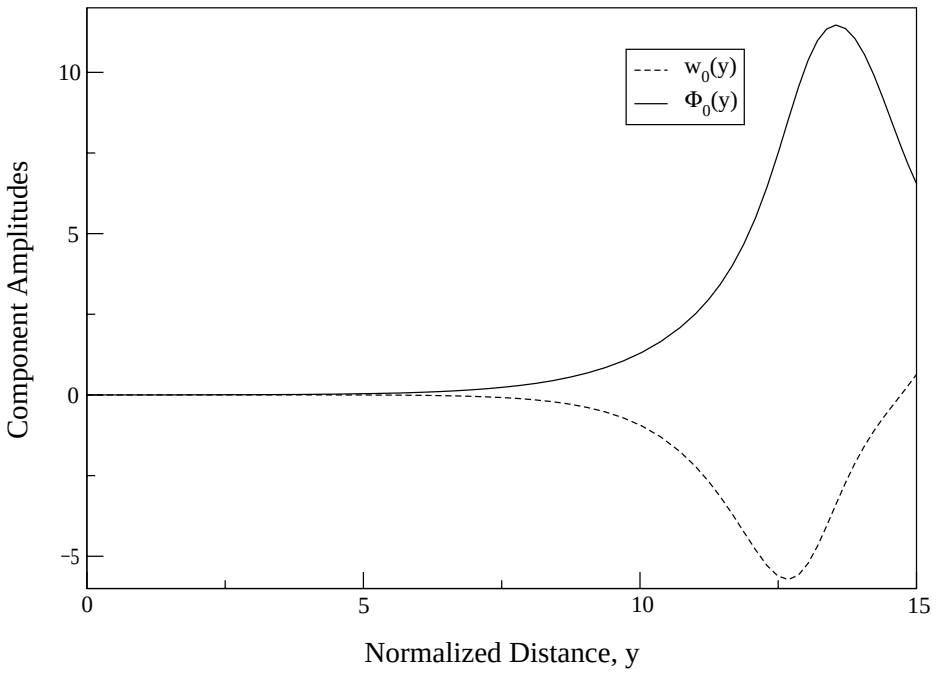


Figure 2.3: Hamiltonian amplitudes, $w_0$ and $\Phi_0$, versus normalized distance $y$.

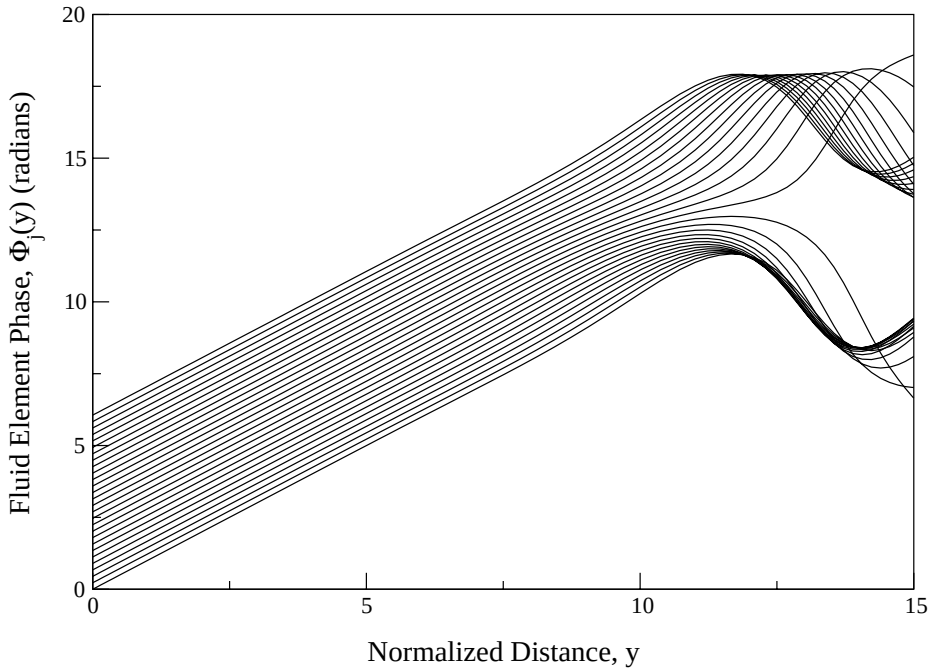


Figure 2.4: Fluid element phases, $\Phi_j(y)$, versus normalized distance $y$.

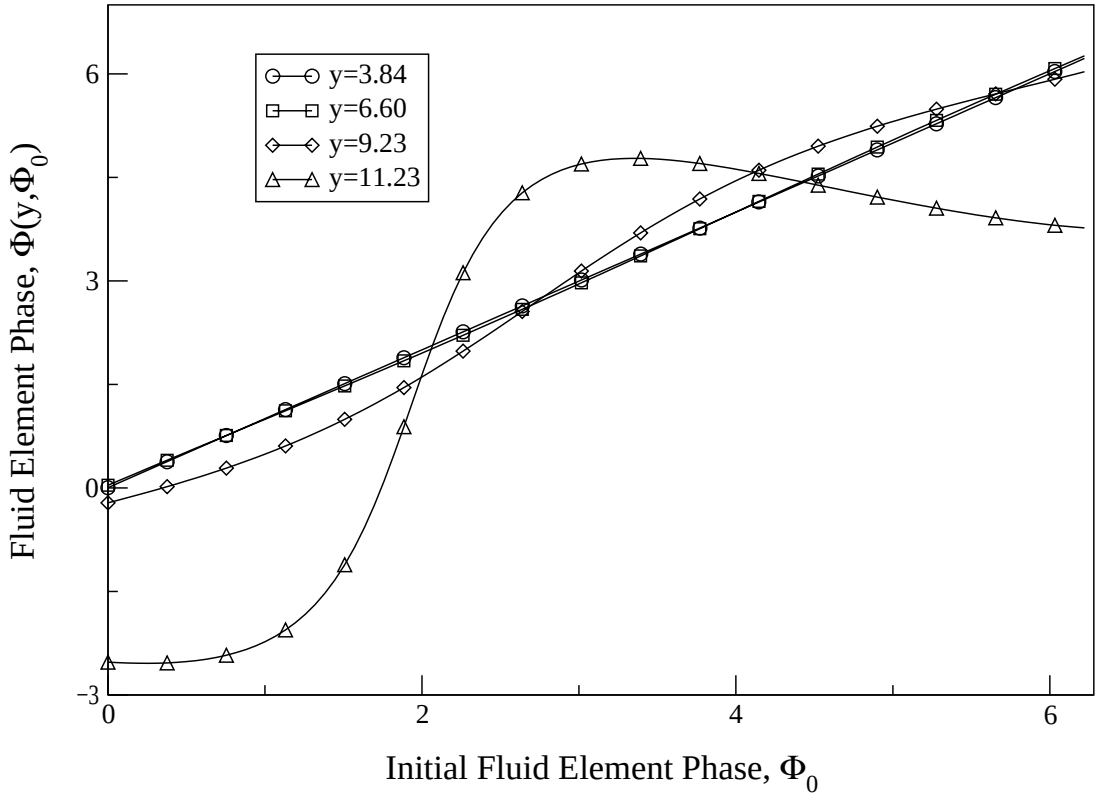


Figure 2.5: Approximate fluid function, $\Phi(y, \Phi_0)$, evaluated at four different $y$ values. Note that the lines in this figure are meant to represent the fluid quantity $\Phi(y, \Phi_0)$, for different values of $y$. In fact the figure is generated with the discretized model and are merely representing the result as a fluid quantity using curve fitting between the data points. Simulation parameters are same as in Table 2.1 except for $b = 0$ and $N = 100$.

General points to note include the saturation in Figure 2.1, fluid element crossover in Figure 2.4, and evolution of the fluid function in Figure 2.5 as discussed in Section 2.1.2.

There is one subtlety with regards to simulating equations (2.26)-(2.29) for varying detuning parameters. To be consistent with a choice of $b \neq 0$ the initial velocities must also be initialized to this value of $b$. The motivation being that if one chooses $b \neq 0$ then by definition (2.15) we have $u_0 \neq v_0$; since $w_j(0)$ should be proportional to the difference between $u_0$ and $v_0$ we see that setting $w_j(0) = 0$ makes no physical sense. Rearranging (2.7) and (2.15) one can convince oneself further that the normalized variables $b$ and $w_j(0)$ are of the same "units".

## 2.2 Equilibrium and Linearization

As discussed in Section 2.1.3 we have identified an equilibrium of the discretized single tone traveling wave tube model formulated in the electron beam frame. In this section we first identify this equilibrium point of the discretized system. Next, we do a linearization about that point and inspect the eigenvalue spectrum of the linearization. Finally, we linearize by an alternate method known as the method of collective variables.

### 2.2.1 Identification of an Equilibrium

Recall that our equilibrium condition is that of a monoenergetic electron beam evenly distributed over one period of the stream wave, with the circuit voltage amplitude zero. To mathematically realize this condition for arbitrary values of $b$ we need to consider equations (2.37)-(2.40).[17] An equilibrium point for a system of or-

[17] There is an equilibrium condition for equations (2.26)-(2.29) but it is not consistent with our variable definitions when $b \neq 0$. The condition requires $w_j(0) = 0$ for all $j$, but recall from 2.1.4 that to be consistent with our definitions the initial values of $w_j$ have to equal $b$.

dinary differential equations is realized when the right hand side is zero for all of the equations. At the equilibrium point the derivative of the solution is zero; the solution does not change for a changing integration variable. It is clear that setting $\Gamma_j(0) = 0$ implies the right hand side of (2.40) is zero. Setting $\psi_0(0) = \Gamma_0(0) = 0$ implies the right hand side of (2.39) and the last terms on the right hand sides of (2.37) and (2.38) are zero. What is left is to ensure that the sums of the sines and cosines in (2.37) and (2.38) are zero. This is readily accomplished by requiring the initial phases of the electron disks be evenly distributed over $2\pi$ as we expect from the physical idea of a uniformly distributed beam.

The equilibrium discussed above is not unique, and in fact there are several equilibria that can be identified. As discussed, what is required for a point to be an equilibrium point is that the sums of sines and cosines in (2.37) and (2.38) are zero, in addition to the voltage amplitudes and velocities being zero. Thus to identify alternative equilibrium points we search for phase distributions with (2.37) and (2.38) zero. For example, if we take an even number of disks, set half of the disk phases to $\psi_j = 0$ and the other half to $\psi_j = \pi$, one can check that the sums are zero. Similarly, setting half of the disk phases to $\psi_j = \frac{\pi}{2}$, and the other half to $\psi_j = \frac{3\pi}{2}$ corresponds to an equilibrium point also. These distributions are not physically interesting and hence we will not analyze them.

### 2.2.2 Linearization of Hamiltonian System

With the physically interesting equilibrium identified we next look at how the system behaves for state space points very near to the equilibrium point. Specifically we would like to know if an initial condition near the equilibrium tends towards the equilibrium, away from the equilibrium, circles around the equilibrium, or some combination of these options. The simplest form of this question regards stability [10]:

whether a point tends towards or away from the equilibrium. To determine stability we consider eigenvalues of the linearization.

The linearization of equations (2.37)-(2.40) is written as:

$$\dot{\delta\mathbf{x}} = \mathbf{Df}|_{\mathbf{x_0}}\delta\mathbf{x} \tag{2.45}$$

We define the vectors $\mathbf{x} \equiv [\Gamma_0\ \psi_0\ \Gamma_1 \ldots \Gamma_N\ \psi_1 \ldots \psi_N]^{\mathrm{T}}$ and $\delta\mathbf{x} \equiv \mathbf{x} - \mathbf{x_0}$ where $\mathbf{x_0}$ is the point about which we linearize, and the superscript T indicates transpose. The vector function $\mathbf{f}(\mathbf{x})$ is obtained from the right hand side of (2.37)-(2.40), and $\mathbf{Df}|_{\mathbf{x_0}}$ is the Jacobian matrix of $\mathbf{f}(\mathbf{x})$ evaluated at the point $\mathbf{x_0}$. For our system the Jacobian has the following structure:

$$\mathbf{Df} = \left[\begin{array}{c|c|c} \mathbf{A_{st}} & \mathbf{B_{st}} & \mathbf{C_{st}} \\ \hline \mathbf{D_{st}} & \mathbf{E_{st}} & \mathbf{F_{st}} \\ \hline \mathbf{G_{st}} & \mathbf{H_{st}} & \mathbf{K_{st}} \end{array}\right] \qquad (2N+2)\times(2N+2) \tag{2.46}$$

The blocks in (2.46) are given by:

$$\mathbf{A_{st}} = \begin{bmatrix} 0 & b \\ -b & 0 \end{bmatrix} \tag{2.47}$$

$$\mathbf{B_{st}} = [\mathbf{0}] \qquad 2\times N \tag{2.48}$$

$$\mathbf{C_{st}} = \begin{bmatrix} \sqrt{\frac{2}{N}}\sin\psi_1 & \cdots & \sqrt{\frac{2}{N}}\sin\psi_N \\ -\sqrt{\frac{2}{N}}\cos\psi_1 & \cdots & -\sqrt{\frac{2}{N}}\cos\psi_N \end{bmatrix} \qquad 2\times N \tag{2.49}$$

$$\mathbf{D_{st}} = \begin{bmatrix} \sqrt{\frac{2}{N}}\cos\psi_1 & \sqrt{\frac{2}{N}}\sin\psi_1 \\ \vdots & \vdots \\ \sqrt{\frac{2}{N}}\cos\psi_N & \sqrt{\frac{2}{N}}\sin\psi_N \end{bmatrix} \qquad N\times 2 \tag{2.50}$$

$$\mathbf{E_{st}} = [\mathbf{0}] \qquad N\times N \tag{2.51}$$

$$\mathbf{F_{st}} = \begin{bmatrix} \sqrt{\frac{2}{N}}\left[\psi_0 \cos\psi_1 - \Gamma_0 \sin\psi_1\right] & 0 & \cdots & 0 \\ 0 & \sqrt{\frac{2}{N}}\left[\psi_0 \cos\psi_2 - \Gamma_0 \sin\psi_2\right] & \cdots & 0 \\ \vdots & & \ddots & \vdots \\ 0 & 0 & \cdots & \sqrt{\frac{2}{N}}\left[\psi_0 \cos\psi_N - \Gamma_0 \sin\psi_N\right] \end{bmatrix} \qquad N \times N \tag{2.52}$$

$$\mathbf{G_{st}} = [\mathbf{0}] \qquad N \times 2 \tag{2.53}$$

$$\mathbf{H_{st}} = \begin{bmatrix} 1 & 0 & \cdots & 0 \\ 0 & 1 & \cdots & 0 \\ \vdots & & \ddots & \vdots \\ 0 & 0 & \cdots & 1 \end{bmatrix} \qquad N \times N \tag{2.54}$$

$$\mathbf{K_{st}} = [\mathbf{0}] \qquad N \times N \tag{2.55}$$

Equations (2.48), (2.51), (2.53), and (2.55) are zero matrices of the indicated dimensions.

For our analysis we evaluate (2.46) at the fixed point which results in the linear system in (2.45). The eigenvalues of $\mathbf{Df}|_{\mathbf{x_0}}$ indicate how the system behaves near the equilibrium.[18] Specifically, if there are any eigenvalues with real part greater than zero the equilibrium point is unstable. The eigenvector associated with the unstable eigenvalues gives the direction in the state space in which the solution grows. There

[18] See any of [54, 28, 30, 43, 48] to see why this is so.

are similar conclusions that can be drawn if eigenvalues have either negative real part or zero real part, but we shall not discuss them here.

For general qualitative behavior of equations (2.37)-(2.40) near the equilibrium we present the computation of the spectrum of $\mathbf{Df}|_{\mathbf{x_0}}$ with $b = 1.0$ and six electron disks. As $\mathbf{Df}|_{\mathbf{x_0}}$ has nontrivial Jordan form [9] we present the Jordan matrix and eigenvectors below. The structure of the Jordan matrix is:

$$\mathbf{J} = \begin{bmatrix} \mathbf{J_1} & & & & & \\ & \mathbf{J_2} & & & & \\ & & \mathbf{J_3} & & & \\ & & & \mathbf{J_4} & & \\ & & & & \mathbf{J_5} & \end{bmatrix} \tag{2.56}$$

Everything in $\mathbf{J}$ that is not in one of the blocks is understood to be zero. The first block has the nondegenerate eigenvalues; the block is:

$$\mathbf{J_1} = \begin{bmatrix} i0.755 & 0 & 0 & 0 & 0 & 0 \\ 0 & -i0.755 & 0 & 0 & 0 & 0 \\ 0 & 0 & 0.745-i0.877 & 0 & 0 & 0 \\ 0 & 0 & 0 & -0.745+i0.877 & 0 & 0 \\ 0 & 0 & 0 & 0 & 0.745+i0.877 & 0 \\ 0 & 0 & 0 & 0 & 0 & -0.745-i0.877 \end{bmatrix} \tag{2.57}$$

The eigenvectors ($\mathbf{v}_\lambda$) associated with the eigenvalues ($\lambda$) in (2.57) are given in (2.58) -

(2.59). The components of the vectors are given in $\mathbf{v}$.

$$\mathbf{v}=\begin{bmatrix}\Gamma_0\\ \psi_0\\ \Gamma_1\\ \Gamma_2\\ \Gamma_3\\ \Gamma_4\\ \Gamma_5\\ \Gamma_6\\ \psi_1\\ \psi_2\\ \psi_3\\ \psi_4\\ \psi_5\\ \psi_6\end{bmatrix} \quad \lambda=\pm i0.755 \qquad \mathbf{v}_\lambda=\begin{bmatrix}0.293\\ \mp i0.293\\ \mp i0.224\\ -0.194\mp i0.112\\ -0.194\pm i0.112\\ \pm i0.224\\ 0.194\pm i0.112\\ 0.194\mp i0.112\\ -0.297\\ -0.148\pm i0.257\\ 0.148\pm i0.257\\ 0.297\\ 0.148\mp i0.257\\ -0.148\mp i0.257\end{bmatrix} \tag{2.58}$$

$$\lambda{=}0.745{\pm}i0.877 \qquad \mathbf{v}_\lambda{=}\begin{bmatrix} -0.188{\pm}i0.424 \\ -0.424{\mp}i0.188 \\ 0.101{\pm}i0.210 \\ -0.131{\pm}i0.192 \\ -0.232{\mp}i0.017 \\ -0.101{\mp}i0.210 \\ 0.131{\mp}i0.192 \\ 0.232{\pm}i0.017 \\ 0.196{\pm}i0.051 \\ 0.054{\pm}i0.195 \\ -0.142{\pm}i0.144 \\ -0.196{\mp}i0.051 \\ -0.054{\mp}i0.195 \\ 0.142{\mp}i0.144 \end{bmatrix} \qquad \lambda{=}-0.745{\pm}i0.877 \qquad \mathbf{v}_\lambda{=}\begin{bmatrix} -0.424{\pm}i0.188 \\ -0.188{\mp}i0.424 \\ 0.209{\pm}i0.101 \\ 0.017{\pm}i0.232 \\ -0.192{\pm}i0.131 \\ -0.209{\mp}i0.101 \\ -0.017{\mp}i0.232 \\ 0.192{\mp}i0.131 \\ -0.051{\mp}i0.196 \\ 0.144{\mp}i0.142 \\ 0.195{\pm}i0.054 \\ 0.051{\pm}i0.196 \\ -0.144{\pm}i0.142 \\ -0.195{\mp}i0.054 \end{bmatrix} \tag{2.59}$$

The remaining Jordan blocks, $\mathbf{J_2}$ through $\mathbf{J_5}$, are identical to each other:

$$\mathbf{J_2} = \mathbf{J_3} = \mathbf{J_4} = \mathbf{J_5} = \begin{bmatrix} 0 & 1 \\ 0 & 0 \end{bmatrix} \tag{2.60}$$

With each of these blocks is associated an eigenvector and a generalized eigenvector.

We provide only the four eigenvectors here:

$$\begin{bmatrix} 0 \\ 0 \\ 0 \\ 0 \\ 0 \\ 0 \\ 0 \\ 0 \\ 0 \\ 1.0 \\ 0 \\ 0.3802 \\ 0.9249 \\ 0 \\ 0 \end{bmatrix} \begin{bmatrix} 0 \\ 0 \\ 0 \\ 0 \\ 0 \\ 0 \\ 0 \\ 0 \\ 0 \\ 0 \\ 1.0 \\ 0.9249 \\ -0.3802 \\ 0 \\ 0 \end{bmatrix} \begin{bmatrix} 0 \\ 0 \\ 0 \\ 0 \\ 0 \\ 0 \\ 0 \\ 0 \\ 0 \\ 0 \\ 0 \\ 0 \\ 0 \\ 1 \\ 0 \end{bmatrix} \begin{bmatrix} 0 \\ 0 \\ 0 \\ 0 \\ 0 \\ 0 \\ 0 \\ 0 \\ 0 \\ 0 \\ 0 \\ 0 \\ 0 \\ 0 \\ 1 \end{bmatrix} \tag{2.61}$$

From the results notice how eigenvalues with real part greater than zero have eigenvector components along the $\Gamma_0$ and $\psi_0$ directions, implying that these are unstable directions in the state space. We have observed that the real parts of the eigenvalues with real part greater than zero remain unchanged for increasing the number of disks up to 20 disks. It is conjectured that these values do not change for an arbitrary number of disks. Also notice that the eigenvalues are symmetric about the real and imaginary axis of the complex plane; this is expected because the system is Hamiltonian [13, pg. 36].

Finally we note that $b$ has a radical effect on the eigenstructure of the linear system. In particular a bifurcation occurs with changing $b$; for $b \geq 1.89$ the TWT collective interaction fails to occur. That is, for $b \geq 1.89$ the uniform beam fixed

point becomes stable against small perturbations. One way this can be seen is by how $b$ appears in the calculation of the eigenvalues. We will discover an alternative method for arriving at this bifurcating $b$ value in the next section.

### 2.2.3 Linearization by Method of Collective Variables

The final bit of analysis we do on the single tone system (2.37)-(2.40) is another linearization about the equilibrium point. The method is inspired by the work done by Casagrande *et al.* on FELs [8] in which new variables are defined by taking moments of the discretized equations. Interestingly, the result of this calculation produces the same cubic equation for linear growth rates as an Eulerian analysis of a TWT. Furthermore, the value of detuning above which the collective interaction takes place is found to be this value of $b \approx 1.89$. We present the analysis and resulting cubic equation.

The first collective variable we define is a complex bunching parameter given by:

$$\mathcal{B} \equiv -\sqrt{\frac{2}{N}} \sum_{j=1}^{N} [\cos\psi_j + i \sin\psi_j] \tag{2.62}$$

The parameter $\mathcal{B}$ measures bunching of the particle phases with respect to sine and cosine waves. Furthermore, we define the amplitude variable:

$$\Xi = \Gamma_0 + i\psi_0 \tag{2.63}$$

With this definition and the definition in (2.62) we may write equations (2.37) and (2.38) as:

$$\dot{\Xi} = \mathcal{B} - ib\Xi \tag{2.64}$$

Next we desire a differential equation for $\mathcal{B}$. We obtain this by differentiating the definition in (2.62). The differentiation results in:

$$\dot{\mathcal{B}} = -i\sqrt{\frac{2}{N}} \sum_{j=1}^{N} \Gamma_j e^{i\psi_j} \tag{2.65}$$

In (2.65) we have used (2.40). We now define another variable based on (2.65).

$$\mathcal{P} \equiv -\sqrt{\frac{2}{N}} \sum_{j=1}^{N} \Gamma_j e^{i\psi_j} \tag{2.66}$$

With this definition we may write the differential equation for $\mathcal{B}$ as:

$$\dot{\mathcal{B}} = i\mathcal{P} \tag{2.67}$$

Finally, we desire a differential equation for $\mathcal{P}$. This is obtained by differentiating (2.66) and using (2.39) and (2.40); with the help of (A.3) the result is:

$$\dot{\mathcal{P}} = -\Xi - \frac{1}{N} \sum_{j=1}^{N} \left[ \Xi^* e^{i2\psi_j} + i\sqrt{2N}\Gamma_j^2 e^{i\psi_j} \right] \tag{2.68}$$

In (2.68) the quantity $\Xi^*$ is the complex conjugate of $\Xi$.

We can consider linearization of (2.64), (2.67), and (2.68) about the equilibrium point. The linearization results in:[19]

$$\dot{\Xi} = \mathcal{B} - ib\Xi \tag{2.69}$$

$$\dot{\mathcal{B}} = i\mathcal{P} \tag{2.70}$$

$$\dot{\mathcal{P}} = -\Xi \tag{2.71}$$

This can be written in matrix form $\dot{\mathbf{w}} = \mathbf{A}\mathbf{w}$ where the matrix $\mathbf{A}$ is given by:[20]

$$\mathbf{A} = \begin{bmatrix} -ib & 1 & 0 \\ 0 & 0 & i \\ -1 & 0 & 0 \end{bmatrix} \tag{2.72}$$

The characteristic equation of this matrix is:

$$\lambda^3 + ib\lambda^2 + i = 0 \tag{2.73}$$

[19] To linearize we use the fact that $\sum_{j=1}^{N} \alpha^{(j-1)} = \frac{1-\alpha^N}{1-\alpha}$ where $\alpha = e^{i\frac{4\pi}{N}}$ and require $N > 2$. See Appendix C for more details of a similar linearization.

[20] This is not the same matrix as in (2.47)

Equation (2.73) is the classic TWT dispersion relation from Pierce's analysis ([45], pg. 118) for the case of no attenuation and the neglect of space charge.

The roots of this cubic equation bifurcate at $b \approx 1.89$. For values of $b > 1.89$ none of the roots of (2.73) have a positive real part and hence the exponential growth of the linearization disappears. One can refer to [45] for plots showing the real and imaginary parts of the roots of (2.73) as a function of $b$.

# Chapter 3

# Multitone Analysis

Chapter 2 demonstrates that even the simplest version of a TWT model in Lagrangian coordinates is not trivial. Of ultimate concern is the behavior of the output spectrum of a TWT when driven by multiple input carrier tones. This chapter is devoted to the modeling of the multitone drive situation in as intuitive manner as possible. To this end a completely detailed derivation is presented with physical meanings elucidated where possible. Logically following the multitone model derivation is the exploration of a fixed point of the system and linearization about that point.

## 3.1 Multitone Model

In essence, the model derived here is a "small $C$" version of the model presented by Giarola [25]. Major differences between our model and Giarola's are:

(1) Giarola defines phase variables with respect to a reference frame moving at the cold circuit phase velocity where we choose the initial electron beam velocity frame.

(2) Giarola defines a normalized distance variable for each frequency where we use one distance variable normalized to the fundamental frequency.

(3) Giarola defines velocity variable components for each tone where we define a

total velocity variable.

(4) Giarola defines a phase variable with respect to each tone while we define a phase variable with respect to only the fundamental frequency.

### 3.1.1 Model Derivation

The derivation of the multitone TWT model proceeds in much the same fashion as the single tone derivation. The foundational equations are the same as in the single tone case, namely (2.1)-(2.3). To handle an input signal with more than single tone frequency content a Fourier series form for the circuit voltage and the beam charge density is assumed, which is equivalent to assuming that these variables are periodic in time for a fixed point in space. This seems to be a reasonable assumption if one also assumes that the tones forcing the beam evolution and interaction (drive tones) have frequencies that are related by some rational number,[1] for then the sum of the individual tones is periodic in time with a period related to that of the individual tones. Along these lines we must identify a fundamental frequency $\omega_f$ of which all other tones present are harmonics. This frequency is not considered as a tone that exists in the tube, rather just a mathematical artifact of the Fourier assumption. The common periodicity of the variables previously mentioned is then $T_f = \frac{2\pi}{\omega_f}$. Note that in this time all of the higher frequency tones execute several of their own periods but the signal as a whole has period $T_f$. Further assumptions will need to be made about the frequency dependence of the helix circuit (or transmission line equivalent), and following our simplified methodology we will make the simplest assumptions possible.

[1] This is also a reasonable assumption to first order. The fact that the rational numbers are dense in the real numbers implies that for any irrational number there is a rational number arbitrarily close by.

**Fundamental Equations**

We begin by writing the fundamental equations in the lab frame variables and postulating the Fourier type solutions for circuit voltage and beam charge density. The telegrapher's equation, Newton's force equation, and the continuity equation are as in Chapter 2. We state them here again:

$$\frac{\partial^2 V(z,t)}{\partial t^2} - {v_0}^2 \frac{\partial^2 V(z,t)}{\partial z^2} = v_0 Z_0 \frac{\partial^2 \rho(z,t)}{\partial t^2} \tag{3.1}$$

$$\frac{\partial^2 z(z_0,t)}{\partial t^2} = -\frac{e}{m_e}\frac{\partial V(z,t)}{\partial z} \tag{3.2}$$

$$\rho(z,t) = \frac{I_0}{u_0}\left|\frac{\partial z_0(z,t)}{\partial z}\right|_t \tag{3.3}$$

The assumption of a Fourier series form for $V(z,t)$ and $\rho(z,t)$ is written as in [25]:

$$V(z,t) = \sum_{m=-\infty}^{\infty} V_m(z) e^{\,jm\omega_f t} \tag{3.4}$$

$$\rho(z,t) = \sum_{m=-\infty}^{\infty} \rho_m(z) e^{\,jm\omega_f t} \tag{3.5}$$

We see from equations (3.4) and (3.5) that the harmonic nature of the signals is postulated to be in the time variable (i.e. at a fixed value of $z$) as we mentioned it would be.[2] Also we notice that $V_m(z)$ and $\rho_m(z)$ are spatially dependent complex Fourier coefficients. As Giarola notes, substitution of equations (3.4) and (3.5) into equation (3.1) results in an infinite number of partial differential equations, one for each Fourier coefficient or "tone".

**Variable Definitions**

First we define a new variable based on the lab distance variable $z$. The new variable $y$ is defined with respect to the fundamental frequency discussed previously.

[2] Equations (3.4) and (3.5) are really for demonstration purposes in that while we will do a Fourier expansion later, it will be with different independent variables so we will not use these equations directly.

The definition is:

$$y \equiv C\frac{\omega_f}{u_0}z \tag{3.6}$$

Notice that $\frac{\omega_f}{u_0}$ is the wave number of a traveling wave of frequency $\omega_f$ traveling at the initial electron beam velocity $u_0$; this wave is called the "stream wave". Writing the definition of wave number: $\frac{\omega_f}{u_0} = \frac{2\pi}{\lambda_s}$ with $\lambda_s$ being the "stream wavelength", we may write equation (3.6) as:

$$y \equiv 2\pi C\frac{z}{\lambda_s} \tag{3.7}$$

We see that $y$ is proportional to the number of stream wavelengths for a particular $z$ value. The $C$ proportionality is Pierce's gain parameter [45] (see Chapter 2 for a definition of $C$ in terms of other TWT parameters). We emphasize that the stream wave does not exist in the tube, rather it is merely a convenient reference wave.

We next consider the definition and interpretation of the phase variable. The phase is defined by:[3]

$$\psi \equiv \omega_f\left(\frac{z}{u_0} - t\right) \tag{3.8}$$

As in Chapter 2 one should view the definition of $\psi$ as a coordinate transformation. Then $\psi$ describes the phase of a traveling wave or the phase trajectory of a fluid element, $\psi(y, \psi_0)$. The latter comes from substituting the fluid element time function, $t(z, z_0)$, into the $t$ component of (3.8) and appropriately rescaling the $(z, z_0)$ variables. One can see by inserting the constant phase trajectory $z = u_0 t$ into the $z$ component of $\psi$ that the phase is with respect to the stream wave.

One of the independent variables will be initial fluid element phase $\psi_0$, so we

[3] This is different than the definition commonly used in the TWT literature. The common definition is with respect to a wave traveling at $v_0$, or the cold circuit phase velocity. Our choice is again motivated by the fact that when the equations are written in the initial beam velocity frame there will be a fixed point of the system as discussed in the single tone case.

define it now. At $t = 0$ the fluid element positions are $z = z_0$ and (3.8) gives:[4]

$$\psi_0 \equiv \omega_f \frac{z_0}{u_0} \tag{3.9}$$

To label the electron beam in one period of the stream wave we assign $\psi_0$ values in the interval $[0, 2\pi]$.

Next, we define variables that will describe the fluid state of the electron beam. The required variables will be the fluid phase and the fluid velocity. As discussed above the fluid phase is given by $\psi(y, \psi_0)$. The velocity variable $\Gamma(y, \psi_0)$ is defined by:

$$\frac{\partial z(z_0, t)}{\partial t} \equiv u_0[1 + C\Gamma(y, \psi_0)] \tag{3.10}$$

**Differential Operators**

Ultimately we want to write equations (3.1)-(3.3) in terms of the new variables. The next logical step is therefore to see how differential operators in $(z, t)$ coordinates translate into differential operators in $(y, \psi)$ coordinates. We can do the calculations to get $\frac{\partial}{\partial t}$, $\frac{\partial^2}{\partial t^2}$, $\frac{\partial}{\partial z}$, and $\frac{\partial^2}{\partial z^2}$ in the new coordinates using the chain rule. First we do the calculation for $\frac{\partial}{\partial t}$:

$$\frac{\partial}{\partial t} = \frac{\partial y}{\partial t}\frac{\partial}{\partial y} + \frac{\partial \psi}{\partial t}\frac{\partial}{\partial \psi} \tag{3.11}$$

From equation (3.6) we see the first term on the right hand side of (3.11) is zero and from equation (3.8) we can write:[5]

$$\frac{\partial}{\partial t} = -\omega_f \frac{\partial}{\partial \psi} \tag{3.12}$$

[4] This can equivalently be written based on the time when each fluid element crosses the $z = 0$ plane: $\omega_f t_0$.

[5] One might think that since $y = C\frac{\omega_f}{u_0}z$, and $\frac{\partial z(z_0,t)}{\partial t} \neq 0$ from equation (3.10), that $\frac{\partial y}{\partial t} \neq 0$. This is not the case since $z(z_0, t)$ is a function, and not one of the independent variables in the coordinate transformation we are considering. It may have been more appropriate to name $z(z_0, t)$ as $s(z_0, t)$, and, when necessary, substitute $s$ into the $z$ coordinate of a function (e.g. $\psi(z, t)$) to get quantities relating to fluid elements (e.g. $\psi(z_0, t)$). We have chosen to be consistent with the literature and use $z(z_0, t)$.

Applying this result to itself (i.e. take $\frac{\partial}{\partial t}$ of both sides, but on the right hand side use the definition given by the right hand side) gives:

$$\frac{\partial^2}{\partial t^2} = \omega_f^2 \frac{\partial^2}{\partial \psi^2} \tag{3.13}$$

The derivation is slightly more complicated for $\frac{\partial^2}{\partial z^2}$ since both $y$ and $\psi$ depend on $z$. Similarly to equation (3.11) we have:

$$\frac{\partial}{\partial z} = \frac{\partial y}{\partial z}\frac{\partial}{\partial y} + \frac{\partial \psi}{\partial z}\frac{\partial}{\partial \psi} \tag{3.14}$$

We use the definitions of $y$ in (3.6) and $\psi$ in (3.8) to get:

$$\frac{\partial}{\partial z} = \frac{C\omega_f}{u_0}\frac{\partial}{\partial y} + \frac{\omega_f}{u_0}\frac{\partial}{\partial \psi} \tag{3.15}$$

Applying this result to itself gives:

$$\frac{\partial^2}{\partial z^2} = \frac{C^2\omega_f^2}{u_0^2}\frac{\partial^2}{\partial y^2} + \frac{2C\omega_f^2}{u_0^2}\frac{\partial^2}{\partial \psi \partial y} + \frac{\omega_f^2}{u_0^2}\frac{\partial^2}{\partial \psi^2} \tag{3.16}$$

### The Continuity Equation

The Lagrangian continuity equation in (3.3) is the one-dimensional case of the more general expression:

$$J\rho = \rho_0 \tag{3.17}$$

where $J$ is the Jacobian:

$$J = \left| \frac{\partial(x, y, z)}{\partial(x_0, y_0, z_0)} \right| \tag{3.18}$$

Equation (3.17) results from combining conservation of mass and the method of changing variable in Riemann integration. See Truesdell [55], pg. 93 for a comprehensive discussion.

We require $\rho(z,t)$ in the new variables, i.e. we want $\rho(y,\psi)$. First we write equation (3.3) in the following form using the chain rule:

$$\rho(z,t) = \frac{I_0}{u_0}\left|\frac{\partial z_0(z,t)}{\partial t}\frac{\partial t(z,z_0)}{\partial z}\right|_t \tag{3.19}$$

Assuming $t(z,z_0)$ is well behaved enough[6] we use $\frac{\partial t(z,z_0)}{\partial z} = \left[\frac{\partial z(z_0,t)}{\partial t}\right]^{-1}$ to write (3.19) as:

$$\rho(z,t) = \frac{I_0}{u_0}\left|\frac{\partial z_0(z,t)/\partial t}{\partial z(z_0,t)/\partial t}\right|_t \tag{3.20}$$

Then using (3.10) and $\frac{\partial z_0(z,t)}{\partial t} = -u_0\frac{\partial \psi_0}{\partial \psi}$ [7] we can write:

$$\rho(y,\psi) = \frac{I_0}{u_0}\left|\frac{\partial \psi_0}{\partial \psi}\right|_y \frac{1}{1+C\Gamma(y,\psi_0)} \tag{3.21}$$

The transformation of the continuity equation above uses the method most of the authors use in the Lagrangian TWT literature. An alternative, and we believe more elegant and less confusing, method of doing the transformation is now given. We start with the coordinate transformations given below:

$$y = C\frac{\omega_f}{u_0}z(z_0,t) \tag{3.22}$$

$$\psi_0 = \frac{\omega_f}{u_0}z_0 \tag{3.23}$$

In (3.22) and (3.23) the independent variables are $(z_0,t)$ and $z(z_0,t)$ is some undetermined function of $(z_0,t)$, thus (3.22) and (3.23) are both functions of $(z_0,t)$. The differentials of the transformation are related by:

$$\begin{pmatrix} dy \\ d\psi_0 \end{pmatrix} = \frac{\omega_f}{u_0}\begin{pmatrix} C\frac{\partial z}{\partial z_0} & C\frac{\partial z}{\partial t} \\ 1 & 0 \end{pmatrix}\begin{pmatrix} dz_0 \\ dt \end{pmatrix} \tag{3.24}$$

[6] Recall solutions will in fact not be invertible, but assuming functions are invertible in intermediate steps is allowed.

[7] This relation comes from the chain rule expansion $\frac{\partial z_0}{\partial t} = \frac{\partial z_0}{\partial \psi_0}\frac{\partial \psi_0}{\partial \psi}\frac{\partial \psi}{\partial t}$ and use of (3.9).

We may then compute $\frac{\partial}{\partial y}$ and $\frac{\partial}{\partial \psi_0}$ in terms of $\frac{\partial}{\partial z_0}$ and $\frac{\partial}{\partial t}$ from (3.24) using the inverse of the matrix transforming the differentials:

$$\begin{pmatrix} \frac{\partial}{\partial y} & \frac{\partial}{\partial \psi_0} \end{pmatrix} = \frac{u_0}{\omega_f} \begin{pmatrix} \frac{\partial}{\partial z_0} & \frac{\partial}{\partial t} \end{pmatrix} \begin{pmatrix} 0 & 1 \\ \frac{1}{C\frac{\partial z}{\partial t}} & -\frac{\frac{\partial z}{\partial z_0}}{\frac{\partial z}{\partial t}} \end{pmatrix} \tag{3.25}$$

Next we take $\frac{\partial}{\partial \psi_0}$, as calculated in (3.25), of the definition of $\psi$ in (3.8), $\psi(z_0, t) \equiv \frac{\omega_f}{u_0}[z(z_0, t) - u_0 t]$, which gives:

$$\begin{aligned} \frac{\partial \psi}{\partial \psi_0} &= \left( \frac{\partial}{\partial z_0} - \frac{\frac{\partial z}{\partial z_0}}{\frac{\partial z}{\partial t}} \frac{\partial}{\partial t} \right) [z(z_0, t) - u_0 t] \\ &= \frac{\partial z}{\partial z_0} - \frac{\partial z}{\partial z_0} + u_0 \frac{\frac{\partial z}{\partial z_0}}{\frac{\partial z}{\partial t}} \\ &= u_0 \frac{\frac{\partial z}{\partial z_0}}{\frac{\partial z}{\partial t}} \end{aligned} \tag{3.26}$$

Then we use (3.10) in (3.26) to get:

$$\frac{\partial \psi}{\partial \psi_0} = \frac{\frac{\partial z}{\partial z_0}}{1 + C\Gamma} \tag{3.27}$$

Lastly we write the "inverse functions":

$$\left| \frac{\partial z_0}{\partial z} \right|_t = \left| \frac{\partial \psi_0}{\partial \psi} \right|_y \frac{1}{1 + C\Gamma(y, \psi_0)} \tag{3.28}$$

Substitute this into (3.3) which gives:

$$\rho(y, \psi) = \frac{I_0}{u_0} \left| \frac{\partial \psi_0}{\partial \psi} \right|_y \frac{1}{1 + C\Gamma(y, \psi_0)} \tag{3.29}$$

And (3.29) agrees with (3.21).

Notice that technically $\psi$ on the left hand side of (3.26) is a different function than $\psi(z_0, t)$. In particular, it comes from substituting the inverse transformations of (3.22) and (3.23) into the $z_0$ and $t$ coordinates of $\psi(z_0, t)$. Similarly $\Gamma$ on the right hand side of (3.27) is $\Gamma(z_0, t)$, obtained from substituting (3.22) and (3.23) into the $y$ and $\psi_0$ arguments of $\Gamma(y, \psi_0)$.

**Fourier Series**

We will use a Fourier series representation for two quantities. First we will write the voltage in terms of its Fourier components and let the Fourier coefficients be the dependent variables. We will also assume the charge density is periodic in $\psi$ and use the Fourier coefficients in writing the final set of equations. In preparation we now give the relations for a Fourier series. These relations can be found in any elementary signals and systems text book; we use the so-called trigonometric Fourier series as presented in [31]. For a signal $x(t)$ that is periodic in $t$ with period $T_0$ we write:

$$x(t) = \frac{a_0}{2} + \sum_{k=1}^{\infty} \left(a_k \cos k\omega_0 t + b_k \sin k\omega_0 t\right) \qquad \omega_0 = \frac{2\pi}{T_0} \tag{3.30}$$

$$a_k = \frac{2}{T_0} \int_{T_0} x(t) \cos k\omega_0 t \, dt \tag{3.31}$$

$$b_k = \frac{2}{T_0} \int_{T_0} x(t) \sin k\omega_0 t \, dt \tag{3.32}$$

As stated earlier for the voltage we will leave the integral expressions in (3.31) and (3.32) as variables, i.e. replace the two integral expressions with tone amplitudes $a_{1m}(y)$ and $a_{2m}(y)$. Notice $T_0$ in (3.30)-(3.32) will be in our case $T_f$, or the period of the reference wave.

The final result from Fourier series theory that we will need is the Fourier series for $\frac{d^2x(t)}{dt^2}$. This can easily be calculated from (3.30) noting that neither $a_k$ nor $b_k$ are functions of $t$. The result is:

$$\frac{d^2x(t)}{dt^2} = \sum_{k=1}^{\infty} -k^2\omega_0^2 \left(a_k \cos k\omega_0 t + b_k \sin k\omega_0 t\right) \tag{3.33}$$

**Assumed Solution Forms**

We are almost fully prepared to derive the equations in the new variables. The remaining preparatory step is to write our assumed forms of the voltage and charge density using the Fourier results stated in the previous section. First we consider the voltage solution. The periodic variable of the voltage solution will be $\psi$, where harmonics of the fundamental are $m\psi$.[8] One should keep in mind that in terms of lab frame variables the periodicity is in the $t$ component of $\psi$. For the voltage we choose to let the Fourier coefficients as defined in (3.31) and (3.32) be variables that are functions of $y$. The voltage components are defined by:

$$V(y,\psi) \equiv \frac{Z_0 I_0}{4C} \sum_{m=0}^{\infty} [a_{1m}(y)\cos m\psi + a_{2m}(y)\sin m\psi] \tag{3.34}$$

This expression could be written using equation (A.3) as
$V(y,\psi) = \frac{Z_0 I_0}{8C} \sum_{m=0}^{\infty} \left[A_m(y)e^{-im\psi} + c.c.\right]$ where $A_m(y) \equiv a_{1m}(y) + ia_{2m}(y)$ and c.c. denotes complex conjugate. In most of the literature authors assume a form $V(y,\psi) \equiv \frac{Z_0 I_0}{8C} \sum_{m=0}^{\infty} \left[A_m(y)e^{im\psi} + c.c.\right]$ (the difference being the minus sign in the exponential); the only difference between the choices are differences in sign in the final equations.

We now consider the Fourier series representation of the charge density. In this case we will include the definition of the Fourier coefficients; we write:

$$\begin{aligned} \rho(y,\psi) \;\; = \;\; & \sum_{m=0}^{\infty} \left[ \left( \frac{1}{\pi} \int_0^{2\pi} \rho(y,\psi)\cos m\psi \; d\psi \right) \cos m\psi \right. \\ & \left. + \left( \frac{1}{\pi} \int_0^{2\pi} \rho(y,\psi)\sin m\psi \; d\psi \right) \sin m\psi \right] \end{aligned} \tag{3.35}$$

We note that the Fourier coefficient integral is a function of $y$ only as expected. Also the $2\pi$ is one period of the fundamental frequency, i.e. $T_f = 2\pi$. The goal of this

[8] This definition points out that it might have been clearer to have defined $\psi$ as $\psi_f$ in equation (3.8). However, we are not interested in carrying around the $f$ subscript so will just understand that this is the meaning of definition (3.8).

transformation is to get to a form that we can use on the right side of equation (3.1). To this end we insert (3.21) into the integrals on the right hand side of (3.35) to get:

$$\begin{aligned}\rho(y,\psi) &= \frac{I_0}{u_0}\sum_{m=0}^{\infty}\left[\left(\frac{1}{\pi}\int_0^{2\pi}\left|\frac{\partial\psi_0}{\partial\psi}\right|_y\frac{\cos m\psi\ d\psi}{1+C\Gamma(y,\psi_0)}\right)\cos m\psi\right. \\ &\quad \left.+\left(\frac{1}{\pi}\int_0^{2\pi}\left|\frac{\partial\psi_0}{\partial\psi}\right|_y\frac{\sin m\psi\ d\psi}{1+C\Gamma(y,\psi_0)}\right)\sin m\psi\right] \end{aligned} \tag{3.36}$$

Applying the change of variable to the integrands gives:

$$\begin{aligned}\rho(y,\psi) &= \frac{I_0}{u_0}\sum_{m=0}^{\infty}\left[\left(\frac{1}{\pi}\int_0^{2\pi}\frac{\cos m\psi(y,\psi_0)\ d\psi_0}{1+C\Gamma(y,\psi_0)}\right)\cos m\psi\right. \\ &\quad \left.+\left(\frac{1}{\pi}\int_0^{2\pi}\frac{\sin m\psi(y,\psi_0)\ d\psi_0}{1+C\Gamma(y,\psi_0)}\right)\sin m\psi\right] \end{aligned} \tag{3.37}$$

Lastly we see the right hand side of equation (3.1) requires that we take the second time derivative which is given by equation (3.13) for the new coordinates. We employ the Fourier series property given by (3.33) to get:

$$\begin{aligned}\frac{\partial^2\rho}{\partial t^2}=\omega_f^2\frac{\partial^2\rho(y,\psi)}{\partial\psi^2} &= -\omega_f^2\frac{I_0}{u_0}\sum_{m=0}^{\infty}m^2\left[\left(\frac{1}{\pi}\int_0^{2\pi}\frac{\cos m\psi(y,\psi_0)\ d\psi_0}{1+C\Gamma(y,\psi_0)}\right)\cos m\psi\right. \\ &\quad \left.+\left(\frac{1}{\pi}\int_0^{2\pi}\frac{\sin m\psi(y,\psi_0)\ d\psi_0}{1+C\Gamma(y,\psi_0)}\right)\sin m\psi\right] \end{aligned} \tag{3.38}$$

This is the final form that we will require.

### Transforming the Telegrapher's Equation

We are now prepared to derive the first two differential equations of our model in the transformed Lagrangian coordinates (actually a countable "$2\times\infty$" set of equations). We proceed by using the differential operators given by (3.13) and (3.16) on (3.1), inserting the assumed voltage solution given by (3.34) and the charge density

expression given by (3.38). The result of this operation and some rearrangement is:

$$\begin{aligned}
&\left\{\frac{1}{2C}\left[\frac{u_0^2}{v_0^2}-1\right]\frac{\partial^2}{\partial\psi^2}-\frac{C}{2}\frac{\partial^2}{\partial y^2}-\frac{\partial^2}{\partial\psi\partial y}\right\}\cdot \\
&\left\{\sum_{m=0}^{\infty}\left[a_{1m}(y)\cos m\psi+a_{2m}(y)\sin m\psi\right]\right\} \;=\; \\
-\frac{u_0}{v_0}\sum_{m=0}^{\infty}m^2&\left[\left(\frac{2}{\pi}\int_0^{2\pi}\frac{\cos m\psi(y,\psi_0)\;d\psi_0}{1+C\Gamma(y,\psi_0)}\right)\cos m\psi\right. \\
&\left.+\left(\frac{2}{\pi}\int_0^{2\pi}\frac{\sin m\psi(y,\psi_0)\;d\psi_0}{1+C\Gamma(y,\psi_0)}\right)\sin m\psi\right]
\end{aligned} \tag{3.39}$$

Performing the differentiations as indicated:

$$\begin{aligned}
&\frac{1}{2C}\left[1-\frac{u_0^2}{v_0^2}\right]\sum_{m=0}^{\infty}m^2\left[a_{1m}(y)\cos m\psi+a_{2m}(y)\sin m\psi\right] \\
&\quad+\sum_{m=0}^{\infty}m\left[\frac{da_{1m}(y)}{dy}\sin m\psi-\frac{da_{2m}(y)}{dy}\cos m\psi\right] \\
&\quad-\frac{C}{2}\sum_{m=0}^{\infty}\left[\frac{d^2a_{1m}(y)}{dy^2}\cos m\psi+\frac{d^2a_{2m}(y)}{dy^2}\sin m\psi\right] \;=\; \\
-\frac{u_0}{v_0}\sum_{m=0}^{\infty}m^2&\left[\left(\frac{2}{\pi}\int_0^{2\pi}\frac{\cos m\psi(y,\psi_0)\;d\psi_0}{1+C\Gamma(y,\psi_0)}\right)\cos m\psi\right. \\
&\left.+\left(\frac{2}{\pi}\int_0^{2\pi}\frac{\sin m\psi(y,\psi_0)\;d\psi_0}{1+C\Gamma(y,\psi_0)}\right)\sin m\psi\right]
\end{aligned} \tag{3.40}$$

Define the detuning parameter $\delta$ by:[9]

$$\frac{u_0}{v_0}\equiv 1+C\delta \tag{3.41}$$

Substituting this definition into (3.40) gives:

$$\frac{\delta\,(2+C\delta)}{2}\sum_{m=0}^{\infty}m^2\left[a_{1m}(y)\cos m\psi+a_{2m}(y)\sin m\psi\right]$$

[9] This definition is slightly different than equation (2.15). Nordsieck uses (2.15) in [38] whereas our definition appears in [45, 49]. To avoid confusion between the detuning parameters of Chapters 2 and 3 we use the new variable name $\delta$.

$$
\begin{aligned}
&- \sum_{m=0}^{\infty} m \left[ \frac{da_{1m}(y)}{dy} \sin m\psi - \frac{da_{2m}(y)}{dy} \cos m\psi \right] \\
&+ \frac{C}{2} \sum_{m=0}^{\infty} \left[ \frac{d^2 a_{1m}(y)}{dy^2} \cos m\psi + \frac{d^2 a_{2m}(y)}{dy^2} \sin m\psi \right] \quad = \\
&(1 + C\delta) \sum_{m=0}^{\infty} m^2 \left[ \left( \frac{2}{\pi} \int_0^{2\pi} \frac{\cos m\psi(y, \psi_0)\ d\psi_0}{1 + C\Gamma(y, \psi_0)} \right) \cos m\psi \right. \\
&\qquad \left. + \left( \frac{2}{\pi} \int_0^{2\pi} \frac{\sin m\psi(y, \psi_0)\ d\psi_0}{1 + C\Gamma(y, \psi_0)} \right) \sin m\psi \right] \qquad (3.42)
\end{aligned}
$$

The remaining step to get differential equations for $a_{1m}(y)$ and $a_{2m}(y)$ is to equate terms multiplying the sine and cosine functions respectively. Note that what is represented in (3.42) is an infinite sum of equations, one for each tone. From here on we will simply write one set of these equations which will be indexed by $m$. The differential equations for $a_{1m}(y)$ and $a_{2m}(y)$ are:

$$
\begin{aligned}
&\frac{C}{2} \frac{d^2 a_{1m}(y)}{dy^2} + m \frac{da_{2m}(y)}{dy} + \frac{\delta\,(2 + C\delta)}{2} m^2 a_{1m}(y) \quad = \\
&\qquad (1 + C\delta)\, m^2 \frac{2}{\pi} \int_0^{2\pi} \frac{\cos m\psi(y, \psi_0)\ d\psi_0}{1 + C\Gamma(y, \psi_0)} \qquad m = 0, 1, 2, \ldots \qquad (3.43)
\end{aligned}
$$

$$
\begin{aligned}
&\frac{C}{2} \frac{d^2 a_{2m}(y)}{dy^2} - m \frac{da_{1m}(y)}{dy} + \frac{\delta\,(2 + C\delta)}{2} m^2 a_{2m}(y) \quad = \\
&\qquad (1 + C\delta)\, m^2 \frac{2}{\pi} \int_0^{2\pi} \frac{\sin m\psi(y, \psi_0)\ d\psi_0}{1 + C\Gamma(y, \psi_0)} \qquad m = 0, 1, 2, \ldots \qquad (3.44)
\end{aligned}
$$

Under the physical assumptions stated earlier these are the exact equations for $a_{1m}(y)$ and $a_{2m}(y)$ in the new variables written in Lagrangian coordinates. For now we leave these equations as they are and move on. Shortly we will return and take the "small $C$" approximation of (3.43) and (3.44). We forego physical interpretation until that simplification has been made.

**Transforming Newton's Law**

In this section we derive the $\Gamma(y,\psi_0)$ equation by application of Newton's Law as seen in (3.2). We write (3.2) again in the following form:

$$\frac{\partial}{\partial t}\frac{\partial z(z_0,t)}{\partial t} = -\frac{e}{m_e}\frac{\partial V(z,t)}{\partial z} \tag{3.45}$$

Recall that we used $\frac{\partial z}{\partial t}$ in the definition of $\Gamma(y,\psi_0)$ in equation (3.10). Therefore, to proceed we substitute (3.10) into the left hand side of (3.45) and apply the chain rule of differentiation. On the right hand side we use (3.15) to convert $\frac{\partial}{\partial z}$ to $\frac{\partial}{\partial y}$ and $\frac{\partial}{\partial \psi}$, and substitute in our assumed voltage solution (3.34). This gives:

$$\begin{aligned} Cu_0\frac{\partial\Gamma(y,\psi_0)}{\partial y}\frac{\partial y}{\partial t} &= -\frac{e}{m_e}\left\{\frac{C\omega_f}{u_0}\frac{\partial}{\partial y}+\frac{\omega_f}{u_0}\frac{\partial}{\partial\psi}\right\}\cdot \\ &\quad \left\{\frac{Z_0I_0}{4C}\sum_{m=0}^{\infty}\left[a_{1m}(y)\cos m\psi + a_{2m}(y)\sin m\psi\right]\right\} \end{aligned} \tag{3.46}$$

We can take this further by again using (3.10) and that $\frac{\partial y}{\partial t} = \frac{\partial y}{\partial z}\frac{\partial z}{\partial t}$ where $\frac{\partial y}{\partial z} = C\frac{\omega_f}{u_0}$; we also compute the derivatives on the right hand side:

$$\begin{aligned} \frac{\partial\Gamma(y,\psi_0)}{\partial y}\left[1+C\Gamma(y,\psi_0)\right] &= -\frac{1}{2}\left\{C\sum_{m=0}^{\infty}\left[\frac{da_{1m}(y)}{dy}\cos m\psi(y,\psi_0)\right.\right. \\ &\qquad \left.+\frac{da_{2m}(y)}{dy}\sin m\psi(y,\psi_0)\right] \\ &\quad +\sum_{m=0}^{\infty} m\left[a_{2m}(y)\cos m\psi(y,\psi_0)\right. \\ &\qquad \left.\left.-a_{1m}(y)\sin m\psi(y,\psi_0)\right]\right\} \end{aligned} \tag{3.47}$$

We have also used the definition of Pierce's gain parameter: $C^3 \equiv \frac{Z_0I_0}{4V_0}$, and that $eV_0 = \frac{1}{2}m_eu_0^2$. Equation (3.47) is the exact equation for evolution of $\Gamma(y,\psi_0)$. Occasionally in the literature the left hand side is written as $\frac{1}{2C}\frac{\partial}{\partial y}\left[1+C\Gamma(y,\psi_0)\right]^2$. Rewriting in this fashion is exactly analogous to the common observation that for a velocity function $v$, $\frac{1}{2}\frac{dv^2}{dt} = v\frac{dv}{dt}$.

**An Evolution Equation for $\frac{\partial \psi}{\partial y}$**

The final equation required is for $\psi(y, \psi_0)$. To derive this equation we take the definition of $\psi$ from (3.8), differentiate both sides with respect to $y$ and make the proper substitutions. The differentiation yields (with an application of the chain rule and using $\frac{\partial t}{\partial z} = \left(\frac{\partial z}{\partial t}\right)^{-1}$):

$$\frac{\partial \psi(y, \psi_0)}{\partial y} = \omega_f \frac{\partial z}{\partial y} \left( \frac{1}{u_0} - \left[ \frac{\partial z}{\partial t} \right]^{-1} \right) \tag{3.48}$$

Now we substitute in (3.10) and use that $\frac{\partial z}{\partial y} = \left(\frac{\partial y}{\partial z}\right)^{-1}$ giving:

$$\frac{\partial \psi(y, \psi_0)}{\partial y} = \frac{\Gamma(y, \psi_0)}{1 + C\Gamma(y, \psi_0)} \tag{3.49}$$

This is the final form of the equation for $\psi(y, \psi_0)$.

The derivation of (3.49) is the method most often used in the Lagrangian TWT literature. We again offer an alternative method based on the coordinate transformations (3.22)-(3.23). From (3.25) we have:

$$\frac{\partial}{\partial y} = \frac{u_0}{\omega_f} \frac{1}{C\frac{\partial z}{\partial t}} \frac{\partial}{\partial t} \tag{3.50}$$

We apply (3.50) to the definition of $\psi$ in (3.8):

$$\begin{aligned} \frac{\partial \psi}{\partial y} &= \frac{1}{C\frac{\partial z}{\partial t}} \frac{\partial}{\partial t} (z - u_0 t) \\ &= \frac{\frac{\partial z}{\partial t} - u_0}{C\frac{\partial z}{\partial t}} \end{aligned} \tag{3.51}$$

Then we use the definition of $\Gamma$ in (3.10):

$$\begin{aligned} \frac{\partial \psi}{\partial y} &= \frac{u_0 \left[1 + C\Gamma\right] - u_0}{C u_0 \left[1 + C\Gamma\right]} \\ &= \frac{\Gamma}{1 + C\Gamma} \end{aligned} \tag{3.52}$$

This is the same as (3.49).

**The Small $C$ Equations**

Equations (3.43), (3.44), (3.47) and (3.49) are the fully converted equations under the physical assumptions made. To simplify matters even further we restrict ourselves to low gain TWTs, or ones with $C \ll 1$. In this approximation we get:

$$\frac{da_{1m}(y)}{dy} = -m\frac{2}{\pi}\int_0^{2\pi} \sin m\psi(y,\psi_0)\; d\psi_0 + \delta m a_{2m}(y) \qquad m = 0,1,2\ldots \tag{3.53}$$

$$\frac{da_{2m}(y)}{dy} = m\frac{2}{\pi}\int_0^{2\pi} \cos m\psi(y,\psi_0)\; d\psi_0 - \delta m a_{1m}(y) \qquad m = 0,1,2,\ldots \tag{3.54}$$

$$\frac{\partial\Gamma(y,\psi_0)}{\partial y} = \frac{1}{2}\sum_{m=0}^{\infty} m\left[a_{1m}(y)\sin m\psi(y,\psi_0) - a_{2m}(y)\cos m\psi(y,\psi_0)\right] \tag{3.55}$$

$$\frac{\partial\psi(y,\psi_0)}{\partial y} = \Gamma(y,\psi_0) \tag{3.56}$$

If one sets $m = 1$ in equations (3.53)-(3.56) one will not get the small $C$ equations for the single tone case (2.16)-(2.19). There are two reasons for this:

(1) The multitone model was formulated in the unperturbed beam velocity frame where the single tone model was formulated in the frame moving with the cold circuit phase velocity. The manifestation of this is in the additive terms multiplying the detuning parameter on the right hand side of (3.53) and (3.54). If one refers back to Section 2.1.3 one will find a transformation from the circuit frame to the beam frame for the discretized model, and indeed see the appearance of the additive terms in equations (2.37) and (2.38).

(2) In the multitone model we chose our voltage solution directly from the trigonometric Fourier series, whereas Nordsieck chose a solution for the voltage which had a negative sign in front of the sine component. This choice results in the negative sign in front of (2.17) where it does not appear in (3.54), and a negative sign in (3.55) that does not appear in (2.18).

### 3.1.2 Physical Interpretation

In Chapter 2 we discussed at length how one interprets the growth of the voltage wave and fluid element evolution due to element "positioning" with respect to the wave. Equations (3.53) and (3.54) calculate wave growth by a time integration over a fundamental period (determining the bunchedness of the beam as well as the nominal phase location of the bunch), equation (3.55) determines the acceleration of the fluid due to fluid element phasing with respect to the voltage wave and equation (3.56) determines the velocity of the fluid. There is a fundamental difference, however, in the multitone equations regarding accelerations and wave growth; namely, the term $m$ which multiplies many of the terms on the right hand side of equations (3.53)-(3.56). This term will be considered in this section.

#### Electron Beam Response to Circuit Voltage

We interpret $m$ by looking at equation (3.55). Consider two sine waves of equal amplitude but different frequencies (different values of $m$). The higher frequency wave is steeper from peak to trough and therefore should exert a stronger force on a fluid element than a lower frequency wave for identical element phasing. This indeed is the meaning of the $m$ term; it came to being by differentiating the sine and cosine functions, which is an operation that measures gradient and in this case force. In fact equation (3.55) is proportional to the negative gradient of the voltage as defined in (3.34) where terms multiplied by $C$ have been dropped. Note that the acceleration of a fluid element is then a linear combination of the force contributions of the individual tones.

**Wave Growth**

Recall that $a_{1m}(y)$ and $a_{2m}(y)$ are the Fourier coefficients of tone $m$ of the total circuit voltage as assumed in (3.34). As in the single tone case, the integral computes the bunchedness of the beam by integrating the fluid phase function $\psi(y, \psi_0)$ over all initial fluid element positions $\psi_0$. In the multitone case, however, the integral computes the bunchedness of the beam with respect to tone $m$. The physical argument is identical to the argument of Chapter 2 except for the appearance of the $m$ term. Explaining the appearance of the $m$ term in the argument of the sinusoids in the integrand is straightforward; i.e. to determine bunchedness with respect to a wave with frequency $m\omega_f$ we must integrate with respect to the proper sinusoid of the same frequency.[10]

To determine the reason the $m$ term multiplies the integration consider again two equal amplitude waves of different frequency. According to (3.53) and (3.54) a fluid element at equal phase with respect to the two waves will contribute more to the growth of the higher frequency wave. We can rationalize this by considering the original form of the telegrapher equation in (3.1). Recall that time accelerations in the voltage and charge density contribute to the spatial acceleration, or growth, of the voltage wave. It is clear then that a higher time acceleration for a charge density will cause a higher space acceleration for the voltage wave than would a smaller time acceleration excitation. Said another way, higher frequencies will grow faster in space than will low frequencies.

It is interesting to observe that the growth contribution of a fluid element depends only on its phase with respect to the wave and not the height of the wave.[11] This differs from the calculation of the acceleration of a fluid element as in (3.55) in

[10] The frequency $\omega_f$ is implicit in the definition of $\psi$ so simply $m\psi$ appears in the argument of the sinusoids.

[11] This is the case in the single tone equations also. Although we did not mention it in Chapter 2, it can be determined from the equations.

that amplitudes do appear in the accelerations as one would expect. To understand this amplitude independent contribution we again look to (3.1). If we consider the spatial acceleration of the voltage as being made up of the time acceleration contributions of the voltage and the charge density, then the charge density contribution does not care as to what the voltage amplitude is.[12] The time averaging integrations in (3.53) and (3.54) measure the bunchedness of the beam regardless of what the amplitude of the circuit voltage just as the source term in (3.1) does. This is not to say, however, that if we were to set up two experiments including two waves of the same frequency, unequal amplitudes, and traveling synchronously with the beam ($\delta = 0$) that they would grow the same. Indeed they would immediately take different amplitude trajectories as their fluid accelerations as given in (3.55) would be different.

The other term on the right hand sides of equations (3.53) and (3.54) predicts a detuning effect. If one was able to turn off the interaction for a nonzero amplitude wave (i.e. $a_{1m}(y) \neq 0$ and $a_{2m}(y) \neq 0$) one would still expect the voltage variables to change in $y$. The reason is that the formulation is done in the beam frame. For a value of detuning $\delta > 0$, sitting in the beam frame the voltage wave is traveling to the left. This effect is captured in these terms. For two waves with different frequencies traveling at the same speed (recall the transmission line is assumed to be dispersionless) one would see more cycles of the higher frequency wave go by in unit time; this is predicted by the $m$ multiplier in these terms.

### 3.1.3 Development of Discretized Multitone Small $C$ Equations

As in the single tone case, we have identified Hamiltonian structure in the discretized multitone small $C$ model. In this section we discretize the small $C$ model

[12] We are speaking of explicit dependence of $\rho$ on $V$. There will be implicit dependence since different choices of boundary data for $V$ will influence values of $\rho$ at points further down the tube.

and present the Hamiltonian form of the equations.

**Discretization**

Equations (3.53)-(3.56) are partial differential equations and can be considered to be of infinite dimension; there are an (uncountably) infinite number of fluid elements each identified by its initial value of $\psi_0$ and a (countably) infinite number of harmonics making up the Fourier series representation of the voltage. If we consider a finite number of fluid elements represented by a finite number of initial phase values and a finite subset of the voltage harmonics we may write equations (3.53)-(3.56) as a set of ordinary differential equations finite in dimension. If the number of fluid elements is chosen to be $N$ and the number of tones present is chosen to be $M$ the dimension of the system is $2M + 2N$.

For the finite number of frequencies chosen we will likely pick a set of frequencies with nonconsecutive $m$ values.[13] For notational purposes we therefore consider a set of frequencies, $\Omega$, with $M$ elements where individual elements of the set are identified by $\Omega_n$. With this construction $\Omega$ is indexed by $n = 1, \ldots, M$. The $\Omega_n$'s correspond to values of $m$ we have chosen to keep in selecting a finite number of frequencies. We use the subscript $n$ to label the Fourier coefficients of the tone having frequency $\Omega_n\omega_f$ and the subscript $j$ to label the $j^{\text{th}}$ value of initial phase, or $j^{\text{th}}$ "particle". The system becomes:

[13] Choosing the "most important" frequencies is sometimes referred to as a Galerkin approximation (see pg. 631 of [34]). See Section 3.1.4 for examples of how and why one might do such a thing.

$$\dot{a}_{1n} = -\Omega_n \frac{4}{N} \sum_{j=1}^{N} \sin \Omega_n \psi_j + \delta\Omega_n a_{2n} \qquad n = 1, \ldots, M \quad (3.57)$$

$$\dot{a}_{2n} = \Omega_n \frac{4}{N} \sum_{j=1}^{N} \cos \Omega_n \psi_j - \delta\Omega_n a_{1n} \qquad n = 1, \ldots, M \quad (3.58)$$

$$\dot{\Gamma}_j = \frac{1}{2} \sum_{k=1}^{M} \Omega_k \left[ a_{1k} \sin \Omega_k \psi_j - a_{2k} \cos \Omega_k \psi_j \right] \qquad j = 1, \ldots, N \quad (3.59)$$

$$\dot{\psi}_j = \Gamma_j \qquad j = 1, \ldots, N \quad (3.60)$$

Equations (3.57) and (3.58) are each $M$ in number and equations (3.59) and (3.60) are each $N$ in number. The overdot represents differentiation with respect to $y$.

**Hamiltonian Form of Discretized Equations**

Before presenting the Hamiltonian form of the equations we discuss some more notational conventions. As in the single tone case we desire to have the variables for the tone amplitudes to be $\Gamma$'s and $\psi$'s to emphasize the Hamiltonian nature of the system. However, since there are two amplitude variables per tone we need to modify our indexing notation. For particle quantities we write $\Gamma_{0j}(y)$ and $\psi_{0j}(y)$; for wave quantities we write $\Gamma_{n0}(y)$ and $\psi_{n0}(y)$ as defined below. Therefore, the first index position is for wave quantities and the second index position is for particle quantities. For initial values we will no longer use the 0 subscript, rather indicate a 0 in the argument, e.g. $\Gamma_{0j}(0)$ is particle $j$'s velocity at $y = 0$.

As in the single tone case the tone amplitude variables are not symplectic and we must perform a transformation to get symplectic variables (see B.2.1 in Appendix B for the Hamiltonian and modifications to the equations of motion before the transformation). We make the transformation using the following definitions:

$$\Gamma_{n0}(y) \equiv \sqrt{\frac{N}{8\Omega_n}} a_{1n}(y) \quad (3.61)$$

$$\psi_{n0}(y) \equiv \sqrt{\frac{N}{8\Omega_n}} a_{2n}(y) \quad (3.62)$$

Substituting definitions (3.61) and (3.62) into equations (3.57)-(3.59) we get:

$$\dot{\Gamma}_{n0} = -\sqrt{\frac{2\Omega_n}{N}}\sum_{j=1}^{N}\sin\Omega_n\psi_{0j} + \delta\Omega_n\psi_{n0} \qquad n = 1,\ldots,M \quad (3.63)$$

$$\dot{\psi}_{n0} = \sqrt{\frac{2\Omega_n}{N}}\sum_{j=1}^{N}\cos\Omega_n\psi_{0j} - \delta\Omega_n\Gamma_{n0} \qquad n = 1,\ldots,M \quad (3.64)$$

$$\dot{\Gamma}_{0j} = \sqrt{\frac{2}{N}}\sum_{k=1}^{M}\Omega_k^{\frac{3}{2}}\left[\Gamma_{k0}\sin\Omega_k\psi_{0j} - \psi_{k0}\cos\Omega_k\psi_{0j}\right] \qquad j = 1,\ldots,N \quad (3.65)$$

$$\dot{\psi}_{0j} = \Gamma_{0j} \qquad j = 1,\ldots,N \quad (3.66)$$

The Hamiltonian that generates these equations of motion is:

$$\begin{aligned} H = & \sum_{j=1}^{N}\left[\frac{\Gamma_{0j}^2}{2} + \sqrt{\frac{2}{N}}\sum_{n=1}^{M}\Omega_n^{\frac{1}{2}}\left(\Gamma_{n0}\cos\Omega_n\psi_{0j} + \psi_{n0}\sin\Omega_n\psi_{0j}\right)\right] \\ & -\frac{\delta}{2}\sum_{n=1}^{M}\Omega_n\left(\Gamma_{n0}^2 + \psi_{n0}^2\right) \end{aligned} \quad (3.67)$$

where the equations of motion are generated by:

$$\dot{\Gamma}_{nj} = -\frac{\partial H}{\partial\psi_{nj}} \quad (3.68)$$

$$\dot{\psi}_{nj} = \frac{\partial H}{\partial\Gamma_{nj}} \quad (3.69)$$

In equations (3.68) and (3.69) the indices $n$ and $j$ may not both be nonzero in order for the proper equations to be generated.

### Conserved Quantities

In addition to the conserved quantity of the Hamiltonian, we have another conserved quantity:

$$\Delta_{\mathrm{mt}} \equiv \sum_{j=1}^{N}\Gamma_j + \sum_{n=1}^{M}\frac{\Omega_n}{2}\left(\Gamma_{n0}^2 + \psi_{n0}^2\right) \quad (3.70)$$

See B.2.2 in Appendix B for equations (3.63)-(3.70) in complex form.

### 3.1.4 Numerical Solution to Equations

As a final step in the model presentation we give an example of numerically solving equations (3.63)-(3.66). Generally the statements made in 2.1.4 apply in this section; however, additional comments are needed due to the multifrequency nature of the present model. Therefore, we structure this section nearly identically to Section 2.1.4 except for the appearance of the section entitled "Integration Methods and Stiffness"; stiffness is not an issue in the multitone equations.

#### Defining the Numerical Problem

The primary difference between the model equations in (3.63)-(3.66) and those of Chapter 2 is the existence of multiple frequencies. We have indicated that we are considering a Galerkin approximation, or a finite subset of frequencies that we are going to deem to be more necessary than others; indeed our model equations are for that finite set of frequencies. We choose our finite set $\Omega$ from the countably infinite frequency set, $\Omega_\infty = \{m\omega_f \text{ such that } m \text{ is a positive integer}\}$.[14] It is clear from this set definition that the closest two frequencies may be is $\omega_f$.

To demonstrate how one would choose frequencies we consider an example in which we wish to model two frequency drive, $\omega_1$ and $\omega_2$ with $\omega_1 < \omega_2$, and the nearest third order intermodulation products, $2\omega_1 - \omega_2$ and $2\omega_2 - \omega_1$. Say we choose $\omega_1 = 7\omega_f$ and $\omega_2 = 10\omega_f$. Then our frequency set becomes $\Omega = \{4, 7, 10, 13\}$. Note that 1 (or $\omega_f$) does not appear in the set and need not appear. The obvious question is to consider what might be the implications for leaving out the frequencies between those present. The answer is seen by running simulations with and without them present; they are not particularly "important" frequencies if their inclusion only slightly modifies the results of simulations. Indeed if one wanted more accurate

[14] Technically we choose the finite subset from $\Omega_\infty$, and then divide all elements by $\omega_f$ to arrive at $\Omega$.

results one would want to include harmonic frequencies of the drives before including the frequencies between those in $\Omega$. Also note that frequency choices must be carefully considered as we are assuming in the model infinite bandwidth which would not occur in practice. In other words some physical reasoning regarding what frequencies are entered into our set is appropriate; e.g. $10\omega_1$ is likely out of the bandwidth of any real TWT and hence its inclusion into our frequency set is not realistic.

Another very important consideration due to the multifrequency nature of the model is the choice of the number of initial phases, or the number of "disks". From a "digital sampling" viewpoint we must ensure that the period difference between closely spaced frequencies is sufficiently sampled. If we consider the spatial variation of the waves (related to $\omega$ by $v_0$) we might require a minimum number of particles initially distributed over the wavelength difference of closely spaced frequencies.[15] Letting the minimum number of particles per wavelength difference be $n$ (a quantity one establishes with experience), the wavelength associated with $\omega_f$ to be $\lambda_f$, the total particle number $N$, and the difference between two closely spaced frequencies to be $\Delta\lambda \equiv \lambda_b - \lambda_a > 0$ we may write:

$$\frac{\Delta\lambda}{\lambda_f} N \geq n \tag{3.71}$$

Using the relation $\lambda = \frac{v_0 2\pi}{\omega}$ we may rearrange (3.71) to get:

$$\Delta\omega \geq \frac{n}{N} \frac{\omega_a \omega_b}{\omega_f} \tag{3.72}$$

In (3.72) we have $\Delta\omega = \omega_a - \omega_b > 0$. Perhaps a more useful version of (3.72) will be an expression for the minimum number of particles required for a given frequency separation. For a worst case estimate we replace the frequency product $\omega_a\omega_b$ by the larger product $\omega_a^2$ and are left with:

$$N \geq \frac{n}{\Delta\omega} \frac{\omega_a^2}{\omega_f} \tag{3.73}$$

[15] This is equivalently formulated with regards to time period differences between two frequencies, but it is felt that the spatial picture is easier to consider.

Note that the inequality only holds prior to the interaction. When bunching has occurred we obviously cannot guarantee to sample all spatial points evenly. This is another reason the value of $n$ comes with experience.

As a final numerical issue we mention that when doing numerical simulations one might like to rescale the length in (3.6). Namely, one might let:

$$\tilde{y} \equiv C\frac{\omega_{\max}}{u_0}z \tag{3.74}$$

In (3.74) $\omega_{\max}$ is the maximum frequency present in the simulation. The reason for doing this is that saturation lengths in $\tilde{y}$ will come out similar even for disparate frequencies. If one does not employ this definition saturation lengths simply may vary widely for different frequency choices. When using (3.74) the definition of $\psi$ must change as well, namely:

$$\tilde{\psi} \equiv \omega_{\max}\left(\frac{z}{u_0} - t\right) \tag{3.75}$$

The frequency $\Omega_n$ requires a new definition as well:

$$\tilde{\Omega}_n \equiv \frac{\omega_n}{\omega_{\max}} \tag{3.76}$$

With these new definitions one may check that the model equations in (3.57)-(3.60) do not change by substituting the relations between old and new variables: $y = \frac{\omega_f}{\omega_{\max}}\tilde{y}$, $\psi = \frac{\omega_f}{\omega_{\max}}\tilde{\psi}$, and $\Omega_n = \frac{\omega_{\max}}{\omega_f}\tilde{\Omega}_n$.[16] The differentiation is then with respect to $\tilde{y}$ [17] and the meaning of the phase variables in the equations are now phases with respect to the highest frequency present. As such one must handle phase initialization differently as well; initial phases must take values from 0 to $\frac{\omega_{\max}}{\omega_f}2\pi$. The set of frequencies $\tilde{\Omega}$ is now a set of fractions rather than a set of integers; the largest entry in $\tilde{\Omega}$ is $\frac{\omega_{\max}}{\omega_{\max}} = 1$.

[16] If one does the substitution into equations (3.63)-(3.66) there are some multiplying factors remaining. The reason for this is that variable changes in Hamiltonian systems are very particular, i.e. only certain types of variable changes preserve Hamiltonian structure.

[17] The expression for $\frac{d}{d\tilde{y}}$ can be obtained by the chain rule for example.

**Simulations**

Lastly we present an example of the results of integrating equations (3.63)-(3.66). We choose the problem discussed previously of two drive tones and the nearest intermodulation frequencies with the frequency set $\Omega = \{4, 7, 10, 13\}$. The beam is initially uniformly distributed and monoenergetic. The simulation parameters and initial data are presented in Table 3.1. The simulation does not use the rescaled variables in (3.74)-(3.76), rather the standard variables.

In Figure 3.1 we plot amplitudes of the tones as defined by:

$$A_n = \sqrt{a_{1n}^2 + a_{2n}^2} \tag{3.77}$$

Transformations between $a_{1n}$, $a_{2n}$ and $\Gamma_{n0}$, $\psi_{n0}$ are made using (3.61) and (3.62). Notice in general that higher frequency components (both drive and intermodulation) tend to grow faster.

In Figure 3.2 we plot a representative group of disk trajectories; we show every $5^{\text{th}}$ disk. Notice the splitting of the disk phases into several sub-bunches due to the multitone drive.

## 3.2 Equilibrium and Linearization

Finally with regards to initial investigation of the multitone TWT model we consider the equilibrium as was done in the single tone case. We identify the equilibrium, consider the linearization about the equilibrium, and finally linearize by way of collective variables.

### 3.2.1 Identification of an Equilibrium and the Jacobian Matrix

One can quickly convince oneself that the equilibrium condition from the single tone case makes physical and mathematical sense in the multitone equations. That

| Parameter | Value |
|---|---|
| $\delta$ | 1.0 |
| $N$ | 130 |
| $n$ | 2 |
| $\omega_f$ | 1.0 |
| $a_{11}(0)$ | 0.0 |
| $a_{21}(0)$ | 0.0 |
| $a_{12}(0)$ | 0.007 |
| $a_{22}(0)$ | 0.0 |
| $a_{13}(0)$ | 0.001 |
| $a_{23}(0)$ | 0.0 |
| $a_{14}(0)$ | 0.0 |
| $a_{24}(0)$ | 0.0 |
| $\Omega_1$ | 4 |
| $\Omega_2$ | 7 |
| $\Omega_3$ | 10 |
| $\Omega_4$ | 13 |
| $\Gamma_j(0)$ | 0.0 |
| $\psi_j(0)$ | $2\pi(j-1)/N$ |

Table 3.1: Simulation parameters and initial data for presented results. The values for $\Gamma_{n0}$ and $\psi_{n0}$ are obtained from (3.61) and (3.62). For $\Gamma_j(0)$ and $\psi_j(0)$ $j$ takes on values $1, \ldots, N$. A lower bound on $N$ was determined from equation (3.73) with $n = 2$, $\Delta\omega = 3$, and $\omega_a = \Omega_4\omega_f$.

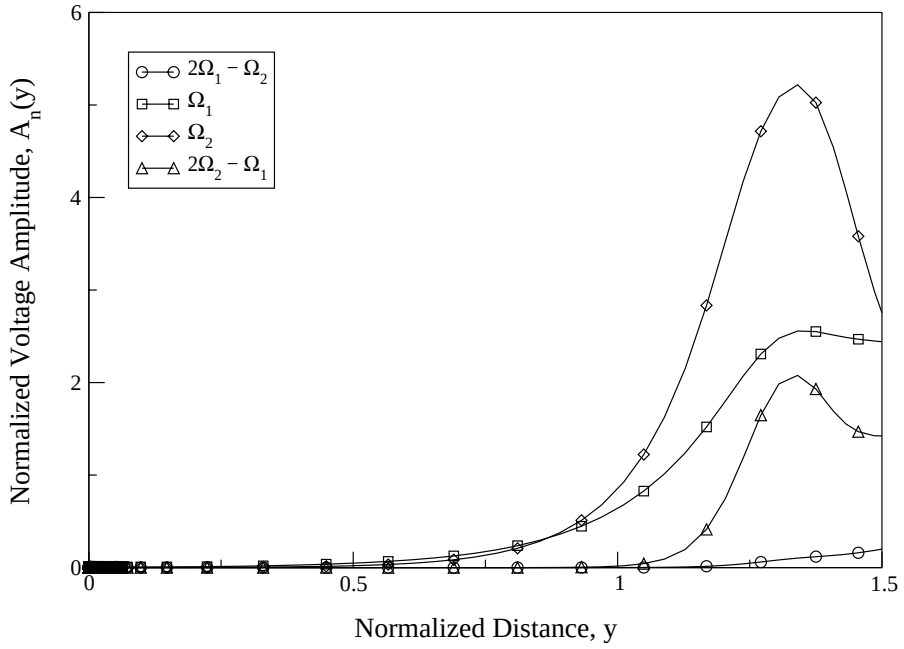


Figure 3.1: Normalized amplitudes, $A_n(y)$ as in (3.77), versus normalized distance $y$.

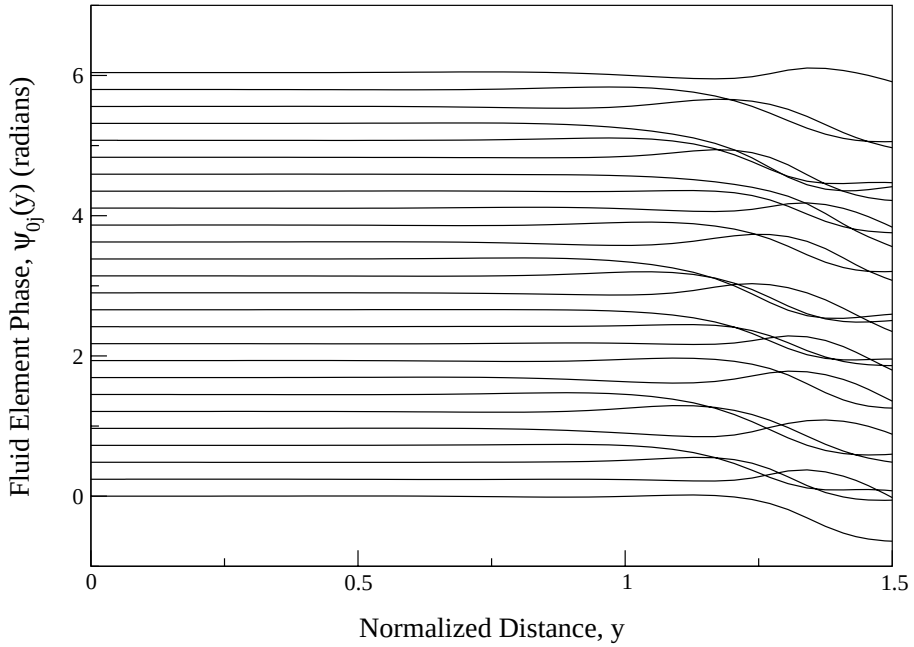


Figure 3.2: Fluid element phases, $\psi_{0j}(y)$, versus normalized distance $y$.

is, for a uniformly distributed monoenergetic beam and zero voltage amplitudes for all tones the right hand sides of equations (3.63)-(3.66) are zero. Small perturbations from this point are characterized by the eigenvalues and eigenvectors of the Jacobian matrix.

For the equilibrium the disk phases are evenly distributed over one period, $T_f$, corresponding to the fundamental frequency. This is also a period shared by all other frequencies (not their fundamental period necessarily); as such the sums of sines and cosines of these phases add to zero. The fact that all other terms on the right hand side of the system are zero is immediately obvious.

We directly present the Jacobian matrix in a similar manner to the method of Chapter 2. The difference in structure is purely due to the presence of multiple tones. That is, the first two columns and first two rows of the Jacobian in the single tone case will be replaced with $2M$ rows and $2M$ columns. The overall structure is:

$$\mathbf{Df} = \left[\begin{array}{c|c|c|c} \mathbf{A_{mt}} & \mathbf{B_{mt}} & \mathbf{C_{mt}} & \mathbf{D_{mt}} \\ \hline \mathbf{E_{mt}} & \mathbf{F_{mt}} & \mathbf{G_{mt}} & \mathbf{H_{mt}} \\ \hline \mathbf{K_{mt}} & \mathbf{L_{mt}} & \mathbf{M_{mt}} & \mathbf{N_{mt}} \\ \hline \mathbf{O_{mt}} & \mathbf{P_{mt}} & \mathbf{Q_{mt}} & \mathbf{R_{mt}} \end{array}\right] \qquad 2(N+M) \times 2(N+M) \tag{3.78}$$

The blocks in (3.78) are given by:

$$\mathbf{A_{mt}} = [\mathbf{0}] \qquad M \times M \tag{3.79}$$

$$\mathbf{B_{mt}} = \begin{bmatrix} \delta\Omega_1 & 0 & \cdots & 0 \\ 0 & \delta\Omega_2 & \cdots & 0 \\ \vdots & & \ddots & \vdots \\ 0 & 0 & \cdots & \delta\Omega_M \end{bmatrix} \qquad M \times M \tag{3.80}$$

$$\mathbf{C_{mt}} = [\mathbf{0}] \qquad M \times N \tag{3.81}$$

$$\mathbf{D_{mt}} = \begin{bmatrix} -\sqrt{\frac{2\Omega_1^3}{N}}\cos\Omega_1\psi_{01} & \cdots & -\sqrt{\frac{2\Omega_1^3}{N}}\cos\Omega_1\psi_{0N} \\ -\sqrt{\frac{2\Omega_2^3}{N}}\cos\Omega_2\psi_{01} & \cdots & -\sqrt{\frac{2\Omega_2^3}{N}}\cos\Omega_2\psi_{0N} \\ \vdots & & \vdots \\ -\sqrt{\frac{2\Omega_M^3}{N}}\cos\Omega_M\psi_{01} & \cdots & -\sqrt{\frac{2\Omega_M^3}{N}}\cos\Omega_M\psi_{0N} \end{bmatrix} \qquad M \times N \tag{3.82}$$

$$\mathbf{E_{mt}} = \begin{bmatrix} -\delta\Omega_1 & 0 & \cdots & 0 \\ 0 & -\delta\Omega_2 & \cdots & 0 \\ \vdots & & \ddots & \vdots \\ 0 & 0 & \cdots & -\delta\Omega_M \end{bmatrix} \qquad M \times M \tag{3.83}$$

$$\mathbf{F_{mt}} = [\mathbf{0}] \qquad M \times M \tag{3.84}$$

$$\mathbf{G_{mt}} = [\mathbf{0}] \qquad M \times N \tag{3.85}$$

$$\mathbf{H_{mt}} = \begin{bmatrix} -\sqrt{\frac{2\Omega_1^3}{N}}\sin\Omega_1\psi_{01} & \cdots & -\sqrt{\frac{2\Omega_1^3}{N}}\sin\Omega_1\psi_{0N} \\ -\sqrt{\frac{2\Omega_2^3}{N}}\sin\Omega_2\psi_{01} & \cdots & -\sqrt{\frac{2\Omega_2^3}{N}}\sin\Omega_2\psi_{0N} \\ \vdots & & \vdots \\ -\sqrt{\frac{2\Omega_M^3}{N}}\sin\Omega_M\psi_{01} & \cdots & -\sqrt{\frac{2\Omega_M^3}{N}}\sin\Omega_M\psi_{0N} \end{bmatrix} \qquad M \times N \tag{3.86}$$

$$\mathbf{K_{mt}} = \begin{bmatrix} \sqrt{\frac{2\Omega_1^3}{N}}\sin\Omega_1\psi_{01} & \cdots & \sqrt{\frac{2\Omega_M^3}{N}}\sin\Omega_M\psi_{01} \\ \sqrt{\frac{2\Omega_1^3}{N}}\sin\Omega_1\psi_{02} & \cdots & \sqrt{\frac{2\Omega_M^3}{N}}\sin\Omega_M\psi_{02} \\ \vdots & & \vdots \\ \sqrt{\frac{2\Omega_1^3}{N}}\sin\Omega_1\psi_{0N} & \cdots & \sqrt{\frac{2\Omega_M^3}{N}}\sin\Omega_M\psi_{0N} \end{bmatrix} \qquad N \times M \tag{3.87}$$

$$\mathbf{L_{mt}} = \begin{bmatrix} -\sqrt{\frac{2\Omega_1^3}{N}}\cos\Omega_1\psi_{01} & \cdots & -\sqrt{\frac{2\Omega_M^3}{N}}\cos\Omega_M\psi_{01} \\ -\sqrt{\frac{2\Omega_1^3}{N}}\cos\Omega_1\psi_{02} & \cdots & -\sqrt{\frac{2\Omega_M^3}{N}}\cos\Omega_M\psi_{02} \\ \vdots & & \vdots \\ -\sqrt{\frac{2\Omega_1^3}{N}}\cos\Omega_1\psi_{0N} & \cdots & -\sqrt{\frac{2\Omega_M^3}{N}}\cos\Omega_M\psi_{0N} \end{bmatrix} \qquad N \times M \tag{3.88}$$

$$\mathbf{M_{mt}} = [\mathbf{0}] \qquad N \times N \tag{3.89}$$

$$\mathbf{N_{mt}} = \begin{bmatrix} \sum_{n=1}^{M}\sqrt{\frac{2\Omega_n^5}{N}}[\Gamma_{n0}\cos\Omega_n\psi_{01} & \cdots & 0 \\ \quad -\psi_{n0}\sin\Omega_n\psi_{01}] & & \\ \vdots & \ddots & \vdots \\ 0 & \cdots & \sum_{n=1}^{M}\sqrt{\frac{2\Omega_n^5}{N}}[\Gamma_{n0}\cos\Omega_n\psi_{0N} \\ & & \quad -\psi_{n0}\sin\Omega_n\psi_{0N}] \end{bmatrix}$$

$$\text{Diagonal} : N \times N \tag{3.90}$$

$$\mathbf{O_{mt}} = [\mathbf{0}] \qquad N \times M \tag{3.91}$$

$$\mathbf{P_{mt}} = [\mathbf{0}] \qquad N \times M \tag{3.92}$$

$$\mathbf{Q_{mt}} = \begin{bmatrix} 1 & 0 & \cdots & 0 \\ 0 & 1 & \cdots & 0 \\ \vdots & & \ddots & \vdots \\ 0 & 0 & \cdots & 1 \end{bmatrix} \qquad N \times N \tag{3.93}$$

$$\mathbf{R_{mt}} = [\mathbf{0}] \qquad N \times N \tag{3.94}$$

When **Df** is evaluated at the equilibrium point, block $\mathbf{N_{mt}}$ is a zero matrix.

### 3.2.2 Linearization by Method of Collective Variables

Finally we do a linearization by defining collective variables as we did in Section 2.2.3. The development is completely analogous except that now we have collective variables for each tone, i.e. where we had the variable $\mathcal{B}$ in Section 2.2.3 we will have $M$ variables, $\mathcal{B}_n$. Likewise we will have the variables $\mathcal{P}_n$ that will be $M$ in number. After the definitions are made we derive differential equations for the new variables and linearize them about the equilibrium point.

We begin by noting that we will want:

$$\Xi_n \equiv \Gamma_{n0} + i\psi_{n0} \tag{3.95}$$

With this definition one can derive the following differential equation for $\Xi_n$:

$$\dot{\Xi}_n = i\sqrt{\frac{2\Omega_n}{N}} \sum_{j=1}^{N} e^{i\Omega_n \psi_{0j}} - i\delta\Omega_n \Xi_n \tag{3.96}$$

Define a bunching parameter for the $n^{\text{th}}$ tone based on the first term on the right hand side of (3.96).

$$\mathcal{B}_n \equiv i\sqrt{\frac{2}{N\Omega_n}} \sum_{j=1}^{N} e^{i\Omega_n \psi_{0j}} \tag{3.97}$$

With (3.97) the new differential equation for $\Xi_n$ becomes:

$$\dot{\Xi}_n = \Omega_n \mathcal{B}_n - i\delta\Omega_n \Xi_n \tag{3.98}$$

We now want to derive a differential equation for $\mathcal{B}_n$. Differentiating (3.97) and using (3.66) we get:

$$\dot{\mathcal{B}}_n = -\Omega_n \sqrt{\frac{2}{N\Omega_n}} \sum_{j=1}^{N} \Gamma_{0j} e^{i\Omega_n \psi_{0j}} \tag{3.99}$$

From this we define a new variable, $\mathcal{P}_n$, such that (3.99) becomes:

$$\dot{\mathcal{B}}_n = i\Omega_n \mathcal{P}_n \tag{3.100}$$

The definition for $\mathcal{P}_n$ is:

$$\mathcal{P}_n \equiv i\sqrt{\frac{2}{N\Omega_n}}\sum_{j=1}^{N}\Gamma_{0j}e^{i\Omega_n\psi_{0j}} \tag{3.101}$$

We then derive the differential equation for $\mathcal{P}_n$ by differentiating (3.101) and using (3.65), (3.66), and (A.4). After some work we arrive at:

$$\begin{aligned}\dot{\mathcal{P}}_n &= -\frac{1}{N\Omega_n^{\frac{1}{2}}}\sum_{j=1}^{N}\left\{\sum_{k=1}^{M}\Omega_k^{\frac{3}{2}}\left[\Xi_k e^{-i(\Omega_k-\Omega_n)\psi_{0j}} - \Xi_k^* e^{i(\Omega_k+\Omega_n)\psi_{0j}}\right]\right. \\ &\quad \left. + \sqrt{2N}\Omega_n\Gamma_{0j}^2 e^{i\Omega_n\psi_{0j}}\right\}\end{aligned} \tag{3.102}$$

We now separate the term in the summation in which $k = n$. The result may be expressed as:

$$\begin{aligned}\dot{\mathcal{P}}_n &= -\Omega_n\Xi_n - \frac{1}{N\Omega_n^{\frac{1}{2}}}\sum_{j=1}^{N}\left\{\sum_{\substack{k=1\\k\neq n}}^{M}\Omega_k^{\frac{3}{2}}\left[\Xi_k e^{-i(\Omega_k-\Omega_n)\psi_{0j}}\right.\right. \\ &\quad \left.\left. -\Xi_k^* e^{i(\Omega_k+\Omega_n)\psi_{0j}}\right] - \Omega_n^{\frac{3}{2}}\Xi_n^* e^{i2\Omega_n\psi_{0j}} + \sqrt{2N}\Omega_n\Gamma_{0j}^2 e^{i\Omega_n\psi_{0j}}\right\}\end{aligned} \tag{3.103}$$

Linearizing equation (3.103) about the equilibrium leaves the following $3\times 3$ system per tone (see Appendix C for details of the linearization.):

$$\dot{\Xi}_n = \Omega_n\mathcal{B}_n - i\delta\Omega_n\Xi_n \tag{3.104}$$

$$\dot{\mathcal{B}}_n = i\Omega_n\mathcal{P}_n \tag{3.105}$$

$$\dot{\mathcal{P}}_n = -\Omega_n\Xi_n \tag{3.106}$$

Therefore, for a system of $M$ tones one gets the following decoupled block diagonal system:

$$\dot{\mathbf{w}} = \mathcal{D}\mathbf{w} \tag{3.107}$$

The structure of the vector $\mathbf{w}$ is:

$$\mathbf{w} = \left[\Xi_1\ \mathcal{B}_1\ \mathcal{P}_1\ \Xi_2\ \mathcal{B}_2\ \mathcal{P}_2 \ldots \Xi_M\ \mathcal{B}_M\ \mathcal{P}_M\right]^{\mathrm{T}} \tag{3.108}$$

The structure of $\mathcal{D}$ is:

$$\mathcal{D} = \begin{bmatrix} \mathcal{D}_1 & 0 & \dots & 0 \\ 0 & \mathcal{D}_2 & \dots & 0 \\ \vdots & & \ddots & \vdots \\ 0 & 0 & \dots & \mathcal{D}_M \end{bmatrix} \qquad 3M \times 3M \tag{3.109}$$

The blocks, $\mathcal{D}_n$ are given by:

$$\mathcal{D}_n = \begin{bmatrix} -i\delta\Omega_n & \Omega_n & 0 \\ 0 & 0 & i\Omega_n \\ -\Omega_n & 0 & 0 \end{bmatrix} \tag{3.110}$$

Since the frequencies are decoupled in (3.107) we may compute a general expression for the eigenvalues of (3.110) which will apply for all $n$. This expression is:

$$\mu^3 + i\delta\Omega_n\mu^2 + i\Omega_n^3 = 0 \tag{3.111}$$

Note that if we substitute the relation $\mu = \Omega_n\lambda$ we obtain equation (2.73). Therefore solutions to (2.73) need only be scaled by $\Omega_n$ to be a solution to (3.111). In this way we see that higher frequencies have larger growth rates.

# Chapter 4

# Conclusions

## 4.1 Results

The majority of the thesis is devoted to a redevelopment of a Lagrangian multitone model for a TWT. The model developed is not materially novel, but the choice of coordinates is; this includes the multitone model written in Hamiltonian coordinates. The coordinates are chosen in part for the model's amenability to analysis with tools from dynamical systems theory when written in these coordinates. Furthermore, in the model development we stress that Lagrangian coordinates are a fluid description and the TWT model is described by partial differential equations. As a separate step we discretize the partial differential equations by choosing a finite number of fluid elements. The result of this is a TWT description using ordinary differential equations. This distinction between the Lagrangian coordinates and the discretization is often confused in the literature.

Several results of numerical integration of the model equations are presented in the thesis. We discuss the issue of stiffness which occurs in the models, and its effect on integration routines. In Figure 2.5 a novel illustration of electron beam evolution is presented which stresses the partial vs. ordinary differential equation descriptions.

The linearization of the discretized Lagrangian models as performed in the thesis cannot be found elsewhere in the literature. The linearization confirms the instability in the model, and offers a unique perspective on the coupling between

different state variables via the eigenvalue and eigenvector analysis. The linearization by collective variables offers even further physical insight and a reduced dimensional system view of the TWT.

Lastly, the level of detail included in physical descriptions of the model equations is very high and as such is a good place for one unfamiliar with such models to become introduced to them.

## 4.2 Future Work

One can simplify the discretized multitone model and write it as an affine system. This system is "mildly" nonlinear, and in fact contains just the right amount of detail to predict growth of unwanted frequencies. This model is being investigated for insight into the generation of intermodulation and harmonic frequencies. In conjunction with the affine system we are investigating quasi-linear equations that are related to the Lagrangian model to decidedly identify the mechanism of intermodulation and harmonic growth. With information garnered from these studies we hope to prescribe electron beam modulation strategies for reduction of the unwanted spectral content.

## Bibliography


[1] R. Abraham and J. E. Marsden. *Foundations of Mechanics: A mathematical exposition of classical mechanics with an introduction to the qualitative theory of dynamical systems and applications to the three-body problem.* Addison-Wesley Publishing Co., Inc., Reading, Massachusetts, 1978.

[2] T. M. Antonsen, Jr. and B. Levush. Christine: A multifrequency parametric simulation code for traveling wave tube amplifiers. *NRL Memo report NRL/FR/6840-97-9845*, 1997.

[3] T. M. Antonsen, Jr. and B. Levush. Traveling-wave tube devices with nonlinear dielectric elements. *IEEE Transactions on Plasma Science*, 26(3):774–786, 1998.

[4] T. M. Antonsen, Jr., A. Mondelli, B. Levush, J. P. Verboncoeur, and C. K. Birdsall. Advances in modeling and simulation of vacuum electronic devices. *Proceedings of the IEEE*, 87(5):804–839, 1999.

[5] V. I. Arnold. *Mathematical Methods of Classical Mechanics*, volume 60 of *Graduate Texts in Mathematics*. Springer Verlag, New York, 1978.

[6] V. Barger and M. Olsson. *Classical Mechanics: A Modern Perspective*. McGraw-Hill, New York, 1973.

[7] R. Bonifacio, F. Casagrande, and M. Milani. Analogy between free-electron lasers and Josephson junctions. *Lettere Al Nuovo Cimento*, 34(17):520–524, 1982.

[8] F. Casagrande, R. Bonifacio, and A. Airoldi. The self-consistent pendulum picture of the free electron laser revised and the instability threshold for exponential gain. *Nuclear Instruments and Methods in Physics Research*, A304:439–443, 1991.

[9] C.T. Chen. *Linear System Theory and Design*. The Oxford Series in Electrical and Computer Engineering. Oxford University Press, New York, second edition, 1984.

[10] E. A. Coddington and N. Levinson. *Theory of Ordinary Differential Equations*. McGraw-Hill, New York, 1955.

[11] M. C. Converse. Private communication. December, 1999.

[12] C. C. Cutler. The nature of power saturation in traveling wave tubes. *The Bell System Technical Journal*, 35:841–876, July 1956.

[13] H. Dankowicz. *Chaotic Dynamics in Hamiltonian Systems*. World Scientific, Singapore, 1997.

[14] S. K. Datta, P. K. Jain, and B. N. Basu. Third-order saturation effects in a helix traveling-wave tube under Eulerian approximations. *Microwave and Optical Technology Letters*, 16(6):345–349, 1997.

[15] S. K. Datta, P. K. Jain, M. D. Raj Narayan, and B. N. Basu. Eulerian analysis for harmonic generation and its control in a helix travelling-wave tube. *International Journal of Electronics*, 85(3):377–395, 1998.

[16] S. K. Datta, P. K. Jain, M. D. Raj Narayan, and B. N. Basu. Nonlinear Eulerian hydrodynamical analysis of helix traveling-wave tubes. *IEEE Transactions on Electron Devices*, 45(9):2055–2062, 1998.

[17] S. K. Datta, P. K. Jain, M. D. Raj Narayan, and B. N. Basu. Nonlinear Eulerian hydrodynamical analysis of helix traveling-wave tubes for harmonic generation and its control. *IEEE Transactions on Electron Devices*, 46(2):420–426, 1999.

[18] S. K. Datta, S. U. M. Reddy, B. N. Basu, and K. U. Limaye. A novel Lagrangian simulation technique for helix traveling-wave tubes. *Microwave and Optical Technology Letters*, 18(4):308–310, 1998.

[19] D. del-Castillo-Negrete. Self-consistent chaotic transport in fluids and plasmas. *Chaos*, 10(1):75–88, March 2000.

[20] N. J. Dionne. Harmonic generation in octave bandwidth traveling-wave tubes. *IEEE Transactions on Electron Devices*, ED-17(4):365–372, 1970.

[21] H. P. Freund. Nonlinear theory of helix traveling wave tubes in the frequency domain. *Physics of Plasmas*, 6(9):3633–3646, 1999.

[22] H. P. Freund and E. G. Zaidman. Nonlinear theory of collective effects in helix traveling wave tubes. *Physics of Plasmas*, 4(6):2292–2301, 1997.

[23] C. William Gear. *Numerical Initial Value Problems in Ordinary Differential Equations*. Prentice-Hall, Inc., Englewood Cliffs, N.J., 1971.

[24] J. W. Gewartowski and H. A. Watson. *Principles of Electron Tubes*. D. Van Nostrand Co., Inc., Princeton, 1965.

[25] A. J. Giarola. A theoretical description for the multiple-signal operation of a TWT. *IEEE Transactions on Electron Devices*, ED-15(6):381–395, June 1968.

[26] A. S. Gilmour, Jr. *Principles of Traveling Wave Tubes*. Artech House, Boston, 1994.

[27] H. Goldstein. *Classical Mechanics*. Addison-Wesley Publishing Co., Inc., Reading, Massachusetts, 1980.

[28] J. Guckenheimer and P. Holmes. *Nonlinear Oscillations, Dynamical Systems, and Bifurcations of Vector Fields*, volume 42 of *Applied Mathematical Sciences*. Springer Verlag, New York, 1981.

[29] W. Hansard, editor. *Eulerian and Lagrangian Descriptions in Fluid Mechanics*. Fluid Mechanics Films. Encyclopedia Britannica Educational Corp., Chicago, 1985.

[30] M. Hirsch and S. Smale. *Differential Equations, Dynamical Systems, and Linear Algebra*. Academic Press, San Diego, 1974.

[31] H.P. Hsu. *Signals and Systems*. Schaum's Outline Series. McGraw-Hill, New York, 1995.

[32] L. Lapidus and J. H. Seinfeld. *Numerical Solution of Ordinary Differential Equations*. Academic Press, New York, 1971.

[33] S. Liao. *Microwave Electron-Tube Devices*. Prentice Hall, Englewood Cliffs, 1988.

[34] A. J. Lichtenberg and M. A. Lieberman. *Regular and Chaotic Dynamics*, volume 38 of *Applied Mathematical Sciences*. Springer Verlag, New York, 1992.

[35] J. D. Meiss. Symplectic maps, variational principles, and transport. *Reviews of Modern Physics*, 64:795–848, 1992.

[36] L. M. Milne-Thomson. *Theoretical Hydrodynamics*. MacMillan & Co LTD, London, 1968.

[37] I. J. Morey and C. K. Birdsall. Traveling-wave-tube simulation: The IBC code. *IEEE Transactions on Plasma Science*, 18(3):482–489, 1990.

[38] A. Nordsieck. Theory of the large signal behavior of traveling-wave amplifiers. *Proceedings of the I. R. E.*, 41:630–637, May 1953.

[39] F. Paschke. On the nonlinear behavior of electron-beam devices. *RCA Rev.*, 18:221–242, 1957.

[40] F. Paschke. Generation of second harmonic in a velocity-modulated electron beam of finite diameter. *RCA Rev.*, 19:617–627, 1958.

[41] F. Paschke. Nonlinear theory of a velocity-modulated electron beam with finite diameter. *RCA Rev.*, 21:53–74, 1960.

[42] I. Percival and D. Richards. *Introduction to Dynamics*. Cambridge University Press, New York, 1982.

[43] L. Perko. *Differential Equations and Dynamical Systems*, volume 7 of *Texts in Applied Mathematics*. Springer Verlag, New York, 1996.

[44] J. R. Pierce. Theory of the beam-type traveling-wave tube. *Proceedings of the I.R.E.*, 35:111–123, 1947.

[45] J. R. Pierce. *Traveling Wave Tubes*. Van Nostrand, Princeton, N.J., 1950.

[46] W. H. Press, S. A. Teukolsky, W. T. Vetterling, and B. P. Flannery. *Numerical Recipies in C: The Art of Scientific Computing*. Cambridge University Press, Cambridge, 1997.

[47] A. J. Roberts. *A One-Dimensional Introduction to Continuum Mechanics*. World Scientific, Singapore, 1994.

[48] C. Robinson. *Dynamical Systems: Stability, Symbolic Dynamics, and Chaos*. Studies in Advanced Mathematics. CRC Press, Boca Raton, 1999.

[49] J. E. Rowe. *Nonlinear Electron-Wave Interaction Phenomena*. Academic Press, New York, 1965.

[50] M. K. Scherba and J. E. Rowe. Characteristics of multisignal and noise-modulated high-power microwave amplifiers. *IEEE Transactions on Electron Devices*, ED-18(1):11–34, 1971.

[51] B. Schutz. *Geometrical Methods of Mathematical Physics*. Cambridge University Press, Cambridge, 1980.

[52] S. Sensiper. Electromagnetic wave propagation on helical structures (a review and survey of recent progress). *Proceedings of the I.R.E.*, 43:149–161, 1955.

[53] V. Srivastava and S. N. Joshi. Improved nonlinear model for multisignal analysis of helix TWTs. *IEE Proceedings-H*, 139(2):129–134, 1992.

[54] S. H. Strogatz. *Nonlinear Dynamics and Chaos: With Applications to Physics, Biology, Chemistry and Engineering*. Addison-Wesley Publishing Co., Inc., Reading, Massachusetts, 1994.

[55] C. A. Truesdell. *A First Course in Rational Continuum Mechanics*, volume 71 of *Pure and Applied Mathematics*. Academic Press, San Diego, 1991.

# Appendix A

## Useful Identities

For $A \equiv a_1 + ia_2$, $\psi \in R$:

$$\begin{aligned} \frac{1}{2}\left[Ae^{i\psi} + c.c.\right] &= a_1 \cos\psi - a_2 \sin\psi \\ &= \frac{\partial}{\partial\psi}\left\{\frac{1}{2i}\left[Ae^{i\psi} - c.c.\right]\right\} \end{aligned} \tag{A.1}$$

$$\begin{aligned} \frac{1}{2i}\left[Ae^{i\psi} - c.c.\right] &= a_2 \cos\psi + a_1 \sin\psi \\ &= -\frac{\partial}{\partial\psi}\left\{\frac{1}{2}\left[Ae^{i\psi} + c.c.\right]\right\} \end{aligned} \tag{A.2}$$

$$\begin{aligned} \frac{1}{2}\left[Ae^{-i\psi} + c.c.\right] &= a_1 \cos\psi + a_2 \sin\psi \\ &= -\frac{\partial}{\partial\psi}\left\{\frac{1}{2i}\left[Ae^{-i\psi} - c.c.\right]\right\} \end{aligned} \tag{A.3}$$

$$\begin{aligned} \frac{1}{2i}\left[Ae^{-i\psi} - c.c.\right] &= a_2 \cos\psi - a_1 \sin\psi \\ &= \frac{\partial}{\partial\psi}\left\{\frac{1}{2}\left[Ae^{-i\psi} + c.c.\right]\right\} \end{aligned} \tag{A.4}$$

Where *c.c.* denotes complex conjugate.

# Appendix B

## Alternative Model Equations

In many cases the TWT equations can be written differently from what is presented in the body of the thesis. Since these alternate representations do not add conceptually to the material we present them in this appendix. In B.1 the single tone equations are presented in variables similar to that used in the FEL theory of [8]. Additionally, the single tone equations are written with magnitude and phase variables for the voltage amplitude. In B.2 we present similar results for the multitone model.

### B.1 Single Tone Model in Alternative Variables

The single tone discretized TWT model as presented in Chapter 2 is essentially identical to the model derived for a high gain FEL in [8]. The variables in [8] differ from our choices and therefore we present our models in the complex notation of [8]. In B.1.1 the cold circuit phase velocity reference frame formulation including model equations and Hamiltonian is presented. In B.1.2 we transform the results in B.1.1 to the initial electron beam velocity reference frame. In B.1.3 equations (2.37)-(2.44) are written in complex variables. Finally, in B.1.4 equations (2.37)-(2.44) are written in magnitude and phase variables.

### B.1.1 Equations (2.20)-(2.23) in Complex Variables

See section 2.1.3 for the discretized TWT model as formulated in the cold circuit phase velocity reference frame.

#### Model Equations

The variables $a_1$ and $a_2$ may be combined into a complex variable and equations (2.20)-(2.23) may be written as:

$$\dot{A} = -i\langle e^{-i\Phi_j}\rangle \tag{B.1}$$

$$\dot{w}_j = -i[Ae^{i\Phi_j} - c.c.] \qquad j = 1, \ldots, N \tag{B.2}$$

$$\dot{\Phi}_j = w_j \qquad j = 1, \ldots, N \tag{B.3}$$

where $A \equiv \frac{a_1}{4} + i\frac{a_2}{4}$ and $\langle\cdot\rangle$ indicates average over all particles ($\langle\cdot\rangle = N^{-1}\sum_{j=1}^{N}$).

#### Hamiltonian

Hamiltonian function:

$$H = \sum_{j=1}^{N} \frac{{w_j}^2}{2} + \left[A\sum_{j=1}^{N} e^{i\Phi_j} + c.c.\right] \tag{B.4}$$

The equations of motion are generated by:

$$\dot{\Phi}_j = \frac{\partial H}{\partial w_j} \qquad j = 1, \ldots, N \tag{B.5}$$

$$\dot{w}_j = -\frac{\partial H}{\partial \Phi_j} \qquad j = 1, \ldots, N \tag{B.6}$$

$$\dot{A} = -\frac{i}{N}\frac{\partial H}{\partial A^*} \tag{B.7}$$

### B.1.2 Equations (B.1)-(B.3) in the Beam Frame

**Model Equations**

Equations (B.1)-(B.3) may be transformed from the circuit frame to the beam frame by letting $\mathcal{A} \equiv Ae^{iby}$ and using transformations (2.35) and (2.36). The transformation yields:

$$\dot{\mathcal{A}} = -i\langle e^{-i\psi_j}\rangle + ib\mathcal{A} \tag{B.8}$$

$$\dot{\Gamma}_j = -i[\mathcal{A}e^{i\psi_j} - c.c.] \qquad j = 1, \ldots, N \tag{B.9}$$

$$\dot{\psi}_j = \Gamma_j \qquad j = 1, \ldots, N \tag{B.10}$$

**Hamiltonian**

Hamiltonian function:

$$H = \sum_{j=1}^{N} \frac{\Gamma_j^2}{2} + \left[\mathcal{A}\sum_{j=1}^{N} e^{i\psi_j} + c.c.\right] - Nb\mathcal{A}\mathcal{A}^* \tag{B.11}$$

The equations of motion are generated by:

$$\dot{\psi}_j = \frac{\partial H}{\partial \Gamma_j} \qquad j = 1, \ldots, N \tag{B.12}$$

$$\dot{\Gamma}_j = -\frac{\partial H}{\partial \psi_j} \qquad j = 1, \ldots, N \tag{B.13}$$

$$\dot{\mathcal{A}} = -\frac{i}{N}\frac{\partial H}{\partial \mathcal{A}^*} \tag{B.14}$$

### B.1.3 Equations (2.37)-(2.44) in Complex Variables

**Model Equations**

If we define $\Xi \equiv \Gamma_0 + i\psi_0$, then equations (2.37)-(2.40) become:

$$\dot{\Xi} = -\sqrt{2N}\langle e^{i\psi_j}\rangle - ib\Xi \tag{B.15}$$

$$\dot{\Gamma}_j = \frac{1}{\sqrt{2N}}\left[\Xi e^{-i\psi_j} + c.c.\right] \qquad j = 1, \ldots, N \tag{B.16}$$

$$\dot{\psi}_j = \Gamma_j \qquad j = 1, \ldots, N \tag{B.17}$$

$\langle\cdot\rangle$ indicates average over all particles ($\langle\cdot\rangle = N^{-1}\sum_{j=1}^{N}$).

**Hamiltonian**

Equation (2.41) becomes:

$$H = \sum_{j=1}^{N}\frac{\Gamma_j^2}{2} - \frac{i}{\sqrt{2N}}\left[\Xi\sum_{j=1}^{N} e^{-i\psi_j} - c.c.\right] - \frac{b}{2}\Xi\Xi^* \tag{B.18}$$

$\Xi^*$ is the complex conjugate of $\Xi$. Equations (2.42)-(2.43) become:

$$\dot{\psi}_j = \frac{\partial H}{\partial \Gamma_j} \qquad j = 1, \ldots, N \tag{B.19}$$

$$\dot{\Gamma}_j = -\frac{\partial H}{\partial \psi_j} \qquad j = 1, \ldots, N \tag{B.20}$$

$$\dot{\Xi} = 2i\frac{\partial H}{\partial \Xi^*} \tag{B.21}$$

The conserved quantity in equation (2.44) becomes:

$$\Delta_{\mathrm{st}} = \sum_{j=1}^{N}\Gamma_j + \frac{1}{2}\Xi\Xi^* \tag{B.22}$$

### B.1.4 Equations (2.37)-(2.44) in Magnitude and Phase Variables

Another useful way of writing equations (2.37)-(2.44) is by the introduction of magnitude (squared) and phase variables for the voltage amplitude. The variable transformation we will use is:

$$J = \frac{\psi_0^2 + \Gamma_0^2}{2} \tag{B.23}$$

$$\theta = \tan^{-1}\frac{\Gamma_0}{\psi_0} \tag{B.24}$$

One can show that $\frac{\partial J}{\partial \psi_0}\frac{\partial \theta}{\partial \Gamma_0} - \frac{\partial J}{\partial \Gamma_0}\frac{\partial \theta}{\partial \psi_0} = 1$. Thus the transformation preserves the Hamiltonian structure of equations (2.37)-(2.43) [51, pg. 169].

**Model Equations**

Differential equations for $J$ and $\theta$ are derived by using equations (2.37)-(2.40). The resulting equations are:

$$\dot{J} = -\frac{2}{\sqrt{N}}\sqrt{J}\sum_{j=1}^{N}\sin(\psi_j+\theta) \tag{B.25}$$

$$\dot{\theta} = -\frac{1}{\sqrt{N}\sqrt{J}}\sum_{j=1}^{N}\cos(\psi_j+\theta)+b \tag{B.26}$$

$$\dot{\Gamma}_j = \frac{2}{\sqrt{N}}\sqrt{J}\sin(\psi_j+\theta) \qquad j=1,\ldots,N \tag{B.27}$$

$$\dot{\psi}_j = \Gamma_j \qquad j=1,\ldots,N \tag{B.28}$$

**Hamiltonian**

Equation (2.41) becomes:

$$H=\sum_{j=1}^{N}\frac{\Gamma_j^2}{2}+\frac{2}{\sqrt{N}}\sqrt{J}\sum_{j=1}^{N}\cos(\psi_j+\theta)-bJ \tag{B.29}$$

Equations (2.42)-(2.43) become:

$$\dot{\psi}_j = \frac{\partial H}{\partial \Gamma_j} \qquad j=1,\ldots,N \tag{B.30}$$

$$\dot{\Gamma}_j = -\frac{\partial H}{\partial \psi_j} \qquad j=1,\ldots,N \tag{B.31}$$

$$\dot{J} = \frac{\partial H}{\partial \theta} \tag{B.32}$$

$$\dot{\theta} = -\frac{\partial H}{\partial J} \tag{B.33}$$

The conserved quantity in equation (2.44) becomes:

$$\Delta_{\mathrm{st}}=\sum_{j=1}^{N}\Gamma_j+J \tag{B.34}$$

## B.2 Multitone Model in Alternative Variables

Model equations and Hamiltonians are presented in complex variables for the multitone equations (3.57)-(3.60) in B.2.1 and for (3.63)-(3.70) in B.2.2. In B.2.3 equations (3.63)-(3.70) are written with magnitude and phase variables for the tone amplitudes.

### B.2.1 Equations (3.57)-(3.60) in Complex Variables

**Model Equations**

$$\dot{\mathcal{A}}_n = i\Omega_n\langle e^{i\Omega_n\psi_j}\rangle - i\delta\Omega_n\mathcal{A}_n \qquad n=1,\ldots,M \tag{B.35}$$

$$\dot{\Gamma}_j = i\sum_{k=1}^{M}\Omega_k\left[\mathcal{A}_k e^{-i\Omega_k\psi_j} - c.c.\right] \qquad j=1,\ldots,N \tag{B.36}$$

$$\dot{\psi}_j = \Gamma_j \qquad j=1,\ldots,N \tag{B.37}$$

where $\mathcal{A}_n \equiv \frac{a_{1n}}{4} + i\frac{a_{2n}}{4}$ and $\langle\cdot\rangle$ denotes average over all particles($\langle\cdot\rangle = N^{-1}\sum_{j=1}^{N}$).

**Hamiltonian**

Hamiltonian function:

$$H = \sum_{j=1}^{N}\left[\frac{\Gamma_j^2}{2} + \sum_{n=1}^{M}\left(\mathcal{A}_n e^{-i\Omega_n\psi_j} + c.c.\right)\right] - N\delta\sum_{n=1}^{M}\mathcal{A}_n\mathcal{A}_n^* \tag{B.38}$$

where $\mathcal{A}_n^*$ denotes complex conjugate. The equations of motion are generated by:

$$\dot{\Gamma}_j = -\frac{\partial H}{\partial\psi_j} \qquad j=1,\ldots,N \tag{B.39}$$

$$\dot{\psi}_j = \frac{\partial H}{\partial\Gamma_j} \qquad j=1,\ldots,N \tag{B.40}$$

$$\dot{\mathcal{A}}_n = \frac{i\Omega_n}{N}\frac{\partial H}{\partial\mathcal{A}_n^*} \qquad n=1,\ldots,M \tag{B.41}$$

### B.2.2 Equations (3.63)-(3.70) in Complex Variables

**Model Equations**

$$\dot{\Xi}_n = i\sqrt{2\Omega_n N}\langle e^{i\Omega_n\psi_{0j}}\rangle - i\delta\Omega_n\Xi_n \qquad n=1,\ldots,M \tag{B.42}$$

$$\dot{\Gamma}_{0j} = \frac{i}{\sqrt{2N}}\sum_{k=1}^{M}\Omega_k^{\frac{3}{2}}\left[\Xi_k e^{-i\Omega_k\psi_{0j}} - c.c.\right] \qquad j=1,\ldots,N \tag{B.43}$$

$$\dot{\psi}_{0j} = \Gamma_{0j} \qquad j=1,\ldots,N \tag{B.44}$$

where $\Xi_n \equiv \Gamma_{n0} + i\psi_{n0}$ and $\langle\cdot\rangle$ denotes average over all particles ($\langle\cdot\rangle = N^{-1}\sum_{j=1}^{N}$).

**Hamiltonian**

Hamiltonian function:

$$H = \sum_{j=1}^{N}\left[\frac{\Gamma_{0j}^2}{2} + \frac{1}{\sqrt{2N}}\sum_{n=1}^{M}\Omega_n^{\frac{1}{2}}\left(\Xi_n e^{-i\Omega_n\psi_{0j}} + c.c.\right)\right] - \frac{\delta}{2}\sum_{n=1}^{M}\Omega_n\Xi_n\Xi_n^* \tag{B.45}$$

where $\Xi_n^*$ denotes complex conjugate. The equations of motion are generated by:

$$\dot{\Gamma}_{0j} = -\frac{\partial H}{\partial\psi_{0j}} \qquad j=1,\ldots,N \tag{B.46}$$

$$\dot{\psi}_{0j} = \frac{\partial H}{\partial\Gamma_{0j}} \qquad j=1,\ldots,N \tag{B.47}$$

$$\dot{\Xi}_n = 2i\frac{\partial H}{\partial\Xi_n^*} \qquad n=1,\ldots,M \tag{B.48}$$

The conserved quantity in (3.70) becomes:

$$\Delta_{\mathrm{mt}} = \sum_{j=1}^{N}\Gamma_{0j} + \sum_{n=1}^{M}\frac{\Omega_n}{2}\Xi_n\Xi_n^* \tag{B.49}$$

### B.2.3 Equations (3.63)-(3.70) in Magnitude and Phase Variables

We define magnitude (squared) and phase variables by the transformation:

$$J_n = \frac{\psi_{n0}^2 + \Gamma_{n0}^2}{2} \tag{B.50}$$

$$\theta_n = \tan^{-1}\frac{\Gamma_{n0}}{\psi_{n0}} \tag{B.51}$$

**Model Equations**

Differential equations for $J_n$ and $\theta_n$ are derived using equations (3.63)-(3.66). The resulting equations are:

$$\dot{J}_n = 2\sqrt{\frac{\Omega_n}{N}}\sqrt{J_n}\sum_{j=1}^{N}\cos(\Omega_n\psi_{0j}+\theta_n) \qquad n=1,\ldots,M \tag{B.52}$$

$$\dot{\theta}_n = \left[-\sqrt{\frac{\Omega_n}{N}}\frac{1}{\sqrt{J_n}}\sum_{j=1}^{N}\sin(\Omega_n\psi_{0j}+\theta_n)\right]+\delta\Omega_n \qquad n=1,\ldots,M \tag{B.53}$$

$$\dot{\Gamma}_{0j} = -\frac{2}{\sqrt{N}}\sum_{k=1}^{M}\sqrt{J_k}\Omega_k^{\frac{3}{2}}\cos(\Omega_k\psi_{0j}+\theta_k) \qquad j=1,\ldots,N \tag{B.54}$$

$$\dot{\psi}_{0j} = \Gamma_{0j} \qquad j=1,\ldots,N \tag{B.55}$$

**Hamiltonian**

Hamiltonian function:

$$H=\sum_{j=1}^{N}\left[\frac{\Gamma_{0j}^2}{2}+\frac{2}{\sqrt{N}}\sum_{n=1}^{M}\sqrt{J_n\Omega_n}\sin(\Omega_n\psi_{0j}+\theta_n)\right]-\delta\sum_{n=1}^{M}\Omega_n J_n \tag{B.56}$$

The equations of motion are generated by:

$$\dot{\Gamma}_{0j} = -\frac{\partial H}{\partial\psi_{0j}} \qquad j=1,\ldots,N \tag{B.57}$$

$$\dot{\psi}_{0j} = \frac{\partial H}{\partial\Gamma_{0j}} \qquad j=1,\ldots,N \tag{B.58}$$

$$\dot{J}_n = \frac{\partial H}{\partial\theta_n} \qquad n=1,\ldots,M \tag{B.59}$$

$$\dot{\theta}_n = -\frac{\partial H}{\partial J_n} \qquad n=1,\ldots,M \tag{B.60}$$

The conserved quantity in (3.70) becomes:

$$\Delta_{\mathrm{mt}} = \sum_{j=1}^{N} \Gamma_{0j} + \sum_{n=1}^{M} \Omega_n J_n \tag{B.61}$$

## Appendix C

## Multitone Collective Variable Linearization

In this appendix we linearize (3.103) restated here as:

$$\dot{\mathcal{P}}_n \;=\; g(\Gamma_{n0}, \psi_{n0}, \Gamma_{k0}, \psi_{k0}, \psi_{0j}, \Gamma_{0j}) \tag{C.1}$$

$$\begin{aligned} &g(\Gamma_{n0}, \psi_{n0}, \Gamma_{k0}, \psi_{k0}, \psi_{0j}, \Gamma_{0j}) = \\ &\quad -\Omega_n(\Gamma_{n0} + i\psi_{n0}) - \frac{1}{N\Omega_n^{\frac{1}{2}}} \sum_{j=1}^{N} \left\{ \sum_{\substack{k=1 \\ k\neq n}}^{M} \Omega_k^{\frac{3}{2}} \left[ (\Gamma_{k0} + i\psi_{k0}) e^{-i(\Omega_k - \Omega_n)\psi_{0j}} \right.\right. \\ &\quad \left.\left. - (\Gamma_{k0} - i\psi_{k0}) e^{i(\Omega_k + \Omega_n)\psi_{0j}} \right] - \Omega_n^{\frac{3}{2}} (\Gamma_{n0} - i\psi_{n0}) e^{i2\Omega_n\psi_{0j}} + \sqrt{2N}\Omega_n \Gamma_{0j}^2 e^{i\Omega_n\psi_{0j}} \right\} \end{aligned} \tag{C.2}$$

The definition of $\Xi_n$ given in (3.95) is used above. Even though $g$ depends on $\Xi_k$ for $k = 1, \ldots, M$ and $\psi_{0j}$, $\Gamma_{0j}$ for $j = 1, \ldots, N$, we indicate each variable only once in $g$'s definition. Also $\Xi_n$ is indicated differently than $\Xi_k$, that is $\Xi$ for $n \neq k$, since $g$ depends on these quantities differently.

We define the vector $\mathbf{x}$ as:

$$\mathbf{x} \equiv [\Gamma_{n0}\ \psi_{n0}\ \Gamma_{k0}\ \psi_{k0}\ \psi_{0j}\ \Gamma_{0j}]^{\mathrm{T}} \qquad \begin{matrix} k = 1, \ldots, M \\ k \neq n \end{matrix} \qquad j = 1, \ldots, N \tag{C.3}$$

We indicate the value of $\mathbf{x}$ about which we are going to Taylor expand as:

$$\begin{aligned} \overline{\mathbf{x}} \;&\equiv\; [\overline{\Gamma}_{n0}\ \overline{\psi}_{n0}\ \overline{\Gamma}_{k0}\ \overline{\psi}_{k0}\ \overline{\psi}_{0j}\ \overline{\Gamma}_{0j}]^{\mathrm{T}} \qquad \begin{matrix} k = 1, \ldots, M \\ k \neq n \end{matrix} \qquad j = 1, \ldots, N \\ &=\; [0\ 0\ 0\ 0\ \frac{(j-1)2\pi}{N}\ 0]^{\mathrm{T}} \end{aligned} \tag{C.4}$$

And finally we have the perturbation of the vector $\mathbf{x}$:

$$\begin{aligned}\delta\mathbf{x} &\equiv \mathbf{x}-\overline{\mathbf{x}} \\ &= [\delta\Gamma_{n0}\ \delta\psi_{n0}\ \delta\Gamma_{k0}\ \delta\psi_{k0}\ \delta\psi_{0j}\ \delta\Gamma_{0j}]^{\mathrm{T}} \quad \begin{matrix} k=1,\ldots,M \\ k\neq n \\ j=1,\ldots,N \end{matrix}\end{aligned} \tag{C.5}$$

The Taylor series expansion to first order of $g$ is:

$$\begin{aligned} g(\Gamma_{n0},\psi_{n0},\Gamma_{k0},\psi_{k0},\psi_{0j},\Gamma_{0j}) \approx \\ g(\overline{\mathbf{x}}) + \left.\frac{\partial g}{\partial\Gamma_{n0}}\right|_{\overline{\mathbf{x}}}\delta\Gamma_{n0} + \left.\frac{\partial g}{\partial\psi_{n0}}\right|_{\overline{\mathbf{x}}}\delta\psi_{n0} + \left.\frac{\partial g}{\partial\Gamma_{k0}}\right|_{\overline{\mathbf{x}}}\delta\Gamma_{k0} \\ + \left.\frac{\partial g}{\partial\psi_{k0}}\right|_{\overline{\mathbf{x}}}\delta\psi_{k0} + \left.\frac{\partial g}{\partial\psi_{0j}}\right|_{\overline{\mathbf{x}}}\delta\psi_{0j} + \left.\frac{\partial g}{\partial\Gamma_{0j}}\right|_{\overline{\mathbf{x}}}\delta\Gamma_{0j}\end{aligned} \tag{C.6}$$

Next we compute the derivatives in (C.6).

$$\left.\frac{\partial g}{\partial\Gamma_{n0}}\right|_{\overline{\mathbf{x}}} = -\Omega_n + \frac{\Omega_n}{N}\sum_{j=1}^{N} e^{i2\Omega_n\overline{\psi}_{0j}} \tag{C.7}$$

$$\left.\frac{\partial g}{\partial\psi_{n0}}\right|_{\overline{\mathbf{x}}} = -i\Omega_n - i\frac{\Omega_n}{N}\sum_{j=1}^{N} e^{i2\Omega_n\overline{\psi}_{0j}} \tag{C.8}$$

$$\left.\frac{\partial g}{\partial\Gamma_{k0}}\right|_{\overline{\mathbf{x}}} = -\frac{\Omega_k^{\frac{3}{2}}}{N\Omega_n^{\frac{1}{2}}}\sum_{j=1}^{N}\left[e^{-i(\Omega_k-\Omega_n)\overline{\psi}_{0j}} - e^{i(\Omega_k+\Omega_n)\overline{\psi}_{0j}}\right] \tag{C.9}$$

$$\left.\frac{\partial g}{\partial\psi_{k0}}\right|_{\overline{\mathbf{x}}} = -i\frac{\Omega_k^{\frac{3}{2}}}{N\Omega_n^{\frac{1}{2}}}\sum_{j=1}^{N}\left[e^{-i(\Omega_k-\Omega_n)\overline{\psi}_{0j}} + e^{i(\Omega_k+\Omega_n)\overline{\psi}_{0j}}\right] \tag{C.10}$$

$$\begin{aligned}\left.\frac{\partial g}{\partial\psi_{0j}}\right|_{\overline{\mathbf{x}}} = \frac{1}{N\Omega_n^{\frac{1}{2}}}\Bigg\{ &\sum_{\substack{k=1\\k\neq n}}^{M} i\Omega_k^{\frac{3}{2}}\Big[(\Omega_k-\Omega_n)(\overline{\Gamma}_{k0}+i\overline{\psi}_{k0})e^{-i(\Omega_k-\Omega_n)\overline{\psi}_{0j}} \\ &+ (\Omega_k+\Omega_n)(\overline{\Gamma}_{k0}-i\overline{\psi}_{k0})e^{i(\Omega_k+\Omega_n)\overline{\psi}_{0j}}\Big] \\ &+ i2\Omega_n^{\frac{5}{2}}(\overline{\Gamma}_{n0}-i\overline{\psi}_{n0})e^{i2\Omega_n\overline{\psi}_{0j}} \\ &- i\sqrt{2N}\Omega_n^2\overline{\Gamma}_{0j}^2 e^{i\Omega_n\overline{\psi}_{0j}}\Bigg\}\end{aligned} \tag{C.11}$$

$$\left.\frac{\partial g}{\partial\Gamma_{0j}}\right|_{\overline{\mathbf{x}}} = -\sqrt{\frac{8}{N}}\Omega_n^{\frac{1}{2}}\overline{\Gamma}_{0j}e^{i\Omega_n\overline{\psi}_{0j}} \tag{C.12}$$

To determine the values of (C.7)-(C.12) we substitute the values of $\overline{\mathbf{x}}$ in (C.4). By inspection one can see that:

$$\left.\frac{\partial g}{\partial \psi_{0j}}\right|_{\overline{\mathbf{x}}} = 0 \tag{C.13}$$

$$\left.\frac{\partial g}{\partial \Gamma_{0j}}\right|_{\overline{\mathbf{x}}} = 0 \tag{C.14}$$

To compute (C.9)-(C.12) we need the following formula for a finite series:

$$\sum_{j=1}^{N} \alpha^{(j-1)} = \begin{cases} \frac{1-\alpha^N}{1-\alpha} & \alpha \neq 1 \\ N & \alpha = 1 \end{cases} \tag{C.15}$$

Define the set $\mathbb{Z}^+ = \{1, 2, 3, \ldots\}$. We will use the notation $p, q \in \mathbb{Z}^+$ to indicate that $p, q$ belong to $\mathbb{Z}^+$, and $r, s \notin \mathbb{Z}^+$ to indicate that $r, s$ are not in $\mathbb{Z}^+$.

If one substitutes $\overline{\psi}_{0j} = \frac{(j-1)2\pi}{N}$ into (C.7) and (C.8), then uses $\alpha = e^{i\Omega_n \frac{4\pi}{N}}$ in (C.15) noting that $\Omega_n$ is an integer, one gets:

$$\left.\frac{\partial g}{\partial \Gamma_{n0}}\right|_{\overline{\mathbf{x}}} = \begin{cases} -\Omega_n & 2\Omega_n = rN \quad r \notin \mathbb{Z}^+ \\ 0 & 2\Omega_n = pN \quad p \in \mathbb{Z}^+ \end{cases} \tag{C.16}$$

$$\left.\frac{\partial g}{\partial \psi_{n0}}\right|_{\overline{\mathbf{x}}} = \begin{cases} -i\Omega_n & 2\Omega_n = rN \quad r \notin \mathbb{Z}^+ \\ -2i\Omega_n & 2\Omega_n = pN \quad p \in \mathbb{Z}^+ \end{cases} \tag{C.17}$$

Similarly substituting the definition of $\overline{\psi}_{0j}$ into (C.9) and (C.10), using the appropriate definitions of $\alpha$, and noting that $\Omega_k$ and $\Omega_n$ are integers, one gets:

$$\left.\frac{\partial g}{\partial \Gamma_{k0}}\right|_{\overline{\mathbf{x}}} = \begin{cases} 0 & \begin{array}{ll} |\Omega_k - \Omega_n| = rN & \\ \Omega_k + \Omega_n = sN & r, s \notin \mathbb{Z}^+ \end{array} \\ \frac{\Omega_k^{\frac{3}{2}}}{\Omega_n^{\frac{1}{2}}} & \begin{array}{ll} |\Omega_k - \Omega_n| = rN & r \notin \mathbb{Z}^+ \\ \Omega_k + \Omega_n = pN & p \in \mathbb{Z}^+ \end{array} \\ -\frac{\Omega_k^{\frac{3}{2}}}{\Omega_n^{\frac{1}{2}}} & \begin{array}{ll} |\Omega_k - \Omega_n| = pN & p \in \mathbb{Z}^+ \\ \Omega_k + \Omega_n = rN & r \notin \mathbb{Z}^+ \end{array} \\ 0 & \begin{array}{ll} |\Omega_k - \Omega_n| = pN & \\ \Omega_k + \Omega_n = qN & p, q \in \mathbb{Z}^+ \end{array} \end{cases} \tag{C.18}$$

$$\left.\frac{\partial g}{\partial \psi_{k0}}\right|_{\overline{\mathbf{x}}} = \begin{cases} 0 & \begin{array}{ll} |\Omega_k - \Omega_n| = rN & \\ \Omega_k + \Omega_n = sN & r, s \notin \mathbb{Z}^+ \end{array} \\ -i\frac{\Omega_k^{\frac{3}{2}}}{\Omega_n^{\frac{1}{2}}} & \begin{array}{ll} |\Omega_k - \Omega_n| = rN & r \notin \mathbb{Z}^+ \\ \Omega_k + \Omega_n = pN & p \in \mathbb{Z}^+ \end{array} \\ -i\frac{\Omega_k^{\frac{3}{2}}}{\Omega_n^{\frac{1}{2}}} & \begin{array}{ll} |\Omega_k - \Omega_n| = pN & p \in \mathbb{Z}^+ \\ \Omega_k + \Omega_n = rN & r \notin \mathbb{Z}^+ \end{array} \\ -i\frac{2\Omega_k^{\frac{3}{2}}}{\Omega_n^{\frac{1}{2}}} & \begin{array}{ll} |\Omega_k - \Omega_n| = pN & \\ \Omega_k + \Omega_n = qN & p, q \in \mathbb{Z}^+ \end{array} \end{cases} \tag{C.19}$$

Depending on the relations between $\Omega_n$, $\Omega_k$, and $N$, equation (C.6) could take on many different forms based on the various expressions in (C.16)-(C.19). If we base our choice of $N$ on the requirement that there be greater than two disks per period of the highest frequency, the values in (C.16)-(C.19), and hence (C.6), are determined. Recall $N$ is the number of disks in a period of $\omega_f$. The number of periods of the frequency corresponding to $\Omega_n$ in one period of $\omega_f$ is $\Omega_n$. Thus the number of disks per period of the frequency corresponding to $\Omega_n$ is $\frac{N}{\Omega_n}$, and we require:

$$\frac{N}{\Omega_n} > 2 \tag{C.20}$$

Notice then that there are no positive integers such that:

$$2\Omega_n = lN \qquad l \in \mathbb{Z}^+ \tag{C.21}$$

If we consider $\Omega_n$ to be the largest frequency present, then certainly:

$$\Omega_n + \Omega_k < 2\Omega_n \tag{C.22}$$

Imposing (C.20) on $\Omega_n$ leads to the following inequality:

$$\Omega_n + \Omega_k < N \tag{C.23}$$

Thus there are no positive integers such that:

$$\Omega_n + \Omega_k = lN \qquad l \in \mathbb{Z}^+ \tag{C.24}$$

The preclusion of:

$$|\Omega_k - \Omega_n| = lN \qquad l \in \mathbb{Z}^+ \tag{C.25}$$

follows a similar argument. Notice that the conditions we derived in Section 3.1.4 for the number of disks based on frequency separations are even more stringent than having $2\Omega_n < N$.

Finally, we may compute (C.6). Using $g(\overline{\mathbf{x}}) = 0$, $\Xi_n = \delta\Gamma_{n0} + i\delta\psi_{n0}$, and the conditions derived above in (C.16)-(C.19), one gets:

$$\dot{\mathcal{P}}_n = -\Omega_n \Xi_n \tag{C.26}$$

# Appendix D

## Standard Map for Single and Multitone TWT

In this appendix we take the single and multitone models of Appendix B and discretize them to get mappings similar to the standard mapping [35]. The discretization follows a paper by del-Castillo-Negrete [19].

### D.1 Single Tone

We start with equations (B.25)-(B.28) in Appendix B. Let $\tau$ be a time step, and superscript $t$ be the discrete time index. Discretization of the equations gives:

$$J^{t+1} = J^t - \frac{2\tau}{\sqrt{N}}\sqrt{J^{t+1}}\sum_{j=1}^{N}\sin(\psi_j^t + \theta^t) \tag{D.1}$$

$$\theta^{t+1} = \theta^t - \frac{\tau}{\sqrt{N}}\frac{1}{\sqrt{J^{t+1}}}\sum_{j=1}^{N}\cos(\psi_j^t + \theta^t) + \tau b \tag{D.2}$$

$$\Gamma_j^{t+1} = \Gamma_j^t + \frac{2\tau}{\sqrt{N}}\sqrt{J^{t+1}}\sin(\psi_j^t + \theta^t) \qquad j = 1, \ldots, N \tag{D.3}$$

$$\psi_j^{t+1} = \psi_j^t + \tau\Gamma_j^{t+1} \qquad j = 1, \ldots, N \tag{D.4}$$

The discretized version of the constant of the motion in (B.34) becomes:

$$\Delta_{\mathrm{st}}^t = \sum_{j=1}^{N}\Gamma_j^t + J^t \tag{D.5}$$

One can check that $\Delta_{\mathrm{st}}^{t+1} = \Delta_{\mathrm{st}}^t$; the quantity is still conserved. According to del-Castillo-Negrete [19] the discretized Hamiltonian (energy) is not a conserved quantity,

but the mapping is symplectic (volume preserving). Notice that the discretization is a combination of forward and backward Euler integration schemes.

The equation for $J^{t+1}$ is implicit. We can remedy this by defining $\kappa^t \equiv \sqrt{J^t}$, putting this definition into the equation for $J^{t+1}$, and using the quadratic formula. (Notice that $J^t$ is magnitude squared and $\kappa^t$ is magnitude.) The final mapping is:

$$\kappa^{t+1} = \sqrt{\frac{\tau^2}{N}\left[\sum_{j=1}^{N}\sin(\psi_j^t+\theta^t)\right]^2 + (\kappa^t)^2} - \frac{\tau}{\sqrt{N}}\sum_{j=1}^{N}\sin(\psi_j^t+\theta^t) \tag{D.6}$$

$$\theta^{t+1} = \theta^t - \frac{\tau}{\sqrt{N}}\frac{1}{\kappa^{t+1}}\sum_{j=1}^{N}\cos(\psi_j^t+\theta^t) + \tau b \tag{D.7}$$

$$\Gamma_j^{t+1} = \Gamma_j^t + \frac{2\tau}{\sqrt{N}}\kappa^{t+1}\sin(\psi_j^t+\theta^t) \qquad j=1,\ldots,N \tag{D.8}$$

$$\psi_j^{t+1} = \psi_j^t + \tau\Gamma_j^{t+1} \qquad j=1,\ldots,N \tag{D.9}$$

## D.2 Multitone

A directly analogous calculation can be done for the multitone model. Discretization of (B.52)-(B.55) yields:

$$J_n^{t+1} = J_n^t + 2\tau\sqrt{\frac{\Omega_n}{N}}\sqrt{J_n^{t+1}}\sum_{j=1}^{N}\cos(\Omega_n\psi_{0j}^t+\theta_n^t) \qquad n=1,\ldots,M \tag{D.10}$$

$$\theta_n^{t+1} = \theta_n^t - \sqrt{\frac{\Omega_n}{N}}\frac{\tau}{\sqrt{J_n^{t+1}}}\sum_{j=1}^{N}\sin(\Omega_n\psi_{0j}^t+\theta_n^t) + \tau\delta\Omega_n \qquad n=1,\ldots,M \tag{D.11}$$

$$\Gamma_{0j}^{t+1} = \Gamma_{0j}^t - \frac{2\tau}{\sqrt{N}}\sum_{k=1}^{M}\sqrt{J_k^{t+1}}\Omega_k^{\frac{3}{2}}\cos(\Omega_k\psi_{0j}^t+\theta_k^t) \qquad j=1,\ldots,N \tag{D.12}$$

$$\psi_{0j}^{t+1} = \psi_{0j}^t + \tau\Gamma_{0j} \qquad j=1,\ldots,N \tag{D.13}$$

One can check the following is a conserved quantity:

$$\Delta_{\mathrm{mt}}^t = \sum_{j=1}^{N}\Gamma_{0j}^t + \sum_{n=1}^{M}\Omega_n J_n^t \tag{D.14}$$

To get the map for $J_n^{t+1}$ to be explicit we define $\kappa_n^t \equiv \sqrt{J_n^t}$ and produce the new mapping:

$$\begin{aligned}
\kappa_n^{t+1} &= \sqrt{\tau^2 \frac{\Omega_n}{N}\left[\sum_{j=1}^{N}\cos(\Omega_n\psi_{0j}^t+\theta_n^t)\right]^2+(\kappa_n^t)^2} \\
&\quad + \tau\sqrt{\frac{\Omega_n}{N}}\sum_{j=1}^{N}\cos(\Omega_n\psi_{0j}^t+\theta_n^t) \qquad n=1,\ldots,M \quad \text{(D.15)} \\
\theta_n^{t+1} &= \theta_n^t - \sqrt{\frac{\Omega_n}{N}}\frac{\tau}{\kappa_n^{t+1}}\sum_{j=1}^{N}\sin(\Omega_n\psi_{0j}^t+\theta_n^t) \\
&\quad + \tau\delta\Omega_n \qquad n=1,\ldots,M \quad \text{(D.16)} \\
\Gamma_{0j}^{t+1} &= \Gamma_{0j}^t - \frac{2\tau}{\sqrt{N}}\sum_{k=1}^{M}\kappa_k^{t+1}\Omega_k^{\frac{3}{2}}\cos(\Omega_k\psi_{0j}^t+\theta_k^t) \qquad j=1,\ldots,N \quad \text{(D.17)} \\
\psi_{0j}^{t+1} &= \psi_{0j}^t + \tau\Gamma_{0j} \qquad j=1,\ldots,N \quad \text{(D.18)}
\end{aligned}$$